UNIVERSITA' DEGLI STUDI DI VERONA

DIPARTIMENTO DI
SCIENZE MORFOLOGICO-BIOMEDICHE

DOTTORATO DI RICERCA IN
IMAGING MULTIMODALE IN BIOMEDICINA
CICLO XXII

# NEW EVIDENCES OF INFLAMMATORY MEDIATORS IN ABSENCE EPILEPSY

S.S.D. BIO / 16

Coordinatore: Prof. ANDREA SBARBATI

Tutor: Prof. PAOLO FRANCESCO FABENE

Dottorando: Dott. MICHELE PELLITTERI

**TABLE OF CONTENTS**

# -1-

## INTRODUCTION

### 1.1 Definition of absence epilepsy

Epilepsies and epileptic syndromes describe complex disease states that are accompanied by abnormal hyper excitability and/or hyper synchronicity within the central nervous system (CNS). Epilepsy, as a disease entity, has first been mentioned by the ancient Egyptians who called it *nesejet*, or by the ancient Babylonians who called it the *bennu* disease (Temkin, 1994).

About 500 BC, Hippocrates already claimed that the brain is the origin of epileptic seizure activity. Interestingly, however, this approach was consequently ignored over the millennia and there was hardly any substantial progress in understanding the etiopathogenesis of epilepsies till beginning of the modern times (Temkin, 1994). The clinical features of absence epilepsy itself were first described by Poupart in 1705 (Temkin, 1994). Later on, Tissot described a girl with absences "[…] avec un tres leger movement dans les yeux" and, in addition, repetitive generalized tonic–clonic seizures (GTCS) (Tissot, 1770). The term "epileptic absence" was first introduced by Calmeil (1824); shortly thereafter, Esquirol (1838) raised the term *petit mal* in contrast to the generalized *grand mal* seizure group. Interestingly, Gowers (1881) gave a very detailed description of the absence seizures "without conspicuous convulsions" and Friedmann (1906) first reported a long-term favorable prognosis but originally believed that absences were not epileptic. Sauer (1916) was the first to describe an important subtype of typical absence epilepsy, i.e., pyknolepsy (pycnolepsia, pure *petit mal* or socalled Friedmann syndrome), which was later characterized in detail also by Adie (1924). The establishment and characterization of the electroencephalography by Hans Berger in the 1920s enabled Gibbs and colleagues to unravel absence-specific ictal discharges in clinical EEG recordings (Gibbs and Gibbs, 1935). The *petit mal* triad of Lennox (1945), which was misused and misunderstood, was clarified by the Commission on Classification and Terminology of the International League Against Epilepsy (ILAE) with the differentiation of typical from atypical absences (Gastaut, 1970). Later on, several groups studied absence epilepsy in greater detail using video-EEG monitoring (Penry et al., 1975; Stefan, 1982). Panayiotopoulos and colleagues (1997) described

syndrome-related characterization of typical absence seizures with video-EEG analysis in detail. Etiopathogenetically, absence epilepsies represent a most fascinating disease group which is probably one of the most well-characterized seizure types in humans and animal models (Danober et al., 1998; Manning et al., 2003; Steriade, 2005; Llinas and Steriade, 2006; Khosravani and Zamponi, 2006). As will be outlined below, these detailed insights fostered the development of rather effective and specific pharmacological approaches to treat absence epilepsy in humans.

### 1.2 Epidemiology of absence epilepsy

Nowadays, the frequency, importance and sociocultural implications of epilepsy can hardly be overestimated. Manifest epilepsy affects around 0.5–1% of the population in Europe and North America, 5% of the population perceive a single seizure in their lifetime, and about 10–15% exhibit an increased seizure susceptibility (Forsgren et al., 2005a,b; Pugliatti et al., 2007). In the US, the prevalence of epilepsy is 1.77 million (Victor and Ropper, 2001). Estimates of worldwide prevalence of epilepsy suggest 50 million people being affected with strong differences in regional distribution. Epilepsy incidence is age dependent; 70% of the patients suffering from epilepsy are below 25 years of age, with most of the seizures beginning during childhood and early adolescence. About 40% of epilepsies belong to the generalized grand mal seizure family and another 40% represent complex partial, i.e., limbic or psychomotor seizures (Matthes and Schneble, 1999). In contrast, absence epilepsy makes up approximately 10% of the epilepsies and is often accompanied by other types of generalized seizures (Panayiotopoulos et al., 1995). Estimates of the annual incidence of childhood absence epilepsy (CAE), a prototype of pure petit mal in children aged 0–15 years, range from 6.3/100000 (Olsson, 1988; Loiseau et al., 1990) to 8.0/100000 (Blom et al., 1978; Posner, 2006). The prevalence of CAE was estimated at 10% (Callenbach et al., 1998) and 12.1% (Berg et al., 1999) for children younger than 16 years. Further detailed information on current epidemiology is provided by Jallon and Latour (2005). Interestingly, CAE is two- to fivefold more frequent in females than in males (Posner, 2006). Given the severe sociocultural implications, the necessity for efficient pharmacological treatment of absence epilepsies is self-evident (Manning et al., 2003; Rogawski and Loscher,2004).

## 1.3 Classification and clinical phenomenology of absence epilepsy

### 1.3.1 Typical absence epilepsy

Systematically, absence epilepsies can be differentiated into typical and atypical forms with typical absences being further categorized into simple and complex ones. According to the nomenclature proposed by the Commission on Classification and Terminology of the ILAE (Sirven, 2002), typical absence seizures can be found in the following epilepsy syndromes:

a. Typical absence seizures are the archetype of childhood absence epilepsy (CAE, pycnolepsy, pycnoleptic petit mal, pure petit mal, Friedmann syndrome) (Panayiotopoulos, 1999; Panayiotopoulos, 2005b) with an age of onset of 2–8 years and a peak incidence of 5–7 years. There is an ongoing debate whether infantile forms of absence epilepsies with an onset from the 1st to the 4th year of age (early onset absence epilepsy, EOAE) should be separated from childhood absence epilepsy with an onset later on until the 12th year of onset. This debate ranks about different aetiologies, manifestation, semiology, treatment and courses compared to CAE in children over 4 years of age. Patients generally display a normal neurological development and absences exhibit spontaneous remission (>90%) before puberty even without pharmacological treatment. CAE is the prototype of an idiopathic, age-related epileptic syndrome with characteristic ictal bilaterally synchronous, high-amplitude 2.5 to 4 Hz spike-wave discharge (SWD) activity, double to triple spike-waves and slow-waves and normal interictal background activity. Epileptiform SWD episodes are brief (4–20 s) and frequent (10 to 100/day) with abrupt onset and termination. Due to its etiopathogenesis, absences in CAE and other absence entities are accompanied by severe impairment or loss of consciousness. The eyes stare or move slowly and random eyelid blinking, usually not sustained, may occur. In addition, speech and other voluntary activity stop within the first 3 s of the discharge. However, automatisms are also frequent. The diagnosis of CAE is not probable if myoclonic jerks occur shortly before the active stage of the absences, if there are clonic jerks during the absences, if

there is no impairment of consciousness during the SWD activity or if there are multiple spikes and ictal discharge fragmentations.

b. Juvenile absence epilepsy (JAE, spanioleptic or cycloleptic absence epilepsy) is an idiopathic generalized epilepsy (IGE), mainly characterized by typical absences that are similar to, but probably not as severe and frequent as CAE (Panayiotopoulos et al., 1997; Panayiotopoulos, 2005a). Random and infrequent myoclonic jerks as well as infrequent GTCS occur in most of the patients. The predominant age of onset is between 10 and 16 years with a peak at 10 to 12 years. JAE normally persists in adulthood, but absences tend to become less severe with age. The ictal EEG exhibits generalized, spike or multiple spike and slow-waves at 2.5 to 4 Hz. Typical exclusion criteria for JAE are mild impairment of consciousness, brief ictal discharges (less than 4 s), eyelid or perioral myoclonus and rhythmic limb jerking. Single or arrhythmic myoclonic jerks during the absence ictus are incompatible with JAE. Visual and other sensory precipitation of absences may also speak against the diagnosis of JAE as well. In rare cases however, absence episodes might be triggered by intermittent photostimulation in JAE patients who also display photosensibility.

c. Juvenile myoclonic epilepsy (JME, impulsive petit mal, bilateral massive myoclonus, Herpin-Janz syndrome, Janz syndrome) is a genetically determined, common IGE. The prevalence of JME is 5% to 11% among adults and adolescent patients with other epilepsies, and both sexes are equally affected. JME is characterized by myoclonic jerks on awakening, GTCS and typical absences in more than one third of the patients. The seizures have an age related onset (12–25 years) with absences first appearing either in childhood or early adolescence, followed by myoclonic jerks and GTCS in the middle teens. Seizure-precipitating factors like sleep deprivation and fatigue, alcohol, photosensitivity, mental and psychological arousal are prominent. JME seizures probably persist life-long, although absences may become less severe with age. Jerks and GTCS commonly improve after the fourth decade of life. Typical absences are not the predominant type of absence in JME, and they are usually mild and not associated with automatisms or localized limb jerks. Furthermore, the absence related impairment of consciousness is often subtle. Generalized discharges of 3–6 Hz spike-waves have an unstable intradischarge frequency with fragmentations and multiple spikes.

d. Myoclonic absence epilepsy is a rare generalized absence epilepsy of uncertain classification with a typical age of onset of 6–8 years. It is characterized by severe bilateral rhythmical clonic jerks, often associated with tonic contractions.

e. Eyelid myoclonia with absences (also called eyelid myoclonia and absences, Jeavons syndrome) is an IGE manifested with frequent, pycnoleptic-like seizures. Eyelid myoclonia consists of marked, rhythmic and fast jerks of the eyelids and is often associated with jerky upward deviation of the eyeballs and retropulsion of the head. The seizures are brief (3–6 s) and occur mainly after eye closure (eye closure sensitivity). Additionally and concomitantly, absence seizures occur. The onset is usually in early childhood at an age of 10–12 years. Interestingly, patients are highly photosensitive in childhood, but this declines with age. Infrequent GTCS are inevitable in the long term, and they are likely to occur after sleep deprivation, fatigue and alcohol indulgence. Myoclonic jerks of the limbs may emerge, but they are infrequent and random. Eyelid myoclonia with absences often turns out to be pharmacoresistant and to persist life-long. The ictal EEG manifestations mainly consist of generalized polyspikes and slowwaves at 3–6 Hz, although the latter are more likely to occur after eye closure in an illuminated room. Total darkness abolishes the abnormalities related to eye closure. Photoparoxysmal responses are recorded from all untreated young patients.

In clinical routine, the neurological symptoms of typical absence epilepsy can strongly vary among patients (Stefan, 1982; Panayiotopoulos et al., 1997; Capovilla et al., 2001; Loiseau, 2002; Panayiotopoulos, 2005a). Often, patients display a typical, sudden onset of seizure with characteristic open, glassy and staring eyes, turning pale, dropping whatever is in their hand and quivering of the eyelids. Concomitant relaxation of facial muscle often results in a typical absent impression of the patient. The impairment of consciousness may be severe and thus a predominant clinical symptom but sometimes also moderate, mild or inconspicuous so that proper detection may require additional, special cognitive testing to determine the degree of mental arrest. For the duration of ictal activity, patients typically experience a congrade amnesia. In typical simple forms, mental arrest is often associated with other manifestations, such as hypolocomotion and actions such as speaking and writing will be interrupted with no impairment of static

functions, i.e., posture. The ceased actions will be immediately resumed after seizure termination. Based on the impairment of consciousness, the patient will usually be unresponsive when spoken to. The attacks as outlined above typically last from a few seconds to rarely half a minute and terminate as rapidly as they commenced. In less severe absences, the patient may not entirely stop his or her activities, although reaction time and speech may considerably slow down. In their mildest form, absences may even be inconspicuous to the patient and imperceptible to the observer, as disclosed on video-EEG recordings with errors and delays during breath counting or other cognitive testing during hyperventilation. In contrast, typical "complex" forms of absence seizures are often associated with more sophisticated behavioural exacerbations, such as automatisms. These can be de novo automatisms, e.g., oral automatisms or perseverative forms in which patients exhibit stereotype behaviour such as walking, swimming and writing. Automatisms are common in typical absences when consciousness is sufficiently impaired, and they are more likely to occur 4–6 s after onset. Furthermore, these automatisms are more or less coordinated, adapted, i.e., eupractic or dyspractic, involuntary movements that may be an unconscious continuation of the preservative automatisms, de novo automatisms or both. Perioral automatisms such as lip licking, smacking, swallowing, or mute speech movements are also very common. Scratching, fumbling with the clothes and other limb automatisms may also occur. Many of these symptoms of both simple and complex absences can occur in the same patient. Also, one can observe a characteristic falling back of the head or vermiform turning of the head and trunk which is typical for tonic retropulsive, versive and rotatory subtypes of typical complex absence epilepsy. Clonic and myoclonic absence epilepsy usually affects the facial muscle, sometimes also the upper limbs. During the absence itself, clonic motor manifestations, rhythmic or arrhythmic and singular or repetitive are particularly frequent at the onset and can be continuous. However, they may also occur at any other stage of the seizure; usually they present as jerking of the eyelids, eyebrows and eyeballs, together or independently, as well as random or repetitive eye closures. Fast eyelid flickering is probably the most common ictal clinical manifestation and may occur during brief generalized discharges without discernible impairment of consciousness. Myoclonia at the corner of the mouth and jerking of the jaw are less frequently observed. Myoclonic jerks of the head, body and limbs may be singular or rhythmical and repetitive, and they may be mild or violent.

Absences may also be tonic or atonic. In absence with atonic components, the diminution of the muscle tone is usual and may lead to drooping of the head and, occasionally, slumping of the trunk, dropping of the arms and relaxation of the grip. Rarely, tone is sufficiently diminished to cause falls. In absence with tonic components the tonic muscular contraction may affect the extensor or the flexor muscles symmetrically or asymmetrically. The head may be pulled backwards, i.e., retropulsion or to one side, and the trunk may arch. Occasionally, absence seizures can be associated with autonomic signs, so-called vegetative absence epilepsy, including dilatation or constriction of the pupils, i.e., miosis and mydriasis, a flush, sweating, hypersalivation, paleness, enuresis or encopresis. Mixed forms of these absence subtypes are the rule rather than the exception. Absences may be the only type of seizures, as in CAE, or may be mild and non-predominant, as in JME. Typical absences are fundamentally different and pharmacologically unique compared to any other type of seizures, which also results in different pharmacological treatment. Thus, AEDs effective in focal seizures may be deleterious for absence seizures. Finally, the clinical EEG manifestations of typical absences are, by definition, widespread and often not as classical as in their archetype, CAE. If untreated, these seizure events can occur several hundred times a day. This impedes the child's development, often dramatically, and hence, inadequately treated absences can have severe sociocultural and educational impact particularly in young children and bring them into dangerous situations, e.g., in traffic.

### 1.3.2 Atypical absence seizures and absence seizures in other epilepsy syndromes

Atypical forms of absence epilepsy are often part of or accompanied by a complex epilepsy syndrome, such as Lennox–Gastaut syndrome (about two thirds have atypical absences), atypical benign partial epilepsy/pseudo-Lennox–syndrome (about 70% with absences (Hahn et al., 2001) or Doose syndrome (about 60–80% with absences; myoclonic astatic epilepsy (Guerrini, 2005) and thus exhibit a highly differentiated behavioural and electroencephalographic phenotype, whereas simple absence seizure types display more stereotype characteristics. Atypical absences can be symptomatic, e.g., in case of tumour formation in the frontal lobe, tuberous sclerosis (Bourneville–Pringle disease), Aicardi syndrome, Angelman syndrome and neurometabolic disorders. Atypical absences differ from typical absences in the several ways:

1. Atypical absences occur in the context of mainly severe symptomatic or cryptogenic epilepsies of children with learning difficulties, who also suffer from frequent seizures of other types such as atonic, tonic and myoclonic seizures.
2. In atypical absences, onset and termination is not as abrupt as in typical absences and changes in muscle tone are more pronounced. In addition, seizure episodes are unusually long in duration, e.g., more than 30 s.
3. The ictal EEG of atypical absence consists of slow (<2.5 Hz), spike-and-slow waves. The discharge is heterogeneous, often asymmetrical, and may include irregular spike-wave and slow-wave complexes and other paroxysmal activity. The background interictal EEG is usually abnormal. It is noteworthy that absence epilepsies in general can exhibit status-like character. Most absence seizures can further be provoked by hyperventilation or photostimulation and in contrast can often be aborted by strong auditory or other sensory stimuli, as it is known from, e.g., simple-partial seizure types. Finally, absence seizures are more common in tired than in vigilant patients.

### 1.3.3 Additional rare syndromes associated with typical absence seizures

Apart from those absence seizure types outlined above, there are a few rare syndromes (Panayiotopoulos et al., 1997), which should be briefly mentioned here. Perioral myoclonia with absences is an IGE with onset in childhood or early adolescence. They are characterized by rhythmic myoclonus of the perioral facial or masticatory muscles during the absence, together with a variable impairment of consciousness. The absences are frequent and brief.
This seizure type may often be resistant to medication, unremitting and possibly life-long. Phantom absences denote typical absences that are mild and often inconspicuous to the patient and imperceptible to the observer. However, video-EEG recording, breath counting or other cognitive testing during hyperventilation with brief 3–4 Hz spike or multiple spike-wave and slow-wave discharges can be used in order to disclose the occurrence of such absences. The absences are simple, occasionally with eyelid blinking. Although they may be clinically unrecognized, they usually manifest in adult life with GTCS and often with absence status epilepticus (Panayiotopoulos et al., 1997). Reflex absences represent typical absences with specific modes of precipitation, e.g.,

photic pattern, video games, thinking, reading, etc. (Panayiotopoulos, 2005b). Photosensitivity is estimated to occur in approximately 50% of patients with onset of absences in childhood or adolescence, and it is often associated with an unfavourable prognosis (Lu et al., 2008). The best-defined syndrome with photosensitivity is eyelid myoclonia and absences (Jeavons syndrome). Absences with single myoclonic jerks during the absence ictus are typical absences with single, often violent jerks of the head, body or limbs. They may appear in early childhood and continue in adult life—often with other types of generalized seizures. They are difficult to treat and may have a bad prognosis. Symptomatic and cryptogenic absences may be, as the name suggests, symptomatic, arising as a consequence of a known disorder of the central nervous system (Ferrie et al., 1995), or cryptogenic, i.e., resulting from a suspected, but unknown, cause. Symptomatic and cryptogenic absences may be focal or diffuse, traumatic, metabolic or inflammatory.

### 1.4 Animal model of absence epilepsy

Genetic rat model of absence epilepsy have been studied for many years and thought to mimic more accurately the spontaneous seizures of human epilepsy than do drug-induced animal models (Coenen et al., 2003).

GAERS (Genetic Absence Epilepsy Rats from Strasbourg) are a well-validated animal model of human Idiopathic Generalised Epilepsy (IGE), possessing a similar electrophysiological, ontogenic and pharmacological profile to the human condition (Danober et al., 1998). Historically, the GAERS colony was derived from Wistar rat and selectively bred for the seizure phenotype so that 100% of progeny spontaneously develop the epilepsy. A non-epileptic control (NEC) strain was also derived from the original colony by selectively breeding for the lack of seizure expression, providing a powerful control strain, since any differences between the two strains would have a high a priori chance of being aetiologically associated with the epilepsy. In addition to developing epilepsy, the GAERS strain also exhibits a range of behaviours indicative of affective disturbance, including increased anxiety and depressive like behaviours (Jones et al., 2008), intimating that this rat strain also models the well-documented mood disturbances observed in clinical IGE populations (Caplan et al., 1998, 2005; Davies et al., 2003; Jones et al., 2007; Ott et al., 2003; Tellez-Zenteno et al., 2007).

The rats strain named WAG/Rij (Wistar Albino Glaxo strain bread in Rijswijk) exhibits spontaneous SWDs that have a frequency of 7 to 11 Hz, duration of 1 to 45 s and amplitude of 200 to 1000 μV (van Luijtelaar et al.,1986; Coenen et al., 1987,1992). The spike-wave discharges become manifest in the cortical EEG at an age of 2 to 3 months, while at a younger age spike-wave discharges are not detectable. At an age of 6 months, both male and female rats show about 16–20 discharges per hour, with an average duration of about 5 s. This amounts to several hundred discharges per day (Coenen and van Luijtelaar, 1987).

Characteristics in the behaviour of WAG/Rij rats have been studied extensively and are quite similar to those of outbred Wistar rats with which they have been compared. Typical features of WAG/Rij rats are a short latency to emerge from the home cage into familiar and novel environments; low open-field defecation and high open-field ambulation; a low apomorphine-induced gnawing score; a high running-wheel activity; nondistinctive sleep percentages; good two-way, active shock-avoidance acquisition; and only slightly deficient working, albeit normal reference, memory scores in two spatial memory tasks (de Bruin et al., 2001; Festing and Bender, 1984; Harrington, 1972; van Luijtelaar and Coenen, 1988; van Luijtelaar et al., 1989).

### 1.5 Theoretical considerations: classical concepts of absence Epilepsy

The highly synchronous appearance of SWDs in both hemispheres led to the assumption by early researchers that SWDs could arise from a central structure with widespread cortical projections that could distribute paroxysmal activity over the entire cortex. They proposed the existence of a subcortical pacemaker for SWDs (Jasper and Kershman, 1941). A few years later the ‘‘centrencephalic’’ concept was introduced (Penfield and Jasper, 1954). This ‘centrencephalic integrating system’ was thought to be located in the brain stem and diencephalon. Moreover, this system was believed to be responsible for the bilateral onset of the SWDs and the loss of consciousness. Subsequent stimulation studies in cats gave rise to the hypothesis that SWDs are likely to originate from the non-specific part of the thalamus, the intralaminar nuclei, which project diffusely to many cortical regions. The role of these nuclei in the generation of SWDs in humans remained unclear, in part because comparative anatomical studies showed that the thalamus in mammals is less developed than in humans (Ajmone-Marsan, 1965; Pollen

et al., 1963) and depth intracranial recordings were not an option. Despite these drawbacks, the ‘‘centrencephalic’’ concept was gradually transformed into a ‘‘thalamic theory’’. Direct evidence of SWDs beginning in the thalamus with 1–2 s cortical delay was obtained in patients during absence seizures using simultaneous thalamic and cortical local field potentials (Williams, 1953). To date, the ‘‘thalamic theory’’ remains valid and well accepted and, furthermore, has received recent support from modern techniques like positron emission tomography and fMRI (Prevett et al., 1995; Salek-Haddadi et al., 2003), although it can be questioned whether the temporal resolution of PET and fMRI is currently sufficient to establish temporal differences between cortical and subcortical regions. Using depth recordings in epileptic patients, Bancaud (1969, 1972) observed that the spontaneous discharges occurring during spontaneous petit mal or grand mal seizures might initially be localized to the cerebral cortex, in the vicinity of an identified lesion, particularly in the frontal lobe. This and other observations did not fit into the centrencephalic theory (Petsche, 1962). Moreover, similar attacks could be reproduced by electrical stimulation of the same cortical epileptogenic zone (Bancaud et al., 1974). Therefore, it was suggested that generalized SWDs are secondary to a diffuse focal discharge in the frontal cortex. After their cortical onset, they are rapidly propagated throughout the whole cortex through various cortico-cortical pathways (Bancaud, 1971). In addition, the bilateral synchrony during typical SWDs was not as perfect as previously believed (Lüders et al., 1980). Niedermeyer (1996) presented a new ‘‘cortical theory’’: primary generalized epilepsy is the expression of cortical pathology; generalized SWDs are generated in the mesiofrontal cortex, from where they rapidly spread to other cortical areas. The thalamus certainly participates, but only ‘‘plays second fiddle’’ in carrying out normal physiological thalamo-cortical interactions. The third theory combined thalamic and cortical processes for the initiation and maintenance of absence seizures. Gloor (1969) saw a role for the cortex in the production of these generalized discharges and proposed that a ‘‘cortico-reticular’’ mechanism was involved in their generation, using experimental data collected in the feline generalized penicillin absence epilepsy model (Gloor et al., 1990; Kostopoulos, 2000). In this model, systemic injections of penicillin, a weak GABAA receptor antagonist, caused a gradual dose-dependent transformation of spindles into absence seizures. SWDs could also appear after cortical application of penicillin, whereas an injection of penicillin in the thalamus does not have this effect. This indicates that the

epileptiformic discharges are the result of abnormal responses of the cortex and not of the thalamus (Gloor et al., 1979; Gloor and Fariello, 1988). The crucial factor responsible for SWDs here is a presumed diffuse increase in the excitability of the cortex: cortical neurons respond to the afferent thalamo-cortical volleys by producing SWDs instead of passively transferring sleep spindles. In all, this theory assumes that the mechanism responsible for the genesis of SWDs is closely linked to the thalamocortical mechanism that generates sleep spindles.

### 1.6 Recent achievements in animal models of absence epilepsy

It is well accepted that sleep spindles and SWDs have a common thalamic pacemaker in the reticular thalamic nucleus (RTN) (Kostopoulos, 2000). Due to specific membrane properties and reciprocal interactions with thalamo-cortical relay (TCR) cells, neurons in the RTN are capable of producing intrinsic rhythmic bursts, which manifest themselves in field potentials such as sleep spindles. Surgical isolation of the RTN abolished rhythmic bursting in TCR cells, but bursting was preserved in RTN neurons (Steriade et al., 1985). Steriade and coworkers (for review see Steriade, 2003) demonstrated that TCR nuclei could only exhibit spontaneous spindle oscillations (7–14 Hz) when they receive projections from the RTN. These and similar studies were mainly done in cats in vivo and in the ferret in vitro (Von Krosigk et al., 1993). Basic cellular properties of thalamic cells were described and modeled, such as the different firing modalities (tonic and bursting), the crucial role of Ca2+ currents, and the longlasting hyperpolarization and subsequent calcium spike, that control the basic rhythmicity of thalamo-cortical oscillations (Destexhe and Sejnowski, 2002).

In the last decade, genetic rodent models became the model of choice (Danober et al., 1998; van Luijtelaar et al., 2002; Crunelli and Leresche, 2002; Coenen and van Luijtelaar, 2003; Depaulis and van Luijtelaar, 2006). Outcomes of studies in Genetic Absence Epilepsy Rats from Strasbourg (GAERS; Liu et al., 1991, 1992; Marescaux et al., 1984, 1992; Avanzini et al., 2000; Aker et al., 2002) and WAG/Rij rats (Inoue et al., 1993), supported the idea that SWDs are triggered in the thalamus or, more specifically, in its lateral parts implying that cortical SWDs originate from the thalamus. Pharmacological studies showed that local injections of the $GABA_A$ agonist muscimol and a GABA transaminase inhibitor in the ventrobasal complex of the thalamus,

increases SWDs in GAERS, similar to systemic injections of GABAmimetics in GAERS and in WAG/Rij rats (Vergnes et al., 1984; Danober et al., 1998; Coenen and van Luijtelaar, 2003; Bouwman et al., 2004). Interestingly, local injections of muscimol in the RTN decreased SWDs (Liu et al., 1991), most likely by preventing local oscillatory activity (Danober et al., 1998). The results of these pharmacological studies point towards a role of thalamic GABAergic neurons in the control of SWDs and the differential role of two regions of the thalamus in their occurrence. Other evidence was based on lesion studies: SWDs in GAERS were suppressed after large electrolytic lesions of the lateral thalamus (Vergnes and Marescaux, 1992) and also after more restricted chemical lesions of the RTN (Avanzini et al., 1992, 1993). The same observations were made in WAG/Rij rats: SWDs were completely abolished after ibotenic lesions of large parts of the thalamus including the RTN (Meeren, 2002). However, rostral and caudal poles of the RTN seemed to antagonize each other in the sustaining of SWDs: Lesions in the rostral part of the RTN decreased the number of SWDs, but if lesions were restricted to the caudal and middle parts of the RTN, the incidence was unchanged or even increased (Meeren, 2002;van Luijtelaar and Welting, 2001). Most likely, there exists an antagonistic relationship between the rostral and caudal RTN; the caudal region of the RTN may inhibit the activity of a hypothetical pacemaker of SWDs located in the rostral part. This pacemaker may be disinhibited after lesions of the caudal RTN, which would explain the increase in SWDs. Nevertheless, the findings of all these studies corroborate the cortico-reticular theory that the pacemaker is located in the lateral thalamus. Although it is currently believed that SWDs are initiated in the RTN, the synaptic organization of the rostral pole of the RTN of the non-epileptic ACI rat (Agouti Copenhagen Irish, commonly used as a control strain since these rats showed no or at least very few SWDs in a comparative strain study; Inoue et al., 1990) appears to be similar to that of the epileptic WAG/Rij rat, as studied with electron microscopy (van de Bovenkamp-Janssen et al., 2004a), while GAERS also failed to show any essential structural alterations in RTN neurons compared to non-epileptic rats, no neuronal loss occurred in the RTN of epileptic animals (Sabers et al.,1996). It needs to be remarked that some physiological and anatomical features in rodents' brains are crucially different from the feline brain and earlier theories were exclusively based on neurophysiological studies in cats.

This difference might provide unique particularities to the rodent models of epilepsy, or at least account for some of its differences. First, SWDs in cats occur with frequencies from 3 to 4.5 Hz, about the same as in humans, but rats have 7–11 Hz as the intraspike frequency in a train of SWDs (Drinkenburg et al., 1993; Midzianovskaia et al., 2001; Bosnyakova et al., 2006). Second, in cats GABAergic inhibitory interneurons are present throughout the thalamus, including its relay nuclei, which receive an additional inhibitory control from RTN cells (Jones, 1985). In rats, inhibitory interneurons are absent in almost all thalamic relay nuclei (Jones, 1985), except the lateral geniculate nucleus (LGN, Ohara et al., 1983); moreover, the LGN itself gets more powerful monosynaptic inhibitory afferents from the RTN then any other part of the rats' thalamus (Ohara et al., 1980, 1983). Therefore, intrinsic inhibition is absent in the largest part of the thalamus in rats and the vast majority of thalamic nuclei receive only external inhibitory inputs from the RTN. This may significantly influence the oscillatory activity of thalamic neurons and the properties of thalamo-cortical networks.

Finally, the relative contributions of the cortex and thalamus and their exact mechanisms are still a matter of debate, and much of the controversies concerning the exact mechanisms can be ascribed to the usage of different experimental models (Blumenfeld, 2005). A putative disadvantage of the penicillin model is that the role of the cortex may be overemphasized because this model considers pharmacologically induced SWDs in cats, in which the seizures have slightly different mechanisms compared to spontaneous occurring SWDs in genetic rat models (Meeren, 2002). The study of mechanisms of the idiopathic types of epilepsy such as childhood absence epilepsy, however, may benefit from all the animal models that are nowadays available, including the genetic ones.

### 1.7 The role of the cortex in generalized absence epilepsy revisited

In their scheme for the generation of SWDs, the authors of the cortical theory did not assume a single focus or a focal area (Bancaud, 1969, 1972; Niedermeyer, 1996) nor did the authors of the cortico-reticular theory, who assumed a diffuse and global role of the cortex in the transformation of sleep spindles (Gloor, 1969; Gloor et al.,1990). Regarding the mechanisms of SWDs, both theories considered the cortex in general and did not address the specific local neurophysiological properties that could make one

cortical region more favourable for epileptogenesis than another, as is done in cases of focal epilepsies. Some studies in GAERS and WAG/Rij rats suggested a global role of the cortex in absence epilepsy after cortical deactivation was demonstrated by the spreading depression technique (unilateral diffusion of KCl resulted in immediate abolishment of SWDs not only in the injected cortex but also in the ipsilateral thalamus; Vergnes and Marescaux, 1992; Meeren, 2002). The same effect was found in cats with penicillin-induced SWDs during cortical spreading depression (Avoli and Gloor, 1981; Gloor et al., 1990). This observation was used as an argument for the corticoreticular theory that the cortex is a key element for generation of SWDs. The idea that an intact cortex interconnected in a thalamo-cortical network is a prerequisite for the occurrence of SWDs is also supported by the fact that surgical removal of the cortex abolishes SWDs, cortical slices do not show spontaneous, widely synchronized bursting activity, and that only in a thalamocortical slice preparation some stimulus-elicited oscillatory activity can be found if reciprocal thalamo-cortical connectivity was present (Avoli and Gloor, 1982; Tancredi et al., 2000). The cortico-reticular theory assumes that the cortex is more easily excitable in epileptic subjects than in nonepileptic ones. Consequently, the cortex produces abnormal paroxysmal responses to normal thalamic excitation.

In such a way, thalamic sleep spindles, reaching the cortex through afferent volleys, could be transferred into SWDs (Kostopoulos, 2000). The penicillin model also showed that cortical blockade of $GABA_A$ receptors facilitates the presence of SWDs. Tolmacheva and colleagues (2004) investigated the excitability of the sensorimotor cortex for various types of afterdischarges and seizure types in WAG/Rij rats. No differences between WAG/Rij and ACI (non-epileptic control) rats were found in the seizure thresholds and afterdischarges irrespective of age, only the threshold for limbic seizures was reduced in WAG/Rij rats compared to ACI rats. Therefore, it does not seem likely that the cortex of WAG/Rij rats is in general more hyperexcitable than the cortex of nonepileptic control rats, at least in terms of thresholds of various types of epileptoform afterdischarges. Cortical excitability was also investigated in vitro. Some basic electrophysiological properties of cortical tissue in GAERS, WAG/Rij rats and in non-epileptic rats were not principally different. This mainly concerns passive cortical properties such as the complex waveform of the evoked local field potentials, the percentage of pyramidal neuron populations (intrinsically bursting and regular spiking

cells), and intrinsic membrane properties. (Luhmann et al., 1995; Avanzini et al., 1996; D'Antuono et al., 2006).

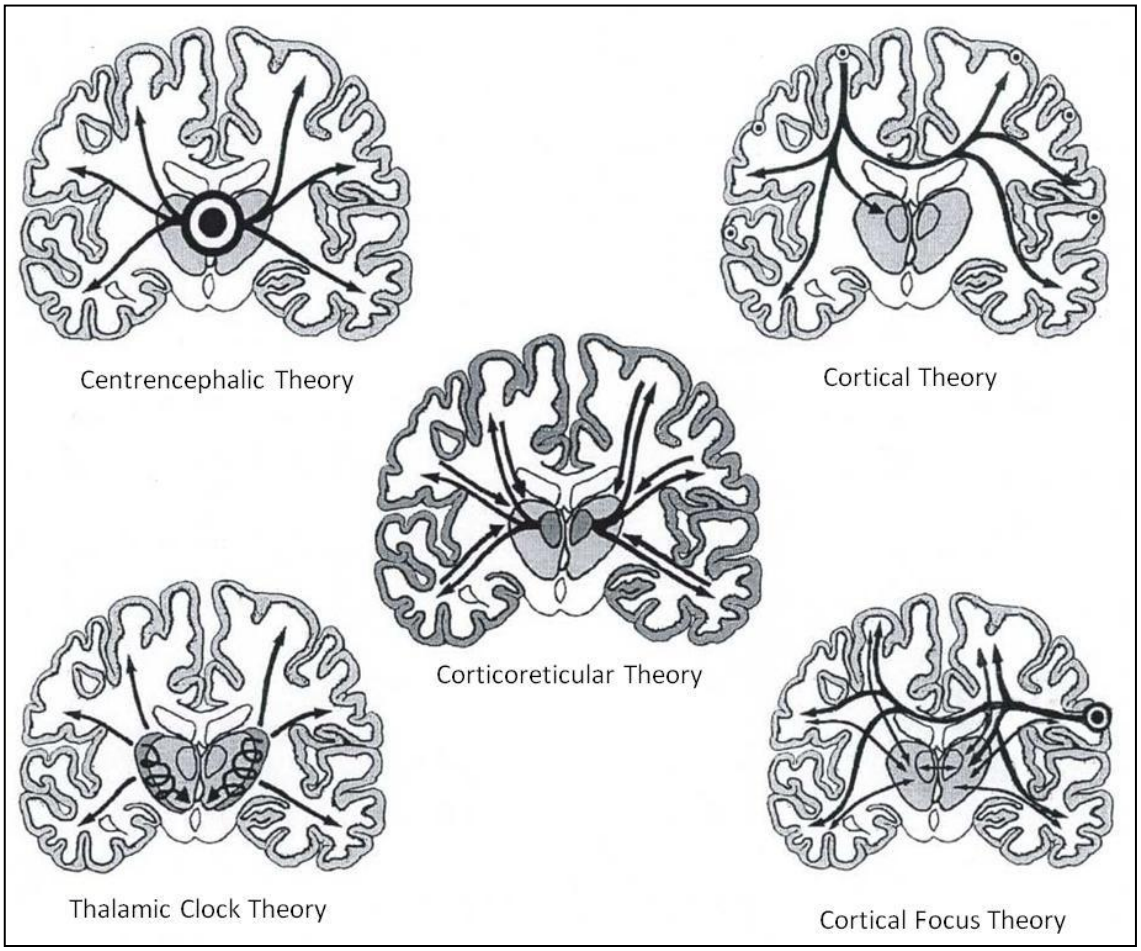


**Figure 1.1.** Schematic impression of the 5 theories on the origin of generalized absence epilepsy. On the left are the thalamic theories: the centrencephalic theory of Penfield and Jasper (1954) and the thalamic clock theory of Buzsáki (1988). On the right are the cortical theories: the cortical theory of Bancaud, Lüders and collegues and Niedermeyer (1972) and the cortical focus theory of Meeren et al (2002). In the middle is the corticoreticular theory of Gloor (1968) (modified from Lüders et al.,1984).

## 1.8 A focal cortical theory of absence epilepsy in WAG/Rij rats

The role of the cortex in triggering SWDs became more obvious after a comprehensive study of network mechanisms responsible for the immediate onset, widespread generalization and high synchrony of SWDs (Meeren et al., 2002). Simultaneous, recorded field potentials from multiple cortical and thalamic sites were studied. The

cortico-cortical, intrathalamic, and cortico-thalamic interrelationships between these field potentials were quantified using non-linear association analysis (Pijn et al., 1989). This method included direct measurements of the strength of association (the degree of correlation) and the time delay between signals recorded at different cortical and thalamic sites. These parameters together characterized functional coupling between populations of interacting neuronal populations. Fig. 1 illustrates a generalized SWD in the WAG/Rij rat and the results of the non-linear analyses, that is, the existence of a cortical focus originating from one of the 16 electrodes in the SmI (somatosensory cortex) (it is shown in graphs at the bottom, the starting point of arrows reflects the beginning of activity at the SmI in all eleven time frames). SWDs recorded at other cortical sites consistently lagged behind this focal site, with time delays that increased with electrode distance, resulting in a mean propagation velocity of about 1.5 m/s. Intrathalamic relationships were more complex and could not account for the observed cortical propagation pattern. Functionally interconnected cortical and thalamic sites appeared to influence each other, while the direction of this bidirectional coupling could vary throughout one seizure. However, during the first five hundred milliseconds the cortical focus was consistently found to lead its thalamic counterpart. Thereafter, the cortex and thalamus were found to alternately lead and lag in an unpredictable way.

These results are incompatible with the common assumption that the thalamus acts as the primary driving source for the discharges. Instead, they indicate that a cortical focus plays a leading role in the origin of generalized SWDs characteristic of absence seizures in the rat. The large-scale synchronization characterizing bilateral synchronized SWDs appears to be mediated by the fast propagation of seizure activity from this focal site through cortico-cortical networks. Once the oscillation has been set into motion, however, the cortex and thalamus form a unified oscillatory network in which both structures drive each other. The role of the thalamus probably lies in providing a resonant circuitry to amplify and sustain the discharges (Meeren et al., 2002). It has been mentioned that the intrathalamic nuclei play a major role in synchronization and maintenance of neuronal oscillations (Seidenbecher and Pape, 2001). In light of these findings, it is proposed that the generation of bilaterally synchronous SWDs is only possible in an anatomically and functionally intact cortico-thalamic network that is in a suitable state. This most beneficial state is characterized by a light to moderate hyperpolarization of the intrinsically bursting cortical pyramidal cells and of the TCR

and the RTN cells, which makes them highly prone to produce high-frequency bursts of action potentials, as is the case during transitions from waking to sleeping, during drowsiness and light non-REM sleep, the most favorable vigilance states for the occurrence of SWDs in WAG/Rij rats (Drinkenburg et al., 1991; Coenen et al., 1991; Coenen, 1995). The initial event was the generation of an epileptic spike at the site of the cortical focus. Fig. 2 illustrates the pooled results of 8 WAG/Rij rats. In each of the 8 rats investigated, the focal zone was found to occupy a small (2-5 mm) zone in the projective area of the snout and vibrissae, as was established with functional mapping using evoked potentials. SWDs were initiated in a distinct (perioral) area of the somatosensory cortex, SmI (Meeren et al., 2002). Also, Steriade (2006) concluded that in a feline seizure model with SWDs, the latter are generated in the neocortex and thalamic involvement was instigated by cortical evoked excitation of mainly RTN neurons.

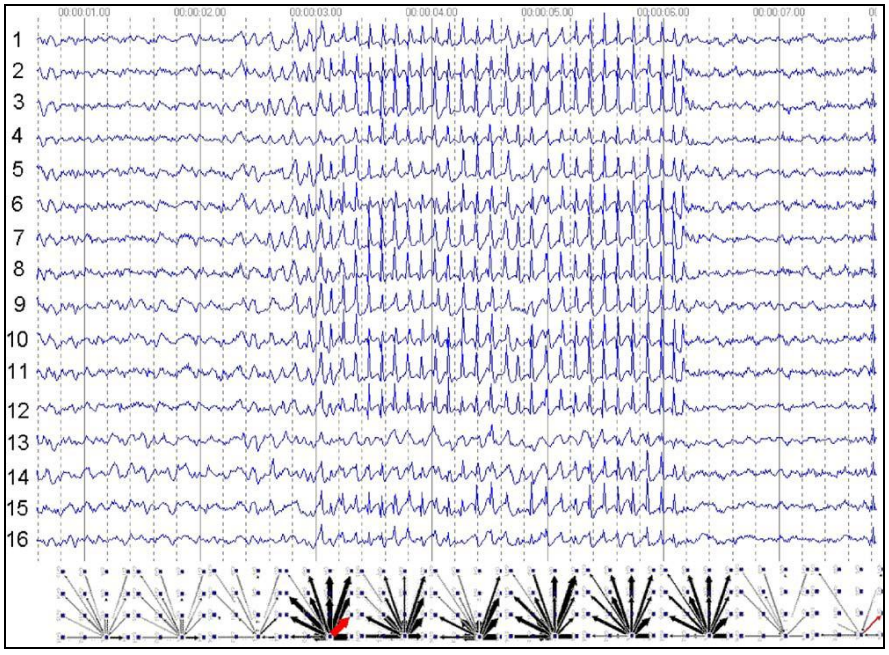


**Fig. 1.2**. A generalized SWD recorded from the lateral convexity of the neocortex of a WAG/Rij rat. Results of the non-linear association analysis are presented underneath; calculations are done on EEG epochs of 500 ms. The thickness of the arrows represents the strength of the association, while the arrowheads point in the direction of the lagging site. The results of the analysis consistently suggest a cortical focus located in the projection area of the upper lip. SWDs recorded at other cortical sites lag behind the focal site with time delays that increase with electrode distance (adapted from Meeren et al., 2002).

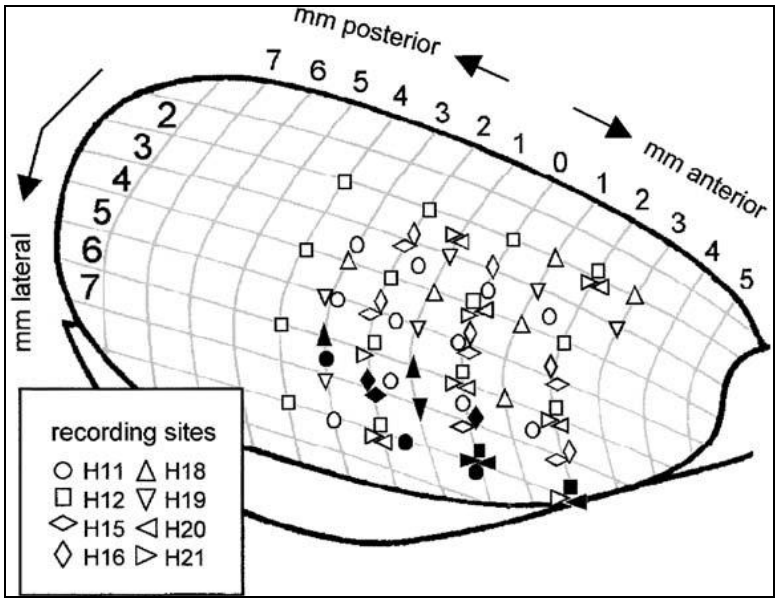


**Fig. 1.3.** Pooled data from eight rats, in all animals leading sites of SWDs, filled symbols, located in the somatosensory cortex. Open symbols represent lagging sites. The numbers represent the coordinates of the cortical surface in mm with zero point at the Bregma. Leading sites of SWDs occupy an area with the anterior-posterior coordinates from 2 (anterior to the bregma) to 3 (posterior to the bregma) mm, extending laterally from 6 to 8mm (adapted from Meeren et al., 2002)

## 1.9 Experimental support of the focal cortical theory: local Deactivation

The role of the SmI in the incidence of SWDs was examined using unilateral microinjections (1 ml) of 2% lidocaine into the vibrissal area of SmI (Sitnikova and van Luijtelaar, 2004). As is known, lidocaine temporarily blocks sodium channels and reversibly prevents neuronal activity (Malpeli and Schiller, 1979; Tehovnik and Sommer, 1997). It was hypothesized that blocking the neural activity in the SmI would unilaterally eliminate the cortical trigger of SWDs, which might result in a temporary decrease in their number. This hypothesis was tested in WAG/Rij rats. Animals were equipped with four epidural recording electrodes: bilaterally over the frontal cortex, unilaterally in the occipital area, and in the SmI adjacent to the injected site. As a control, an equal amount of saline was injected in the same area. A decrease in the number of SWDs emerged immediately after injection of 2% lidocaine as compared to saline. The difference between lidocaine and saline treated animals gradually diminished within two hours after injection. These results demonstrate that pharmacological deactivation of the driving cortical source caused a temporary reduction in the frequency of SWDs, which was observed at all recording sites

suggesting that deactivation of a certain cortical area is capable of decreasing generalized spike-wave activity throughout the entire cortex. Taken together, our results imply a crucial role of the vibrissae projecting area of the neocortex in the process of initiating SWDs. A bilateral blockade is much more effective than an unilateral one, at least as implied by the results of a preliminary pharmacological study: bilateral local injections in the peri-oral region of the SmI of the sodium channel blocker phenytoin in WAG/Rij rats and GAERS showed an almost complete abolishment of SWDs, while systemic administration of the drug increased SWDs. An earlier study was performed in GAERS: the anti-absence drug ethosuximide was bilaterally injected at multiple cortical and thalamic loci. The incidence of SWDs was strongly diminished if ethosuximide was injected in the SmI, and not or much less when injected in other cortical areas or in thalamic sites (e.g. the RTN or ventral basal thalamic complex). Therefore, treatment within thalamic target nuclei is insufficient for ethosuximide to have the full anti-absence effect; instead, the action of this agent may reside exclusively, or least primarily, in the cortex (Manning et al., 2003, 2004).

The outcome of these studies demonstrated that the WAG/Rij rats are not unique in the existence and location of the focal cortical origin of SWDs. In a combined EEG, in situ hybridization and immunohistochemical study in WAG/Rij rats, it was found that some types of sodium channels (Nav1.1 and Nav1.6) were up regulated and over expressed selectively at ML +6mm in the transverse plane at bregma (Klein et al., 2004). This region of the cortex approximately matches the electrophysiologically determined region of seizure onset within the perioral area of the SmI (Meeren et al., 2002). The upregulation was age dependent (only in 5–6 months old rats, not in younger ones), and this corresponds with the age-dependent increase in SWDs. The findings of this very elegant study clearly show that the age-dependent increase in SWDs is closely related to the age-dependent upregulation of certain types of sodium channels in the superficial layers of the perioral area of the somatosensory cortex only.

Neurophysiological studies showed functional differences in excitability in the somatosensory cortex between WAG/Rij rats and non-epileptic controls. An NMDAsensitive late EPSP that led to action potential discharges was found in 44% of regular bursting cells in the neocortical deep layers of WAG/Rij rats, and only in 8% of the cells in control rats in vitro (D'Antuono et al., 2006). Inherent properties of hyperpolarisation-activated currents of pyramidal neurons (layers II–III) in the

somatosensory cortex of WAG/Rij rats differed in this area from those of two other rat strains (Wistar and ACI), and this modification of the physiological properties of neurons was accompanied by a reduced protein expression of subunits HCN1 (Strauss et al., 2004). It was proposed that the above-mentioned changes increase excitability especially in the perioral region of the SmI and thus facilitate the initiation of SWDs (Strauss et al., 2004). It is not clear however, whether these differences between strains are found exclusively in the perioral region of the somatosensory cortex or if other cortical regions differ between the epileptic and control rats. Therefore, it cannot be established that the perioral region of genetic epileptic rats is unique in the sense that only this region is hyperexcitable. High-level impairment of the inhibitory processes was found in the frontal cortex of WAG/Rij rats in vivo when compared to three other rat strains (ACI, APO-SUS and APO-UNSUS) in a paired pulse inhibition paradigm (sensory gating) while recording auditory evoked potentials (De Bruin et al., 2001), suggesting functional inhibitory disturbances in the neocortex of WAG/Rij rats. A functional change in the BOLD (blood-oxygen-leveldependent) signal during SWDs was found in fully conscious WAG/Rij rats. Significant increases in bold responses were found in widespread thalamic areas and the neocortex, including the SmI (Tenney et al., 2004). Other BOLD effects from functional MRI (fMRI) measurements (7 T) were measured in WAG/Rij rats under fentanyl/haloperidol anesthesia in combination with simultaneous recordings of field potentials (Nersesyan et al., 2004a, b). It was shown that spontaneous SWDs intensively involve the somatosensory area in addition to the thalamus and the electrical activity was accompanied by increased oxygen needs.

## 1.10 Morpho-functional substrates of absence epilepsy in WAG/Rij rats

### 1.10.1Cytoarchitectural abnormalities of the neocortex

It is a common belief that typical absence epilepsy is a purely ‘‘functional’’ disease since no structural lesion of any kind has ever been identified (Berkovic et al., 1987; Niedermeyer, 1996). An increased number of dystrophic neurons were found in neocortex and the subcortical white matter of the frontal lobe in patients with absence epilepsy (Meencke, 1989). In animal models of absence epilepsy, the cellular structure of cortical tissue appears to have entirely escaped consideration. Within the framework

of the focal theory of absence seizures (Meeren et al., 2002), Karpova and co-workers examined the cytoarchitecture of the anterior part of the neocortex in WAG/Rij rats, paying attention to the frontal (motor) region and to the parietal cortex, including the perioral region of the SmI (Karpova et al., 2005). The cellular composition and geometry of dendrite trees were established with the Golgi-staining technique and this was followed by qualitative and quantitative morphometric analysis. Typical for both the SmI and motor cortex of WAG/Rij rats was a disorder in the distribution of pyramidal cells in the superficial cortical layers (I–III). Apical dendrites of superficial pyramidal cells were often split in two branches, declined and went in non-perpendicular directions (Fig. 5). Quantitative morphometric measurements of dendrites such as the total length of dendrites, mean length of a dendritic segment and the size of the dendritic arbor, were increased when data from within and outside the epileptic area were compared, indicating that the pattern of dendritic arborization is abnormal in the epileptic zone in WAG/Rij rats. Disturbances in dendritic trees, a receptive part of pyramidal neurons, may cause impairment in communication between individual neurons. As mentioned, the differences were found in the superficial pyramidal cells, which, owing to long-range projections to remote cortical regions, may synchronize intrinsic cortical oscillations (Gray and McCormick, 1996). Therefore, the perioral area of SmI in WAG/Rij rats (the plausible trigger site of SWD) may express abnormal associations with other cortical areas that may facilitate synchronization and propagation of SWDs.

Age-dependent changes in the cytoarchitecture of cortical neurons may facilitate absence epilepsy. In all rodent models of absence epilepsy, SWDs appear at the age of 2–3 months and gradually increase with age (e.g. Coenen and van Luijtelaar, 1987; Willoughby and Mackenzie, 1992; Danober et al., 1998; Marescaux et al., 1992; Snead, 1992; Schridde and van Luijtelaar, 2005), which could be due to aging processes. Aging has an effect on cytomorphometric parameters of neuronal and glial populations in the SmI of the limbs and in the frontal cortex in Wistar rats (Peinado et al., 1993, 1997). Using serial sections stained with cresyl-fast-violet and quantitative morphometric techniques, the cellular composure found in younger (4–6 months old) rats was compared to that in older (30–32 months old) subjects. Cortical volume and neuronal density did not change with age, while glial density was significantly increased in older rats (mean for all layers 17%). Also, cytometric parameters of neurons in layer II–IV

altered with age: the shape of neurons was changed (major/minor diameter ratio was decreased) and the area of the neuronal soma was diminished. The overwhelming majority of synapses in the SmI are excitatory. The ratio between excitatory and inhibitory synapses in young adults is 4.2:1, and in older animals (32 month old) it is 4.9:1 (Poe et al., 2001). Therefore, there is a deficit in the intrinsic inhibitory circuitry of the aging neocortex that may contribute to a hyperexcitable state in the SmI and lead to absence seizures. Intracortical inhibition plays an important role in absence epilepsy, and genetic factors might influence this process of agerelated inhibitory impairment. In the following section more properties of the GABAergic system in the brain of WAG/Rij rats will be discussed.

### 1.10.2 Impairment of the Gabaergic system: immonocytochemistry and neurophysiology

It is already known for more than 10 years that synaptic network properties in the neocortex of WAG/Rij rats are impaired in comparison to non-epileptic Wistar controls. More precisely, the efficiency of GABAergic inhibition (as measured with intracellular recordings) is considerably reduced in the fronto-parietal cortical areas (Luhmann et al., 1995). As is known, inhibitory GABAergic interneurons form 20% to 30% of the neocortical population; their axons are relatively short and rarely spread further than 0.3mm (Peters and Jones, 1984; Markram et al., 2004). Inhibitory interneurons are subdivided into several classes: large, small and nested basket cells, chandelier cells, and double bouquet cells (for review see Markram et al., 2004). About 50% of all inhibitory interneurons are basket cells. They effectively control the firing activity of target cells (pyramidal and other interneurons): they synchronize the activity in neuronal networks. Basket cells typically express two calcium-binding proteins, parvalbumin (PV) and calbindin. PV is co-expressed with GABA in 90% of the GABAergic neurons (Miettinen et al., 1996; Celio, 1986), and PV-immunostaining is an appropriate way to mark basket cells (Kawaguchi and Kubota, 1997). This technique has been recently used in WAG/Rij rats to study the distribution of GABAergic neurons over various brain regions. It was suggested that an increase in cortical excitability in WAG/Rij rats and a low efficacy of the GABAergic inhibitory system could be the result of a smaller

amount of inhibitory neurons or from the impairment of metabolism of GABA in GABAergic neurons. The number of PV-immunopositive cells was quantified in various brain structures of WAG/Rij rats and compared with that in non-epileptic control ACI rats. It was found that some brain regions are much more strongly stained than others, like the molecular hippocampal layers and the thalamic nuclei, in agreement with data from, e.g. Houser et al. (1980). Both WAG/Rij and (non-epileptic control rats) ACI rats showed structures or even large cortical regions that hardly contained PVimmunoreactive cells. These cortical regions were not devoid of neurons but they simply could not be stained with the anti-PV serum. Apparently, these cells do not contain enough PV to become immunopositive. WAG/Rij rats showed a tendency to have more unstained regions than ACI rats but this difference was not statistically significant and no specific cortical area was consistently unstained in each WAG/Rij rat examined, demonstrating that there are individual differences in the affected regions. Quantification of PV-positive cells showed clear differences in the parietal (Par1) and in the forelimb area of the somatosensory cortex (FL), where ACI rats showed about two times as many PV-positive cells as WAG/Rij rats. Par1 and FL are parts of the somatosensory cortex, and Par1 contains the perioral projections. The lack of PV in these regions may destabilize intraneuronal Ca2+ homeostatic processes such as excitability, intracellular signaling and neurotransmitter release. Considering the co-localization of PV with GAD and GABA, it is assumed that the cortex contains areas with a lesser amount or even a lack of GABAergic cells in both strains (WAG/Rij and ACI). Probably, in WAG/Rij rats PV-immunoreactive (GABAergic) neurons in the somatosensory cortex and olfactory tubercle contain less PV or PV could even be absent, which would cause local cortical alterations of inhibition. A neurophysiological study aimed to establish whether differences in excitability or inhibition could underlie the presence of a focal area. Local field potentials were investigated in coronal in vitro brain slices containing Par1 and FL of the somatosensory cortex of 6-month-old WAG/Rij rats and age-matched control Wistar rats (Pitra et al., 2005). Field potentials were evoked by paired electrical stimuli (20 ms interpulse interval) applied to layer V, and they were recorded in overlying sites within layer II/III. Generally, the magnitude of the response to the second stimulus of a pair is a result of interplay between short-term dynamics of monosynaptic excitatory glutamatergic transmission and disynaptic inhibitory GABAergic transmission.

The amplitudes of responses to the first pulse of a pair were not different between WAG/Rij and control rats over the wide range of stimulation intensities, suggestive of a lack of difference in excitatory transmission in activated intracortical pathways of both strains. However, in WAG/Rij rats, a significantly smaller amount of paired-pulse depression of responses was observed in Par1 (Fig. 8b). This difference was not observed in the FL area. These results are consistent with a local and selective deficit in intracortical GABAergic transmission in WAG/Rij rats. In this sense it is extremely interesting that the local application of weak or strong $GABA_A$ antagonists in normal cats (penicillin and bicuculline) promotes the development of SWDs (Kostopoulos, 2000; Steriade, 2003). The role of the GABAergic system has been more extensively investigated in GAERS than in WAG/Rij rats. The hypothesis that an abnormal cortical GABAergic activity may underlie absence seizures in GAERS was confirmed by differences between GAERS and controls in thresholds for GABA receptor antagonists and inhibitors of GABA synthesis (Vergnes et al., 2000). Moreover, it was found that GAERS are more prone to seizures elicited by cortical GABA deficiency (Brailowsky et al., 1999). However, the distribution and number of neurons immunoreactive for GABA and GAD (Spreafico et al., 1993) and expressing GAD65 and GAD67 mRNAs (Danober et al., 1998) were similar in the cerebral cortex of GAERS and in age-matched controls. Also, autoradiographic studies showed that ligands binding to $GABA_A$ receptor subtypes in the cortex were not altered in adult GAERS rat, or in other rats with spontaneous SWDs (Knight and Bowery, 1992; Spreafico et al., 1993). Immunohistochemical studies of the $GABA_A$ receptor subunits showed a moderate reduction in the intensity of immunostaining of the 2,3 subunits of the $GABA_A$ receptor, selectively in the cerebral cortex of adult GAERS rats. Interestingly, this reduction was not observed before the occurrence of absence seizures, suggesting that these differences are present only after repetition of seizures in adults (Spreafico et al., 1993). A high affinity to $GABA_B$ receptors was observed in cortical membranes prepared from adult GAERS, whereas the total number of these receptors was similar in epileptic and control strains (Mathivet et al., 1996). A combined autoradiography, in situ hybridization and immunocytochemical study of the $GABA_B$ receptor in the somatosensory cortex in GAERS showed results at variance, although a clear upregulation of $GABA_B$ receptor protein in the cortico-thalamic circuit in GAERS was found (Princivalle et al., 2003). A significant increase in the number of $GABA_B$

receptors occurs in the cortex of lethargic mice, although the affinity of these receptors appears unchanged (Hosford et al., 1992; Caddick and Hosford, 1996). Both alterations of $GABA_B$ receptor composition could account for an increase in cortical excitation through disinhibition by presynaptic autoreceptors. However, it is by all means not clear whether these differences in $GAB_A$-mimetic properties are present throughout the frontal cortex or mainly in the perioral region of the somatosensory cortex, or whether they are the cause of the discharges or caused by the discharges. It is also not clear whether the WAG/Rij rats and GAERS share the same deficits in the GABAergic system since comparative studies are lacking. Anyway, a deficit in the GABAergic system may have two different consequences: on the one hand, the impairment in inhibition may cause hyperexcitation of intracortical microcircuits, as was suggested for the feline penicillin model (Gloor, 1979). Then, excitatory pyramidal cells may start producing paroxysmal bursts and cause absence seizures. On the other hand, inhibitory deficits may decrease synchrony within the cortex because a sufficient amount of inhibition is needed for the synchronization of pyramidal cell bursting activity. How and in which way a reduced number of GABAergic cells available for synchronizing the burst firing of pyramidal cells contribute to more SWDs when rats are getting older remains to be established.

So, all this evidences suggest that inhibitory mechanisms in WAG/Rij rats are impaired in such a way that seizures more easily appear in local cortical regions (probably due to hyperexcitation from a lack of inhibition) and rapidly spread over the brain due to disinhibition of pyramidal neurons with long-range projections. This might imply that intracortical and cortico-subcortical network associations are altered in WAG/Rij rats.

### 1.10.3 Role of the Glutamatergic system in absence epilepsy

Burst firing between reciprocally interconnected glutamatergic thalamic relay neurons in the ventral basal thalamus and neocortical pyramidal neurons is synchronized by GABAergic neurons in the nucleus reticularis thalamic (NRT) (Steriade et al., 1993; Oh et al.,1995; Cox et al., 1997; Kim et al., 1997; McCormick and Bal, 1997). Glutamatergic thalamic relay neurons in fact send projections to cortex, and layer 6 of cortex sends reciprocal glutamatergic projections back to the associated thalamic nucleus (Guillery, 1969; Montero and Singer, 1984). Both of these projections pass

through the NRT where emitting glutamatergic collaterals within the GABAergic reticular neurons (Steriade and Deschenes, 1984; Pinault et al., 1995a,b). Glutamatergic signaling occurs through both iGluRs and mGluRs within the NRT and each of the dorsal glutamatergic thalamic relay nuclei (Bal et al., 1995a; Godwin et al., 1996b; McCormick and von Krosigk, 1992; Salt and Eaton, 1996; Turner and Salt, 1998).

The NRT-driven synchronization that drives the phasic oscillatory activity within this circuitry generates normal rhythms, such as sleep spindles, and pathological phenomena, such as bilaterally SWDs, that characterize generalized absence seizures (Snead, 1995; McCormick and Bal, 1997; Danober et al., 1998; Snead et al., 1999). Perturbations in the presynaptic release of glutamate and GABA within thalamocortical circuitry have been demonstrated in several animal models of absence seizures (Banerjee and Snead, 1995; Lin et al., 1995; Richards et al., 1995). Vigabatrin, a GABA transaminase inhibitor that increases the levels of endogenous GABA, is also known to enhance spike-wave discharges (Bouwman et al., 2003). Cortical synapses in both relay nuclei and the TRN show strong frequency-dependent facilitation (Alexander and Godwin, 2005; Alexander et al., 2006;Turner and Salt, 1998; Granseth et al., 2002). GABAergic thalamic reticular neurons project only to other thalamic reticular neurons and to their associated relay nuclei (Cucchiaro et al., 1991; Wang et al., 2001). GABAergic TRN cells activate chloride channel-associated $GABA_A$ receptors and G-protein coupled $GABA_B$ receptors within the relay nuclei to which the TRN cells project (Sanchez-Vives and McCormick, 1997). According to the cortical focus theory, cortical hyperexcitation initiates 3Hz SWD activity patterns in part by driving TRN synchronization of activity within the thalamus, which contributes to the generalization of the seizure to cortex. Intracortical circuitry in layers 2/3 and 5 are also proposed to contribute to the initiation and generalization of seizures.

The release of glutamate and GABA in thalamocortical circuitry is modulated by presynaptic metabotropic glutamate receptors (mGluRs) (East et al., 1995; Salt et al., 1996; Cochilla and Alford, 1998; Schaffhauser et al., 1998), giving rise to the hypothesis that mGluRs also may play a role in the pathogenesis of absence seizures. The eight mGluR subtypes (mGluR1–mGluR8) have been classified into three groups on the basis of sequence homology, signal transduction mechanisms, and pharmacological profiles (Nakanishi, 1994; Pin and Duvoisin, 1995; Conn and Pin, 1997). Activation of group III mGluRs inhibits the release of glutamate and GABA

from nerve terminals (East et al., 1995; Pin and Duvoisin, 1995; Neugebauer et al., 1997; Schaffhauser et al., 1998). This subgroup of mGluRs is activated selectively by the glutamate analog L-amino-4-hosphonobutyrate (L-AP4). Among the group III mGluRs ultrastructural studies using mGluR4-specific antibodies consistently have shown a presynaptic localization for this receptor (Kinoshita et al., 1996; Shigemoto et al., 1997; Bradley et al., 1999). mGluR4 is highly expressed in the rodent (Thomsen and Hampson, 1999) and human thalamus (Makoff et al., 1996). The presence of mGluR4 mRNA in the thalamic relay neurons (Ohishi et al., 1995) indicates that the receptor protein is expressed on the terminals of these neurons, which make synaptic contacts with neocortical pyramidal neurons and the GABAergic neurons in the NRT.

### 1.11 Perioral area of SmI as a generator of intrinsic oscillations

Meeren et al. (2002) suggested that there is a focal area within the somatosensory-thalamo-cortical network—the projection area of the snout, vibrissae and upper lip—from which SWDs initiate and drive the rest of the corticothalamic circuitry. The hypothesis that SWDs are initiated somewhere in the sensorimotor cortex was also proposed by Seidenbecher et al. (1998), based on work in GAERS. Before the fully developed paroxysm was evident on the gross EEG, precursor activity (‘‘embryonic’’ SW seizures) was typically recorded in cortical units and in the thalamus. The generation of SWDs was associated with spikeconcurrent, rhythmic burst-like activity in (mono-) synaptically connected regions of specific (somatosensory) thalamic areas, the SmI (layers IV/V), and the RTN. SWD-correlated activity in layers IV/V of the SmI started significantly earlier than correlated burst firing in reticular and in ventrobasal thalamic neurons (Seidenbecher et al., 1998). To understand why the projection area of the snout and vibrissae may be primarily involved in the initiation of SWDs, one should consider some peculiarities of this cortical region in rodents. The vibrissal system in rats has a very high behavioral relevance for survival and has evolved from the demands of a nocturnal environment in order to compensate for their poor vision. Interestingly, a genetic predisposition to absence epilepsy is more readily present in albino rats than in others since the incidence of SWDs is higher in albino than in hooded, brown and agouti rats (Inoue et al., 1990). Moreover, GAERS and old Wistar rats (van Luijtelaar et al., 1995), both albinos, have abundant SWDs. Perhaps; the presence of the albino gene in

albino rats deteriorated the visual system while other sensory systems (such as the vibrissal system) might be more sensitive or have a larger receptive field. The SmI in rodents not only has great functional significance, it also has an exclusive ability to generate and sustain oscillations in the 7–12 Hz band. This has to be taken into account when rats and other rodent models are used as a model of absence epilepsy. Based on this theoretical issue and our own data (Meeren et al., 2002; Sitnikova and van Luijtelaar, 2004) as well as the above-mentioned reports of others, we introduced the concept that the perioral area of SmI in rodents with absence epilepsy has specific morpho-physiological properties to initiate and sustain a spontaneous 7–12 Hz rhythm. The SmI is able to activate a corticothalamo-cortical loop and facilitate epileptogenesis in rats with a genetic predisposition to absence seizures. The cortical area where the perioral projections in SmI can be found is a central part of the trigeminal system and is intimately involved in movements of the whiskers. Rats use these rhythmic whisker movements to obtain information about their extra-personal space. This behavioral state is called ‘‘whisking twitching’’ during which robust, coherent oscillations with a frequency of 7–12 Hz take place in the vibrissal areas of the brainstem, thalamus and SmI (Nicolelis et al., 1995; Nicolelis and Fanselow, 2002). SmI initiates whisking activity by producing these oscillations, or the somatosensory rhythm (Nicolelis et al., 1995; Ahissar et al., 1997). This rhythm first appears at the cortical level as synchronous activity in the population of somatosensory neurons. It is less clear whether the somatosensory rhythm could easily be detected in the EEG or in local field potentials in rats as we never recorded it, even with monopolar microelectrodes in the SmI (Meeren et al., 2002; Sitnikova and van Luijtelaar, 2005). However, it can be observed with unit recordings. It has a cortical origin: the burst activity can be blocked by cortical lesions and by local injection of muscimol (GABAaagonist) into the vibrissal region of the SmI (Nicolelis and Fanselow, 2002). The various types of oscillations in rats, such as somatosensory rhythm, sleep spindles and SWDs have the same frequencies (7–12 Hz). Although functionally different, identical or parallel thalamo-cortical circuits may generate these different 10 Hz rhythms: it cannot be excluded that the neuronal mechanisms underlying the generation of these different rhythms are the same (Nunez, 1995). It is well established that sleep spindles and SWDs in cats and WAG/Rij rats have the same cortical profile of sources and sinks (Kostopoulos et al., 1982; Kandel and Buzsaki, 1997). The somatosensory rhythm begins during attentive

immobility and it reliably predicts the imminent onset of rhythmic whisker twitching. Others describe that the sensory mu rhythm is a state of being idle (Shaw and Liao, 2005). SWDs do not regularly occur during attentive states but, rather, when the rats are mentally and physically passive (Coenen et al., 1991; van Luijtelaar et al., 1991). Therefore, it is not very likely that the somatosensory rhythm triggers SWDs; instead, when the rats are idle, oscillations might happen more easily, and the same circuitry that is involved in the generation of a mu rhythm might be used. Whether this is indeed the case, needs to be established. However, the somatosensory rhythm shares some properties with SWDs, such as the same frequency (Nicolelis et al., 1995; Drinkenburg et al., 1993); they are initiated in the same locus of the SmI, that is, in the projection areas of the vibrissae (Nicolelis et al., 1995; Meeren et al., 2002); they show a considerable topographical overlap and widely occupy the cortical and subcortical parts of the trigeminal system, including the ventroposterior complex of the specific thalamus (Inoue et al., 1993; Semba et al., 1980; Semba and Komisaruk, 1984; Nicolelis et al., 1995); and unexpected sensory stimulation of vibrissae can terminate the ongoing ‘‘somatosensory rhythm’’ (Ahissar et al., 1997) as well as SWDs (Coenen et al., 1991). These observations imply an intimate association between SWDs and the non-paroxysmal somatosensory rhythm. It is proposed that not only in rats with the genetic predisposition to absence epilepsy, such as WAG/Rij rats (Coenen and van Luijtelaar, 2003), GAERS Danober et al., 1998), but also in many old Wistar, WKY and Sprague–Dawley (van Luijtelaar et al., 1995; Willoughby and Mackenzie, 1992) and Long Evans rats (Shaw and Liao, 2005; Polack and Charpier, 2006), normal somatosensory oscillations occurring during a less active brain state are transformed into SWDs, which could explain why so many albino rats slowly develop SWDs. During drowsiness, it is easier to trigger SWD oscillations and activate the corticothalamic network because cortical and thalamic neurons are already slightly hyperpolarized and firing in the favorable bursting mode. Wiest and Nicolelis (2003) hypothesized that in rodent strains with a genetic predisposition to absence epilepsy, 7–12 Hz rhythmic activity might undergo some transformation and give rise to SWDs, irrespective of whether it occurs during drowsiness, attentive wakefulness or during light non-REM sleep. The plasticity in neuro-molecular mechanisms (protein and enzyme synthesis, properties of ion channels and membranes, neurotransmission and neuromodulation, etc.) that might be a consequence of the genetic modifications in WAG/Rij rats (Coenen and van Luijtelaar,

2003), may alter cortical excitability and induce a decay in the efficacy of inhibition. This allows epileptic SWDs to emerge from physiological 7–12 Hz somatosensory oscillations. Neuronal mechanisms of oscillatory activity in SmI. Rhythmic activity in the neocortex occurs due to synchronous firing of the excitatory ‘‘intrinsically bursting’’ pyramidal cells and inhibitory interneurons (Fellous et al., 2001; Silva et al., 1991; Steriade, 2001). Intrinsically bursting pyramidal neurons are located in the deep cortical layers and produce rhythmic recurrent spike bursts of 5–10 Hz (Connors and Gutnick, 1990; Flint and Connors, 1996). Network interactions with local inhibitory interneurons govern synchronization of bursting activity in a population of bursting neurons (Fellous et al., 2001): when a large number of neurons start firing in synchrony, a sharp 5–10 Hz rhythm can be recorded as a field potential. The firing pattern of cortical neurons significantly influences thalamic activity, since descending corticothalamic afferents are several times more dense than thalamo-cortical ascending ones (Rouiller and Welker, 2000). The pyramidal neurons of the deep cortical layers (V and VI) send dense descending projections to various subcortical structures; therefore, cortical oscillations could easily be transferred to the thalamus and other subcortical structures (Descheˆnes et al., 1998). These descending projections provide the RTN (Steriade, 2006) with many more excitatory inputs of the AMPA-GluR4 type than the TCR cells in the ventral basal complex, stimulating the GABA-ergic RTN to fire rhythmically and to inhibit the TCR cells. The differential descending excitatory inputs to the two parts of the thalamus were confirmed with quantitative data from both electron microscopy and neurophysiological recordings (Golshani et al., 2001). The cortical inputs produce excitation and rhythmic spike-bursts in RTN neurons. Interestingly, we found more AMPA-GluR4 receptors in the rostral RTN of WAG/Rij rats than in non-epileptic age-matched control rats and in younger WAG/Rij rats with no or very few SWDs (van de Bovenkamp-Janssen et al., 2006). This suggests that the RTN does react differently in genetic epileptic rats to corticofugal inputs and thus implies that the RTN produces more excitation and bursting than in non-epileptic animals. Construction of an oscillatory loop between SmI and subcortical structures. In order to produce high-voltage regular paroxysms as SWDs, cortical and thalamic neurons form so-called closed excitatory loops where cortical neurons are excited by thalamic neurons and cortical neurons excite the thalamus (rule of reciprocity). Cortical neurons also project to other thalamic nuclei that have no direct cortical terminals.

Therefore, corticothalamic connections comply with a more general rule, the rule of parity (Descheˆnes et al., 1998). With this type of connections, excitation could spread throughout and even beyond the thalamo-cortical system, so that paroxysmal activity could be found in different and selective parts of the brain (Steriade, 2003; Blumenfeld, 2005).

### 1.12 Perioral area of the SmI as a part of an oscillatory trigeminal system

A low-amplitude tremor of the vibrissae or jaws can be observed when rats are standing still, immobile, or during a passive behavioral state (Semba et al., 1980; Semba and Komisaruk, 1984). This tremor-like whisker twitching occurred in synchrony with individual bursts of multiunit activity recorded in the ventrobasal complex of the thalamus and with ‘‘alpha’’ waves (SWDs) in the frontaloccipital EEG. In non-epileptic (and young) Long Evans rats, these rhythmic cortical EEG waves were considered as the equivalent of an idling (mu) rhythm (Shaw and Liao, 2005). The resting tremor became more severe in aged rats, and these animals often exhibited SWDs, which were also called high voltage spindles (HVS); they are however, asymmetric, there is a clear large amplitude spike and a slow wave, and the train of spikes and waves do not have the waxing and waning characteristic of spindles so therefore the name HVS is not appropriate (Shaw, 2004; Shaw and Liao, 2005). It was suggested that oscillations, which normally occur within the trigeminal vibrissae system, could be further transformed into absence-like seizures (SWDs). Considering that SWDs are initiated at the vibrissal area of the SmI, it is possible that SWDs as seen during waking (desynchronized EEG) might represent a transformed mu (somatosensory) rhythm (Sitnikova and van Luijtelaar, 2004). Even in the absence of explicit stimulation (perhaps being idle), rats emit patterns of rhythmic whisking movements with a frequency of 5–15 Hz (O’Connor et al., 2002). The organization of these stereotyped movements involves at least three oscillatory loops. A dysfunction of this powerful oscillatory machinery as the vibrissal system in rodents may easily lead to the appearance of pathological rhythms such as SWDs. Fig.1.4 shows that the thalamocortical circuit, which produces SWDs in rats, is to a certain extent part of the much larger multi-loop trigeminal system. In order to produce stable and high-

amplitude oscillations, this loop needs top-bottom, reciprocal feed-forward and feedback connections. To spread more extensively in the brain, SWDs may use pathways of the trigeminal system and in this way may also invade more remote parts of the brain, including afferent and efferent brainstem projections of the whisker pathway. This may explain why absence seizures in rodents are often accompanied with certain latency by a tremor of the vibrissal system (van Luijtelaar and Coenen, 1986; Danober et al., 1998; Buzsaki et al., 1990). This peripheral activity ultimately interacts with superior parts of the oscillatory system and controls the frequency of ongoing oscillations. Local deafferentation of the mystacial pad with xylocaine significantly decreases the frequency of SWDs in Long Evans rats (Shaw and Liao, 2005). Therefore, rhythmical vibrissal tremor during absence seizures seems to provide an essential afferent control of oscillatory activity in the network where SWDs are generated. In summary, frequency-specific peripheral afferent input from trigeminal terminals is necessary for the thalamo-cortical circuit to synchronize its activity during SWDs.

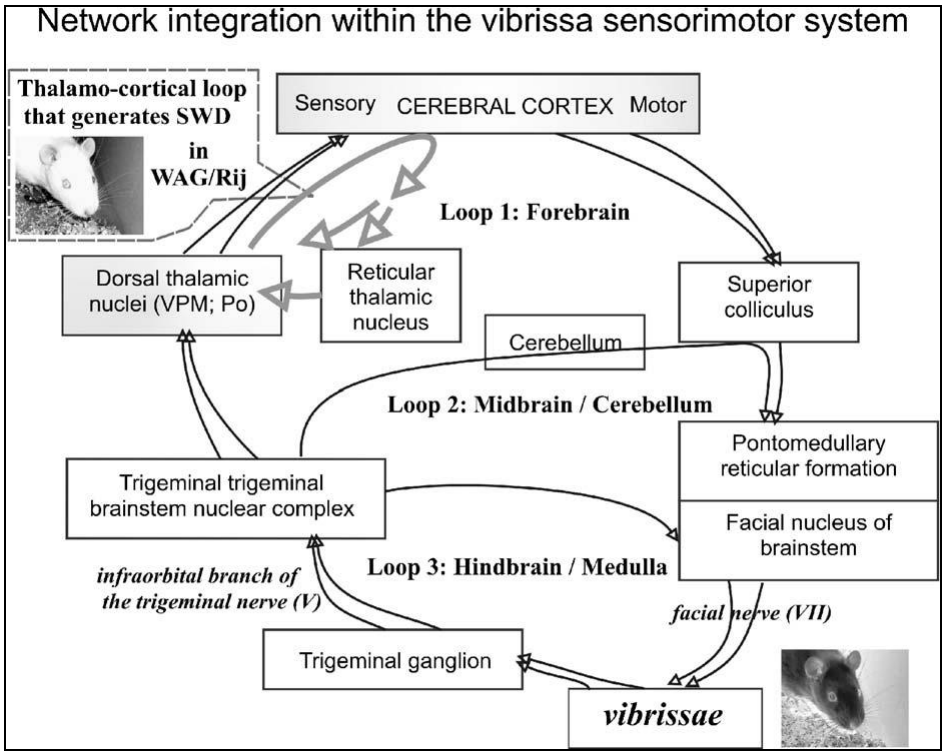


**Fig. 1.4.** The architecture of the vibrissal (trigeminal) system in rodents that involves the hindbrain, cerebellar, and cortical loops (black arrows, see Kleinfeld et al., 1999, for more details). Thalamo-cortical circuit that sustains spike-wave discharges (SWDs) in WAG/Rij rats is indicated with thick gray arrows. This circuit is nested in a forebrain loop (Loop 1), therefore, the major pathways of SWDs largely use forebrain structures of the vibrissa sensorimotor system. The diagram illustrates the major pathways of the trigeminal oscillatory system. It overlaps partly with the cortico-thalamo-cortical loop in which the SWDs are generated. (From van Luijtelaar and Sitnikova, 2006)

## 1.13 Cytokines and absence seizures

The actions of proinflammatory cytokines in the CNS are only at the beginning of being discovered; known is that their central actions include effects on the hypothalamo-pituitary-adrenal (HPA) axis, but also pyrogenic and somnogenic effects have been described as well as a modification of the peripheral immune response (Schotanus, 1995). Some cytokines have been recently shown to affect neurotransmitters, including monoamines, glutamate, GABA, and acetylcholine (ACh), to modulate the preservation of the synaptic strength at excitatory synapses, or affect the expression of various neuropeptides and neurotrophic factors in several brain regions (Rothwell and Hopkins, 1995; Vezzani and Grenata, 2005). Changes in e.g. the neurotransmitter concentrations, some second messenger systems and $Ca^{2+}$ currents induced by changes in the immune system may change the excitability of the central nervous system and alter the susceptibility of exogenous induced or genetically determined types of epilepsy (Kovacs et al., 2006).

There is also some evidence for relations between the immune system and epilepsy. Clinical studies show that the immune system may be activated or disbalanced in childhood epilepsies such as Rasmussen encephalitis (Hauf et al., 2009) and in Lennox-Gastaut syndrome (van Engelen et al., 1995). Increased concentrations of interleukin-6 (IL-6) in cerebrospinal fluid and plasma in patients after tonic-clonic seizures were found and there was also some indication of an increased concentration of IL-1 receptor antagonist (IL-1RA) (Peltola et al., 2000). Experimental studies in rats show that the administration of interleukin-1 beta (IL-1β) prolongs the duration of kainic acid–induced seizures, whereas its effects can be blocked by IL-1RA (Vezzani et al., 2000; 2002). Experimentally triggered status epilepticus with either kainic acid injections in the hippocampus or electrical stimulation increased mRNA expression for hippocampal IL-1β, TNF-α and other cytokines (Vezzani et al., 1999). TNF-α treated rats showed more prolonged epileptiformic discharges than control rats and electrical stimulation of the amygdala enhanced the level of TNF-α in serum and brain tissue (Shandra et al., 2002). In a model of status epilepticus in rats it was established that cytokines affect hyperexcitability (De Simoni et al., 2000). Kindling of the amygdala increased the expression of IL-1β and TNF-α mRNA in various brain areas including cortex, hippocampus and amygdala (Plata-Salaman et al., 2000). Recent work has implicated a

number of cytokines in seizure-related hippocampal pathology. IL-1 protects hippocampal neurons from subsequent kainic acid- induced death at the time of seizure initiation. IL-1 RA icv administration 10 min before and 10 min after systemic kainic acid injection protects neurons in all subfields of the hippocampus from damage in a dose-dependent manner (Jankowsky and Patterson, 2001). Both TNF-α and IL-1β enhanced pentylenetetrazole-induced seizures in mice (Yuhas et al., 1999). It can be concluded that cytokines including IL-1β and TNF-α are more readily expressed following seizures and that seizures can be aggravated when cytokines are added exogenously. Actually, cytokines and other growth factors can be said to affect all aspects of seizure pathology, i.e. seizure itself, neuronal death, neuronal birth, reactive gliosis and mossy fiber sprouting (Jankowsky and Patterson, 2001).

Little is known about the role of these cytokines in other, less malign types of epilepsy such as childhood absence epilepsy. The availability of well accepted genetic absence models such as Genetic Absence Epileptic Rats from Strasbourg (GAERS) and WAG/Rij rats facilitates the research towards the interplay between seizure activity and cytokines. Rats of the WAG/Rij strain are endowed with a genetically determined type of epilepsy (Coenen et al., 1992; van Luijtelaar and Sitnikova, 2006). At an age of two to three months, quite few rats show spike-wave discharges (SWD) in their electroencephalogram (EEG), at six months of age, all rats show SWD concomitant with behavioural signs such as twitching of the vibrissae, accelerated breathing together with an otherwise immobile posture (van Luijtelaar and Coenen, 1986; Coenen and van Luijtelaar, 1987). Age matched ACI rats have much less SWD than WAG/Rij rats (de Bruin et al., 2000; Schridde and van Luijtelaar, 2004) and are therefore often used as controls.

# -2-

## AIM OF THE STUDY

Absence epilepsy is the most pure form of generalized epilepsy characterized in the EEG by widespread bilaterally synchronous spike-wave discharges (SWDs) caused by thalamo-cortical oscillations. Latest Cortical Focus theory suggests a consistent cortical "focus" within the peri-oral region of the somatosensory cortex. In order to raise the evidence of a focal cortical theory, structural and functional MRI data were collected in all the cerebral areas involved in spindles generation and propagation in a genetic model of absence epilepsy *(Experiment 1)*. Four-months-old WAG/Rij rats were used as control (no SWDs) whereas nine-months-old rats (daily SWDs) were referred as experimental group. In order to exacerbate SWDs episodes, rats were treated with Vigabatrin. Moreover to provides chemical information about different brain regions in Wag/Rij rats, we performed MRS analysis for the measure of the levels of different metabolites which reflects specific cellular and biochemical processes *(Experiment 2)*.

It has become increasingly obvious during recent decades that genetic factors play a main role in the idiopathic generalized epilepsies, including absence epilepsy. In this view, gene-array analysis for cell signaling pathways involved in SWDs in different cerebral areas *(experiment 3)*, and qPCR data *(experiment 4)* were performed and correlated with EEG data.

The actions of proinflammatory cytokines in the CNS are only partially discovered. Some cytokines have been recently shown to affect neurotransmitters or are required to preserve the synaptic strength at excitatory synapses, or affect the expression of various neuropeptides and neurotrophic factors in several brain regions. Changes in the immune system may change the excitability of the CNS and alter the susceptibility of exogenous induced or genetically determined types of epilepsy. Here we investigate the role of two cytokines, IL-1β and TNF-α in WAG/Rij rats. Our hypothesis is that cerebral blood flow alterations and cytokines/chemokines release can modulate the occurrence of SWDs. Both controls and WAG/Rij rats were injected i.p. by TNF-α (2µg/kg) and IL-1β (2µg/kg) and EEG was recordered for 72h after the treatment *(experiment 5)*. Furthermore, we analyzed the blood serum by ELISA method for TNF-α and IL-1β in control and epileptic animals *(experiment 6)*.

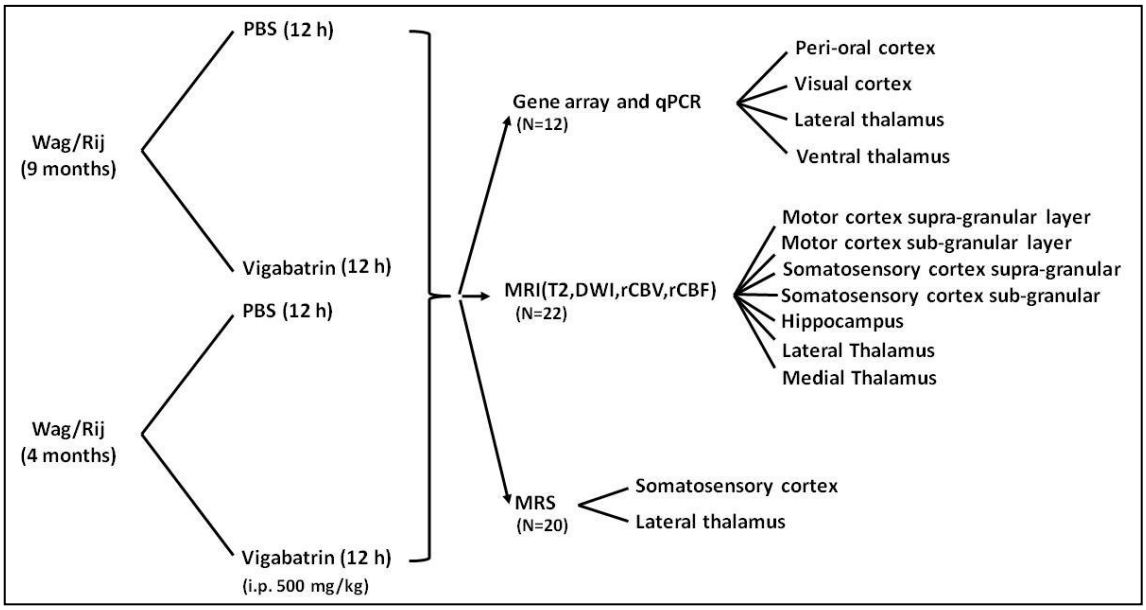


**Fig. 2.1** In the illustration is summarizing the experiment design and number of animals used for experiments 1, 2, 3 and 4.

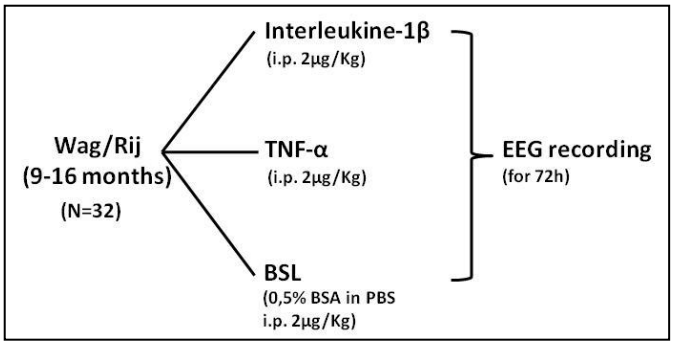


**Fig. 2.2** Schematic description of the experiment design and number of animals used for experiments 5.

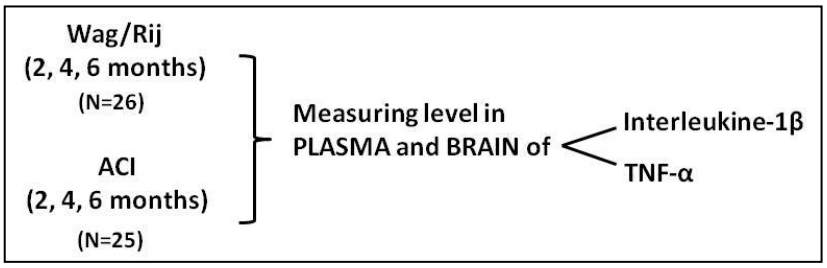


**Fig. 2.3** Summary of the experimental design and number of animals used for experiments 6.

# -3-

## EXPERIMENT 1: STRUCTURAL AND FUNCTIONAL MRI

### 3.1 INTRODUCTION TO EXPERIMENT 1

Usually most epileptic syndromes are associated with widespread structural and functional cerebral damage but patients which suffer of absence epilepsy don't seems to show brain structural damage. Magnetic resonance imaging (MRI) is primarily a medical imaging technique most commonly used in radiology to visualize the structure and function of the body. It provides detailed images of the body in any plane. MRI provides much greater contrast between the different soft tissues of the body than computed tomography (CT) does, making it especially useful in neurological (brain), musculoskeletal, cardiovascular, and oncological (cancer) imaging. It uses no ionizing radiation, but uses a powerful magnetic field to align the nuclear magnetization of (usually) hydrogen atoms in water in the body. Radiofrequency fields are used to systematically alter the alignment of this magnetization, causing the hydrogen nuclei to produce a rotating magnetic field detectable by the scanner. This signal can be manipulated by additional magnetic fields to build up enough information to construct an image of the body.

In order to raise the evidence of a focal cortical theory for absence epilepsy, we studied whether *structural* and *functional* damage or differences occurs in cerebral areas which are known more involved in absence epilepsy.

#### 3.1.1 T2 weighted and diffusion-weighted imaging (DWI) analysis

We performed T2 weighted and diffusion-weighted imaging (DWI) in 7 cerebral regions; hippocampus, ventral and medial thalamus, supra- and sub-granular motor cortex and supra- and sub granular somatosensory cortex in 9 months epileptic Wag/Rij compared to 4 months non-epileptic Wag/Rij. Diffusion-weighted imaging (DWI) is provides image contrast based on differences in diffusion of water molecules within the brain. Diffusion within the brain is determined by a variety of factors including the type of molecule under investigation, the temperature and the microenvironmental architecture in which the diffusion takes place. For example, diffusion of molecules

within the cerebrospinal fluid (CSF) is less limited than diffusion of molecules within the intra- and intercellular space. By using the appropriate magnetic resonance sequences that are sensitive for diffusion, these differences in diffusion rates can be used to produce image contrast.

The microstructural architecture as well as physiological factors influences the diffusion of water molecules within the brain. Within fiber tracts, the effective molecular diffusion is larger in the direction along the long axis of the fiber tract compared with the direction perpendicular to the fiber tract.

### 3.1.2 Regional brain volumes (rCBV) and regional brain flow (rCBF) analysis

In the same groups of animals and for the same 7 cerebral regions used for T2 and DWI analysis, we determined with functional magnetic resonance imaging, regional brain volumes (rCBV) and regional brain flow (rCBF) in order to identify areas of major brain activation during spontaneous spike-and-wave discharges (SWDs). Functional MRI (fMRI) measures signal changes in the brain that are due to changing neural activity. Increased neural activity causes an increased demand for oxygen, and the vascular system actually overcompensates for this. The CBV method requires injection of a class of MRI contrast agents that are now in human clinical trials.

## 3.2 MATERIALS AND METHODS

Male Wag/Rij rats (300-350 g) were kept under controlled environmental parameters and veterinarian control. The animals were habituated to handling for at least 2 weeks prior to the procedures employed in the present study. The experiments received authorization from the Italian Ministry of Health and conformed with the principles of the NIH Guide for the Use and Care of Laboratory Animals and the European Community Council (86/609/EEC) directive. All efforts were made to minimize the number of animals used and avoid their suffering. Two groups af animals were used, epileptic 9 months old rats treated with a single intraperitoneal (i.p.) bolus of Vigabatrin (N=5) (500 mg/kg; Yamanouchi Pharma B.V., The Netherlands) dissolved in saline (0.9%) in a volume of 2 ml/kg, or physiological saline as control (N=5). Second group, non epileptic 4 months old rats, also treated with Vigabatrin (N=6) or saline (N=6) at

the same concentration used for the first group. MRI analysis was performed 12 h after ip treatment. All the animals were analyzed with structural (T2W and DWI) and functional (rCBV and rCBF) MRI in 7 cerebral regions; hippocampus, ventral and medial thalamus, supra- and sub-granular motor cortex and supra- and sub granular somatosensory cortex.

Vigabatrin is irreversible inhibitor of gamma-aminobutyric acid transaminase (GABA-T), the enzyme responsible for the catabolism of the inhibitory neurotransmitter gamma-aminobutyric acid (GABA) in the brain (Hammond and Wilder, 1985). The doses of Vigabatrin administered were chosen based on previous reports that it produce anhancement of SWDs ( Bouwman et al., 2003). MRI experiments were performed using a Bruker Biospec Tomograph equipped with an Oxford, 33-cm-bore, horizontal magnet operating at 4.7 T. Animals were anesthetized with 1% halothane in 1 L of oxygen in air per minute (initial dose: 4% halothane); heart rate were monitored. The rats were placed into a 7.2-cm-i.d. bird cage transmitter coil. The signal was received through a 2-cm surface coil, actively decoupled from the transmitter coil, and placed directly on the animal's head.

### 3.2.1 T2 Weighted Imaging (T2) and Diffusion Weighted Imaging (DWI)

After a sagittal scout spin-echo, twenty contiguous 1-mm-thick slices were imaged starting 1 mm posterior to the olfactory bulbs using a RARE sequence with repetition time (TR) of 5117 ms, echo time (TE) of 65 ms, field of view (FOV) = 3,5×3,5 $cm^2$, number of averages (NEX) = 2, matrix size: 256×256,corresponding to an in-plane resolution of 137 x 137 $\mu m^2$. Five contiguous slices, selected region of interest, were then imaged using a diffusion-weighted spin-echo sequence, with TR of 2200 ms, TE of 30 ms, two b-values (6 and 2000 s/mm2), and matrix size 128 × 64 for apparent diffusion coefficient (ADC) maps and a multiecho spin-echo sequence with 10 echoes, TR of 2000 ms, and TE ranging from 20 to 200 ms for quantitative T2 mapping. Images were analyzed using the software ParaVision 3.0 (Bruker Medical, Ettlingen, Germany). For DWI, the apparent diffusion coefficient (ADC) maps of water in the brain were obtained by two-point linear fit of the logarithm of images intensity versus the b factors according to the expression:

$$M(b)=M0*exp(-ADC*b).$$

Analogously,T2 maps were obtained by a least-squares nonlinear exponential fitting of the signal intensity to the expression:
$M(t)=M0*exp(-t/T2)$.

ADC and T2 values were extracted from maps using the region-of-interest (ROI) method: 5 square ROIs of 2 × 2 pixels were defined in every selected brain region.

### 3.2.2 rCBV and rCBF maps

In this experiment an USPIO particle (Sinerem®, kindly supplied by Guerbet, Aulnay-Sous-Bois, France) was used as a contrast agent. Sinerem® is constituted by an iron-oxide core of about 6 nm diameter coated by dextran (coated particle dimensions of about 20 nm) and is characterized by a blood half-time longer than 2 h in rats. Sinerem® (6 mg iron/kg) was dissolved in saline and injected in the tail vein.The same five contiguous transversal slices, used for ADC and T2 maps, were imaged using Gradient-Echo sequence before and two minutes after administration of Sinerem® with the following parameters: TR/ TE = 200/ 15 ms, flip angle = 30°, Field of view 4×4 cm2, matrix size 256×192 zero-filled at 256x256, slice thickness = 1,5 mm.

After injection of a superparamagnetic contrast agent, the T2* relaxation rate in the brain decreases (compared to the preinjection baseline) proportionally to the local CBV times a certain function of the plasma concentration f(P) of the contrast agent,

$\Delta R2^*=k \cdot f(P) \cdot CBV=K' \cdot CBV,$

where the last equation holds when the agent reaches a plateau concentration in the blood, as in the case of Sinerem. For a gradient-echo sequence with echo time TE, the following equation correlates the natural logarithm (ln) of the ratio between signal intensity (SI) before and after contrast medium ln(SI(pre)/SI(post) to CBV:

$ln(SI(pre)/SI(post)) = (TE \cdot (\Delta R2^*))=K \cdot CBV.$

This equation shows that alterations in the local CBV can be probed by MRI acquisitions and, when keeping constant the contrast agent dose and acquisition parameters, also allows a comparison of CBV values between different animals.

Maps of rCBV were obtained using the algebra tool of ParaVision. Briefly, after absolute reconstruction of images, background noise below threshold value (fixed by the ParaVision software) was cut off, as routinely done. The ln of the ratio between the SI before and after contrast medium administration (R value) was then calculated pixel by pixel and displayed. Values of rCBV were measured using ROIs.

For rCBF maps,first passage images were acquired during the arrival of the contrast agent in the brain. A snapshot flash sequence was used, with TR = 14,2 ms, TE = 10 ms, flip angle = 30°, matrix size 128×32 (zero filled at 128×128). A single slice 1,5mm thickness was acquired. The time interval among images was 0.1 sec: three images were acquired before and 97 images after the bolus administration of Sinerem.

The dynamic data were then analyzed to calculate the peak enhancement and especially the relative TTP. The latter parameter is related to mean transit time and blood flow. TTP was evaluated on the signal intensity plot as the time point of maximal signal reduction. Relative TTP was obtained as a difference between TTP and time of arrival TA: rTTP = TTP−TA, where the time of arrival is the time for contrast material to arrive in the brain.

Peak enhancements were calculated by the relation: (SImin-SIpre)/SIpre, where SImin is the signal intensity at the time of maximal signal drop and SIpre is the average signal intensity of three points before contrast administration.

## 3.3 RESULTS

### 3.3.1. T2 weighted and Diffusion-weighted maging (DWI) analysis

T2 values, calculated from multiecho spin-echo acquisitions, clearly showed the overall pattern of changes in epileptic rats versus controls ($p < 0.05$), 12 h after vigabatrine treatment, highlighting the signal decrease in older animals (characterized by an augmented number of SWDs episodes) throughout the 3 regions involved in absence seizures (the primary circuity of SWDs): Supra somatosensory cortex (SS Supra; 4m: 87.16±0.82, 9m: 83.43±0.90), Sub somatosensory cortex (SS Sub; 4m: 83.62±0.66, 9m:

81.28±0.72) and Lateral Thalamus (Lat Thal; 4m: 79,16±0.34, 9m: 76.40±0.40, Fig.3.1).

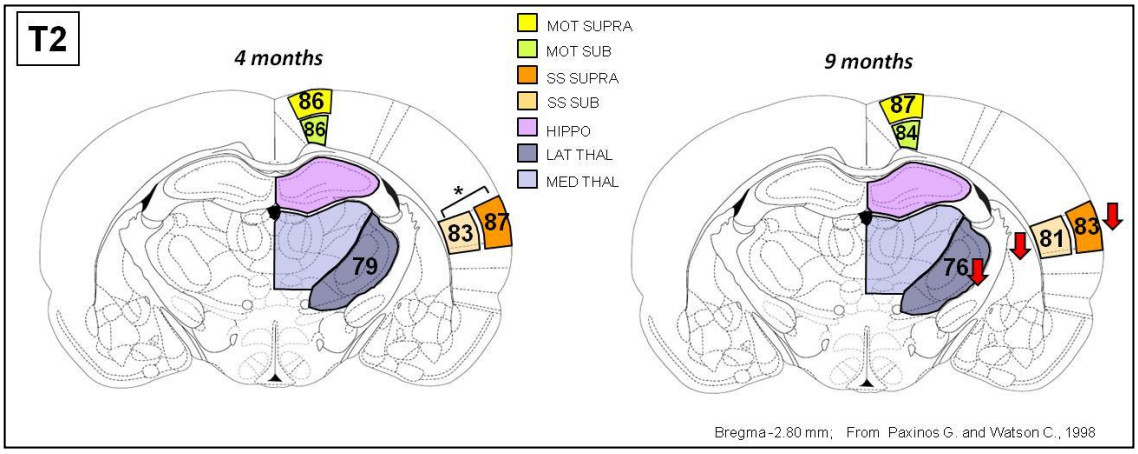


**Fig.3.1** Schematic representation of T2 values comparing epileptic nine months old versus control non epileptic four months old animals; ***= difference for multiple areas in the same group of animals ($p \leq 0.05$), Arrows indicates differences between nine versus four months old rats.

T2 values differ significantly also between SS Supra (87.16±0.82) and SS sub (83.62±0.66; $p < 0.05$) in 4 months old rats only.

Vigabatrin and Age showed an interaction in the lateral thalamus ($p<0.05$). Considering treatment effects, Vigabatrin enhances T2 in the medial thalamus (Med Thal; $p<0.05$; see Tab.3.1). **This interaction should be considered in view of the fact that the lateral thalamus contains GABAergic cells, which are well known to be vigabatrin targets (Meeren et al., 2002).**

| Regions | Age | Treatment | T2 (ms) | |
|---|---|---|---|---|
| | | | mean (ms) | st. dev. |
| Motor cortex supra-granular | 4 months | PBS | 86,93 | 2,42 |
| | | VIGABATTRIN | 86,60 | 1,69 |
| | 9 months | PBS | 88,11 | 0,50 |
| | | VIGABATTRIN | 86,11 | 0,79 |
| Motor cortex sub-granular | 4 months | PBS | 86,85 | 3,04 |
| | | VIGABATTRIN | 85,49 | 2,90 |
| | 9 months | PBS | 84,57 | 2,47 |
| | | VIGABATTRIN | 83,43 | 2,86 |
| Somatosensory -cortex supra-granular | 4 months | PBS | 87,53 | 2,71 |
| | | VIGABATTRIN | 86,79 | 3,56 |
| | 9 months | PBS | 84,25 | 1,80 |
| | | VIGABATTRIN | 82,60 | 2,80 |
| Somatosensory -cortex sub-granular | 4 months | PBS | 83,97 | 1,91 |
| | | VIGABATTRIN | 83,26 | 2,97 |
| | 9 months | PBS | 81,34 | 2,00 |
| | | VIGABATTRIN | 81,21 | 1,99 |
| Lateral Thalamus | 4 months | PBS | 78,10 | 1,02 |
| | | VIGABATTRIN | 80,21 | 2,04 |
| | 9 months | PBS | 76,67 | 0,20 |
| | | VIGABATTRIN | 76,13 | 0,86 |
| Medial Thalamus | 4 months | PBS | 86,6 | 2,04 |
| | | VIGABATTRIN | 87,80 | 7,13 |
| | 9 months | PBS | 84,37 | 1,63 |
| | | VIGABATTRIN | 90,80 | 2,39 |
| Hippocampus | 4 months | PBS | 88,51 | 1,93 |
| | | VIGABATTRIN | 89,84 | 2,07 |
| | 9 months | PBS | 88,09 | 4,24 |
| | | VIGABATTRIN | 90,48 | 6,42 |

**Tab.3.1** Summary of T2 values for all the experimental groups. Data are expressed as mean ± st. dev.

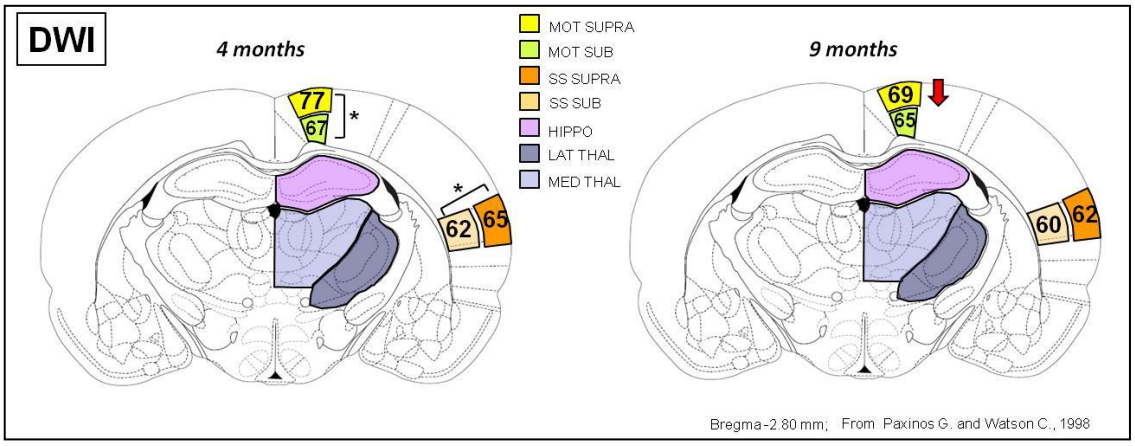


**Fig.3.2** Schematic representation of DWI results comparing epileptic 9 months old with control non epileptic 4 months old animals irrespective to treatment; *****= significative difference for different areas in the same group of animals ($p \leq 0.05$), Arrows = significative differences 9 months Vs 4 months ($p \leq 0.05$)

Diffusion-weighted images, based on the sensitization of the MRI signal to the Brownian motion of water molecules, reveal maps of brain tissue water motion, resulting in hyperintense alterations. ADC maps of brain tissue water, calculated from DWI, showed consistent changes both in cortical and subcortical data.

There is a highly significant difference ($p<0.005$) between cortical areas: sub SS ($0.62\pm0.04$) < supra SS ($0.63\pm0.04$) < sub MOT ($0.66\pm0.05$) < supra MOT ($0.74\pm0.05$). **Thus, WAG/Rij rats have higher Supra than Sub values and less in SS cortex than in Mot cortex.**

| Regions | Age | Treatment | DWI | |
|---|---|---|---|---|
| | | | mean | st. dev. |
| Motor cortex supra-granular | 4 months | PBS | 0,77 | 0,02 |
| | | VIGABATTRIN | 0,73 | 0,06 |
| | 9 months | PBS | 0,76 | 0,05 |
| | | VIGABATTRIN | 0,67 | 0,02 |
| Motor cortex sub-granular | 4 months | PBS | 0,70 | 0,03 |
| | | VIGABATTRIN | 0,70 | 0,06 |
| | 9 months | PBS | 0,65 | 0,02 |
| | | VIGABATTRIN | 0,62 | 0,03 |
| Somatosensory -cortex supra-granular | 4 months | PBS | 0,65 | 0,03 |
| | | VIGABATTRIN | 0,65 | 0,05 |
| | 9 months | PBS | 0,65 | 0,05 |
| | | VIGABATTRIN | 0,60 | 0,02 |
| Somatosensory -cortex sub-granular | 4 months | PBS | 0,63 | 0,03 |
| | | VIGABATTRIN | 0,64 | 0,02 |
| | 9 months | PBS | 0,62 | 0,04 |
| | | VIGABATTRIN | 0,58 | 0,02 |
| Lateral Thalamus | 4 months | PBS | 0,69 | 0,02 |
| | | VIGABATTRIN | 0,67 | 0,03 |
| | 9 months | PBS | 0,46 | 0,04 |
| | | VIGABATTRIN | 0,67 | 0,03 |
| Medial Thalamus | 4 months | PBS | 0,77 | 0,05 |
| | | VIGABATTRIN | 0,81 | 0,04 |
| | 9 months | PBS | 0,75 | 0,06 |
| | | VIGABATTRIN | 0,78 | 0,03 |
| Hippocampus | 4 months | PBS | 0,80 | 0,05 |
| | | VIGABATTRIN | 0,75 | 0,04 |
| | 9 months | PBS | 0,71 | 0,04 |
| | | VIGABATTRIN | 0,69 | 0,05 |

**Tab.3.2** Resume of DWI results for all the experimental groups. Data are expressed as mean ± st. dev

Considering cortical DWI values, older rats show significant ($p<0.05$) lower values ($0.65\pm0.01$) than younger rats ($0.68\pm0.01$). DWI data showed lower values after Vigabatrin treatment ($p<0.05$). Considering drug and region interaction: Vigabatrin decreased DWI values in Hippo, not in other regions. Highly significative differences

($p<0.05$) between subcortical areas have been observed in DWI values: Med Thal (0.77±0.05) > Hippo (0.74±0.06) > Lat Thal (0.67±0.05).

### 3.3.2. Regional brain volumes (rCBV) and regional brain flow (rCBF) analysis

rCBV data obtained by images acquired with gradient-echo sequence before and after USPIO administration showed consistent changes both in cortical and subcortical data. In particular, subgranular layers (4973.08±1820.83) in the motor cortex were found to differ significantly if compared to supragranular layers (6036.12±1671.92; $p< 0.05$). However, this difference was not present in the somatosensory cortex. Differences were observed also in supragranular layers between motor (6036.12±1671.92) and somatosensory cortices (5023.34±1699.35; $p<0.05$); no differences have been noticed in the respective subgranular layers (Tab. 3.3).

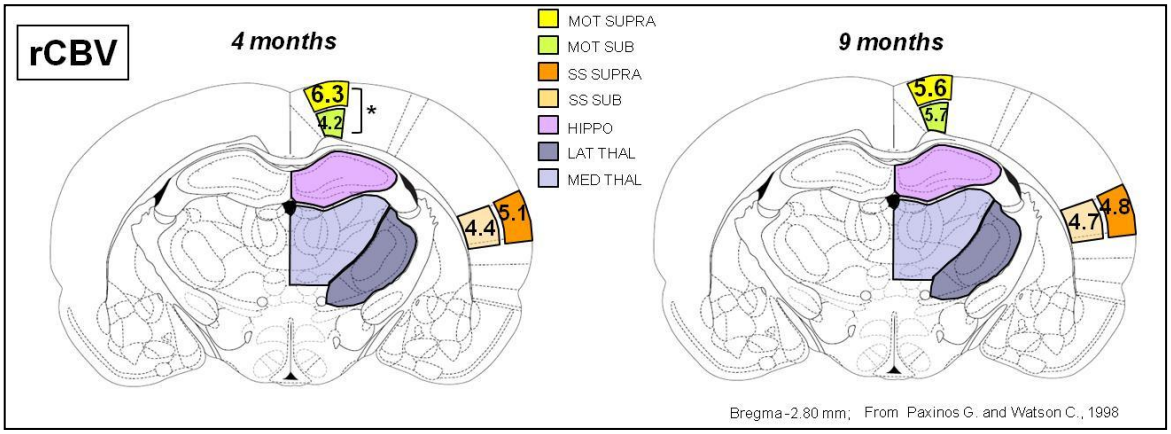


**Fig.3.3** Schematic representation of rCBV results comparing epileptic 9 months old with control non epileptic 4 months old animals irrespective to treatment; ***** = significative difference for different areas in the same group of animals ($p\leq0.05$).

A highly significant ($p<0.001$) effect of Vigabatrin was reported. Treatment reduces rCBV and, in particular, the overall decrease after Viga is more evident in motor cortex (supragranular layer; PBS: 6840.76±1147.94, Viga: 5151.02±1756.64; $p<0.05$ and subgranular layer; PBS: 6277.62±1338.61, Viga: 3538.09±1004.30; $p<0.001$) than other brain regions observed. There was no significant effect of age, nor a significant interaction between age and drug, neither between age, region, and drug. Interaction has

been observed between region and age, and region and drug (Viga vs PBS) ($p<0.05$); post-hoc tests showed that the effect of vigabatrin was restricted to the motor cortex ($p<0.05$). The post-hoc tests did not show significant age differences for the four cortical regions. **The data suggest that the habitual difference between supra- and subgranular layers had disappeared in the somatosensory cortex of WAG/Rij rats and that the effects of vigabatrin were restricted to the motor cortex.**

Referred to subcortical data, evident regional subcortical differences ($p<0.001$) between the 3 subcortical zones Hipp (6519.11±252.37) > Med thal (5513.89±260.41) > Lat thal (4281.14±269.01); There were no age effects, nor effects of Vigabatrin.

| Regions | Age | Treatment | rCBV | |
|---|---|---|---|---|
| | | | mean | st. dev. |
| Motor cortex supra-granular | 4 months | PBS | 7439,52 | 1234,56 |
| | | VIGABATTRIN | 5189,00 | 2443,32 |
| | 9 months | PBS | 6122,25 | 454,08 |
| | | VIGABATTRIN | 5113,04 | 984,71 |
| Motor cortex sub-granular | 4 months | PBS | 5203,73 | 678,06 |
| | | VIGABATTRIN | 3209,26 | 1193,84 |
| | 9 months | PBS | 7566,29 | 3151,17 |
| | | VIGABATTRIN | 3866,94 | 757,52 |
| Somatosensory -cortex supra-granular | 4 months | PBS | 5550,25 | 2618,65 |
| | | VIGABATTRIN | 4654,80 | 1908,82 |
| | 9 months | PBS | 5049,66 | 780,99 |
| | | VIGABATTRIN | 4733,26 | 959,94 |
| Somatosensory -cortex sub-granular | 4 months | PBS | 4610,51 | 811,79 |
| | | VIGABATTRIN | 4137,45 | 1188,48 |
| | 9 months | PBS | 5237,98 | 768,21 |
| | | VIGABATTRIN | 4212,40 | 870,60 |
| Lateral Thalamus | 4 months | PBS | 5025,00 | 1720,00 |
| | | VIGABATTRIN | 3504,00 | 1043,00 |
| | 9 months | PBS | 5121,00 | 924,00 |
| | | VIGABATTRIN | 3474,00 | 884,00 |
| Medial Thalamus | 4 months | PBS | 6310,00 | 1472,00 |
| | | VIGABATTRIN | 5454,00 | 867,00 |
| | 9 months | PBS | 4889,00 | 318,00 |
| | | VIGABATTRIN | 5403,00 | 1567,00 |
| Hippocampus | 4 months | PBS | 7203,00 | 1505,00 |
| | | VIGABATTRIN | 6466,00 | 951,00 |
| | 9 months | PBS | 6269,00 | 640,00 |
| | | VIGABATTRIN | 6138,00 | 1225,00 |

**Tab.3.3** Resume of rCBV results for all the experimental groups. Data are expressed as mean ± st. dev

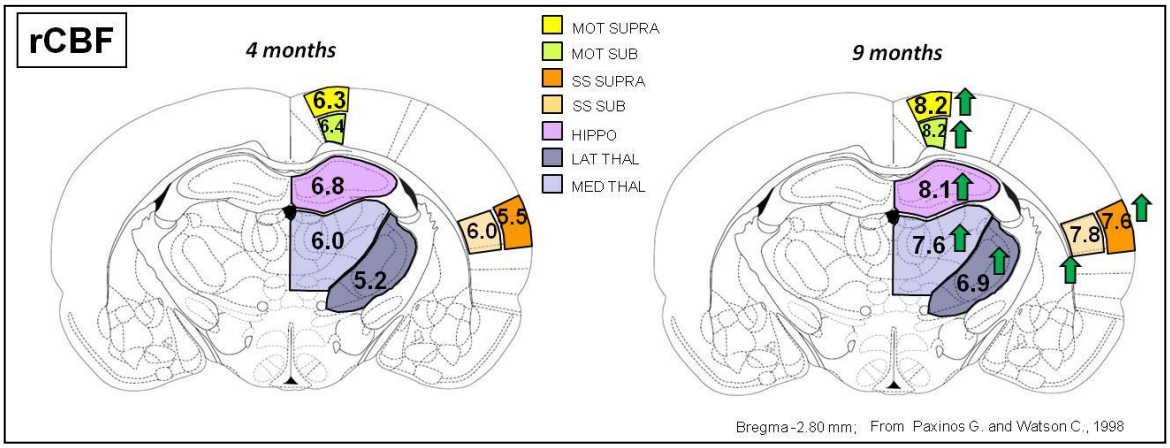


**Fig.3.4** Schematic representation of rCBF results comparing epileptic 9 months old with control non epileptic 4 months old animals irrespective to treatment; Arrows = significative differences 9 months Vs 4 months ($p \leq 0.05$).

Data of rCBF showed consistent changes both in cortical and subcortical regions.

Significant region effect ($p<0.01$) emerged analyzing cortical data: post-hoc tests showed that the values from the Supragranular layer of the somatosensory cortex (SS supra) were lower (6.47±2.18) than of the other 3 cortical regions (SS sub; 6.89±2.06) (Mot supra; 7.16±1.69) (Mot sub; 7.24±1.48). Furthermore, a significant age effect was found ($p<0.05$); 9 months old rats had higher rCBF values (7.94±0.47) than 4 months old rats (6.10±0.45; see Fig. 3.4). There were no interactions, nor a vigabatrine effect.

Furthermore, subcortical differences were found in rCBF ($p<0.001$). The highest values were found in the hippocampus (7.37±1.39), medial thalamus (6.68±1.97), and finally lateral thalamus (5.97±2.16). Significant ($p<0.05$) age effect was found; 9 months old rats had higher rCBF values (7.53±0.50) than 4 months old rats (5.98±0.47).

**Thus, rCBF data demonstrate cortical and subcortical regional differences and higher values for older animals in both cortical and subcortical regions.**

| Regions | Age | Treatment | rCBF | |
|---|---|---|---|---|
| | | | mean | st. dev. |
| Motor cortex supra-granular | 4 months | PBS | 5,62 | 1,67 |
| | | VIGABATTRIN | 7,07 | 2,13 |
| | 9 months | PBS | 8,26 | 0,31 |
| | | VIGABATTRIN | 8,17 | 0,17 |
| Motor cortex sub-granular | 4 months | PBS | 6,01 | 1,15 |
| | | VIGABATTRIN | 6,78 | 1,77 |
| | 9 months | PBS | 8,67 | 0,49 |
| | | VIGABATTRIN | 7,64 | 0,64 |
| Somatosensory -cortex supra-granular | 4 months | PBS | 4,50 | 2,54 |
| | | VIGABATTRIN | 6,69 | 2,37 |
| | 9 months | PBS | 7,73 | 0,29 |
| | | VIGABATTRIN | 7,39 | 1,06 |
| Somatosensory -cortex sub-granular | 4 months | PBS | 5,24 | 2,16 |
| | | VIGABATTRIN | 6,96 | 2,77 |
| | 9 months | PBS | 7,92 | 0,56 |
| | | VIGABATTRIN | 7,75 | 1,04 |
| Lateral Thalamus | 4 months | PBS | 4,53 | 2,70 |
| | | VIGABATTRIN | 5,85 | 2,80 |
| | 9 months | PBS | 7,26 | 0,41 |
| | | VIGABATTRIN | 6,54 | 0,66 |
| Medial Thalamus | 4 months | PBS | 4,85 | 2,20 |
| | | VIGABATTRIN | 7,11 | 2,30 |
| | 9 months | PBS | 7,38 | 0,45 |
| | | VIGABATTRIN | 7,75 | 0,62 |
| Hippocampus | 4 months | PBS | 6,11 | 1,22 |
| | | VIGABATTRIN | 7,44 | 1,71 |
| | 9 months | PBS | 8,10 | 0,30 |
| | | VIGABATTRIN | 8,18 | 0,42 |

**Tab.3.4** Summary of rCBF results for all the experimental groups. Data are expressed as mean ± st. dev

# -4-

## EXPERIMENT 2: MAGNETIC RESONANCE SPETTROSCOPY (MRS)

### 4.1 INTRODUCTION TO EXPERIMENT 2

MRS is used to measure the levels of different metabolites in body tissues. The main difference between standard MRI and MRS is that the frequency of the MR signal is used to encode different types of information. MRI uses high spatial resolution to generate anatomical images, whereas MRS provides chemical information about the tissues. Spatial location determines the frequency with MRI, whereas the tissue's chemical environment determines the frequency in MRS. Rather than images, MRS data are usually presented as line spectra, the area under each peak representing the relative concentration of nuclei detected for a given chemical species. There are many different brain metabolites that are commonly seen on the MR spectrum but in our experiment we considered 3 groups of metabolities; N-acetylaspartate (NAA) + N-acetyl-aspartyl-glutamate (NAAG), creatine (CR) + Phosphocreatine (PCr) and Glutamate (Glu) + Glutamine (Gln). Due to low signal/noise ratio we can consider only the metabolities which have SD<20%, only of this we can be sure that the value is correct.

The common way to analyze clinical spectra is to look at metabolite ratios, glycerophosphoryl-choline (GPC) + phopshorylcholine (PCh) concentration is used as internal control, so all the concentrations of others metabolities are related to GPC+PCh concentration.

Each metabolite reflects specific cellular and biochemical processes. NAA is a neuronal marker and decreases with any disease that adversely affects neuronal integrity. Creatine is an amino acid and provides a measure of energy stores. Glutamate is the predominant excitatory amino acid neurotransmitter in the brain. The observable MR metabolites provide powerful information, but unfortunately, many notable metabolites are not represented in brain MR spectra. DNA, RNA, most proteins, enzymes, and phospholipids are missing. Some key neurotransmitters, such as acetylcholine, dopamine, and serotonin, are absent. Either their concentrations are too low, or the molecules are invisible to MRS.

## 4.2 MATERIALS AND METHODS

MRS experiments were carried out using a Biospec System (Bruker Biospin) equipped with a 4.7T horizontal Oxford Magnet , 33 cm bore size. A 72-mm internal diameter bird-cage coil and a tranceiver surface soil for rat brain were used.
Water signal was suppressed using VAPOR sequence (120-150 Hz bandwidth) and spectra were acquired with a point resolved spectroscopy (PRESS) sequence for localized 1H-MRS spectroscopy with TR/TE=4000/11, number of scans from 256 to 512 and 4 dummy scans. PRESS uses a combination of magnetic fields gradients and a frequency selective 180° pulses to select a three dimensional voxels of a well defined size (20 mm^3) in the regions of interest (ROIs) .

A reference spectra without water suppression were acquired for both the voxels.
Peaks quantification relatively to Cho+PCho was performed by utilizing LCModel (Provencher, 2001).

Two groups af animals were used, one group of epileptic 9 months old rats treated with a single intraperitoneal (i.p.) bolus of Vigabatrin (N=5) (500 mg/kg; Yamanouchi Pharma B.V., The Netherlands) dissolved in saline (0.9%) in a volume of 2 ml/kg, or with physiological saline as control (N=5). Second group, non epileptic 4 months old rats, also treated with Vigabatrin (N=5) or saline (N=5) at the same concentration used for the first group. MRI analysis was performed 12 h after ip treatment and for all the animals ROIs were positioned in lateral thalamus (LT) and somatosensory cortex (SS). Also in this experiment, rats were treated with Vigabatrin in order to exacerbate SWDs episodes.

## 4.3 RESULTS

| Groups | Regions | Metabolites relative concentration (mean ± st. dev) | | |
|---|---|---|---|---|
| | | (NAA+NAAG)/(Ch+Pch) | (Cr+PCr)/(Ch+Pch) | (Glu+Gln)/(Ch+Pch) |
| PBS 4m | Thalamus | 5,18 ± 0,76 | 4,03 ± 0,34 | 7,46 ± 0,46 |
| PBS 9m | | 5,12 ± 0,99 | 4,39 ± 0,26 | 6,15 ± 0,72 |
| Vigabatrin 4m | | 6,04 ± 0,94 | 5,51 ± 1,43 | 8,90 ± 2,18 |
| Vigabatrin 9m | | 6,75 ± 0,78 | 5,70 ± 0,68 | 9,03 ± 0,44 |
| PBS 4m | Somatosensory cortex | 8,34 ± 1,37 | 5,24 ± 0,46 | 10,78 ± 1,20 |
| PBS 9m | | 7,44 ± 1.91 | 5,14 ± 0,71 | 8,89 ± 0,61 |
| Vigabatrin 4m | | 9,35 ± 3,07 | 6,72 ± 0,49 | 12,35 ± 3,82 |
| Vigabatrin 9m | | 9,94 ± 2,93 | 6,80 ± 1,27 | 13,47 ± 2,66 |

**Tab. 4.1** Schematic representation of MRS results. N-acetylaspartate(NAA), N-acetyl-aspartyl-glutamate (NAAG), choline (Ch), phopshorylcholine (PCh), creatine (CR), Phosphocreatine (PCr), Glutamate (Glu) and Glutamine (Gln). GPC+PCh concentration is used as internal control, so all the concentrations of others metabolities are related to GPC+PCho concentration. Values are expressed as mean ± St.dev.

MRS data indicate higher levels of Glutamate+Glutamine vs control after Vigabatrin treatment, both in the thalamus and in the somatosensory cortex in epileptic 9 months rats ($p<0.005$) (Fig. 4.1-4.2).

Also the other groups of metabolities are enhanced by Vigabatrin injection in the thalamus of epileptic animals but this enhancing is only significative for 9 months old animals ($p<0.05$) (Fig. 4.1). Data point out the effect of Vigabatrin on Creatine+Phosphocreatine concentration both for epileptic and non epileptic animals in the somatosensory cortex ($p<0.05$) (Fig. 4.2).

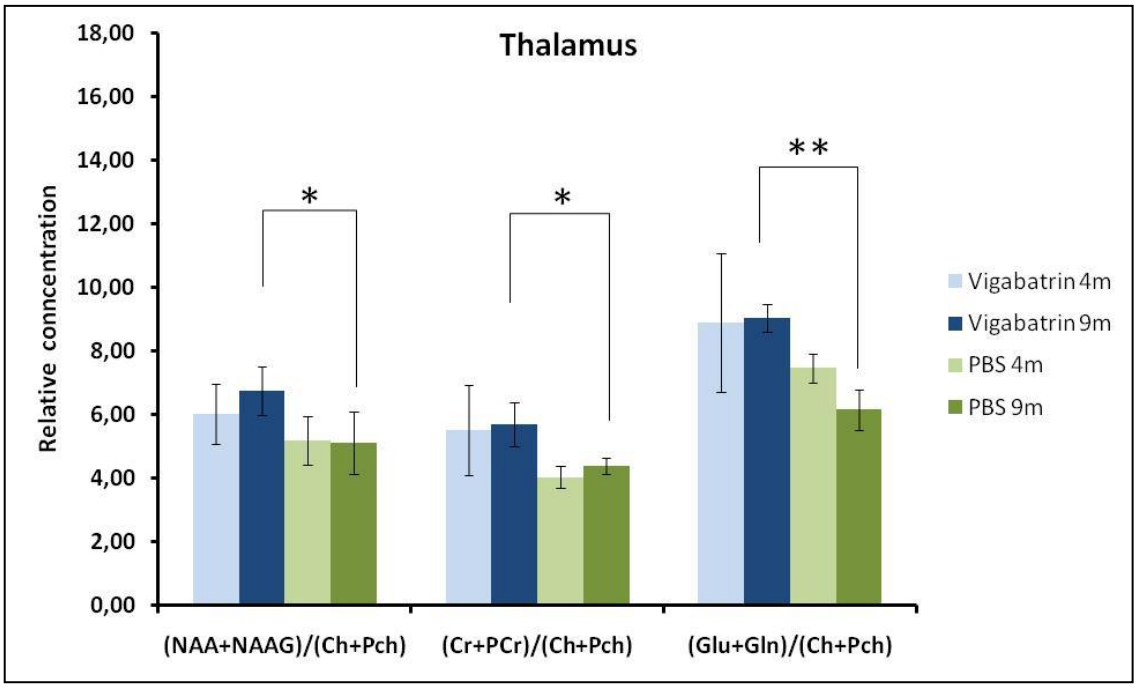


**Fig.4.1** Representation of MRS results performed in the Thalamus of Wag/Rij rats comparing epileptic 9 months animals treated with Vigabatrin or PBS vs control non epileptic treated animals. Relative concentrations of N-acetylaspartate(NAA) + N-acetyl-aspartyl-glutamate (NAAG), creatine (CR) + Phosphocreatine (PCr) and Glutamate (Glu) + Glutamine (Gln) were related to choline (Ch) + phopshorylcholine (PCh) concentration used as internal standard. *****= ($p \leq 0.05$); ******= ($p \leq 0.005$);

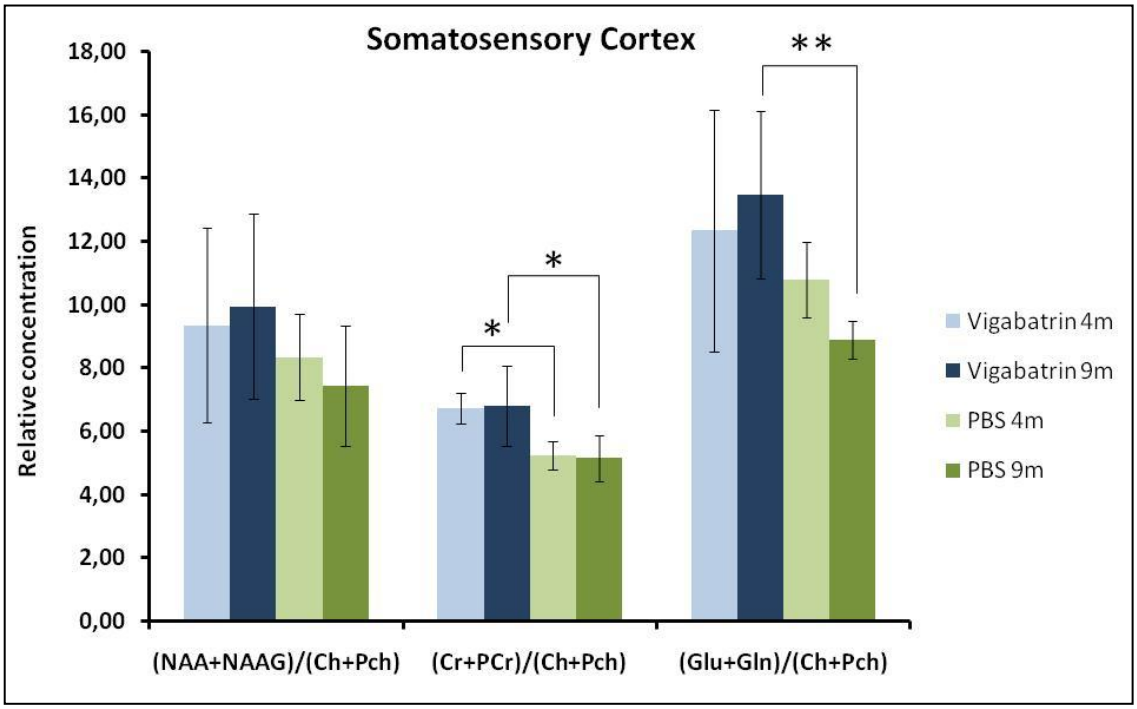


**Fig.4.2** Representation of MRS results performed in the Somatosensory cortex of Wag/Rij rats comparing epileptic 9 months animals treated with Vigabatrin or PBS vs control non epileptic treated animals. Relative concentrations of N-acetylaspartate(NAA) + N-acetyl-aspartyl-glutamate (NAAG), creatine (CR) + Phosphocreatine (PCr) and Glutamate (Glu) + Glutamine (Gln) were related to choline (Ch) + phopshorylcholine (PCh) concentration used as internal standard. *****= ($p \leq 0.05$); ******= ($p \leq 0.005$);

# -5-

## EXPERIMENT 3: GENE ARRAY

### 5.1 INTRODUCTION TO EXPERIMENT 3

It has become increasingly obvious during recent decades that genetic factors play a main role in the idiopathic generalized epilepsies, including absence epilepsy.

Evidence for a genetic predisposition in this type of epilepsy arose from twin studies, where it was found that both pairs of monozygotic twins suffered more frequently from this disorder than pairs of dizygotic twins (Lennox and Jolly, 1954).

To determine whether specific cerebral regions are differently activated in a animal model of absence seizures and to identify characteristic genes involved in absence epilepsy the present study analyzed the expression of 113 genes rapresentative of 18 signal transduction pathways. We used Microarray technology which utilizes RNA from tissue to simultaneously determine the expression levels of many genes.

Microarrays are composed of a set of distinct, gene-specific, nucleic acid probes immobilized on a solid support. During a microarray experiment, RNA is enzymatically converted to labeled cDNA (complementary DNA) or cRNA, and then hybridized to the immobilized nucleic acid probe. The labeled target bound at each gene-specific spot is typically detected using chemiluminescent methods. The signal produced at each spot is representative of the amount of message in the original RNA sample. This microarray system provides a economical and productive methods for monitoring a focused large panel of genes in a particular biological pathway or disease state. In order to reveal changes in expression of biological important subsets of genes, microarray data were subjected to hierarchical clustering and statistical parametric and non-parametric analysis.

Validation of the direction and magnitude of changes in gene expression indicated by microarray analyses was performed by real-time quantitative polymerase chain reaction (qPCR) *(*see *experiment 4).*

## 5.2 MATERIALS AND METHODS

Male WAG/Rij (~250–300 g) housed individually in standard polycarbonate cages in a temperature and humidity controlled environment on a 12:12 light–dark cycle (lights off at 0600 h). Animals had access to food and water ad libitum.

For microarray experiments, two groups af animals were used, epileptic 9 months old rats treated with a single intraperitoneal (i.p.) bolus of Vigabatrin (N=3) (500 mg/kg; Yamanouchi Pharma B.V., The Netherlands) dissolved in saline (0.9%) in a volume of 2 ml/kg, or physiological saline as control (N=3). Second group, non epileptic 4 months old rats, also treated with Vigabatrin (N=3) or saline (N=3) at the same concentration used for the first group. Drugs were administered 12h prior to dissection of cerebral tissue (at approximately 0900 pm) in a single dose via the intraperitoneal (i.p.) route. The doses of Vigabatrin administered were chosen based on previous reports that it produce anhancement of SWDs ( Bouwman et al., 2003).

*Tissue preparation*, *i*n order to reduce variability of the results, the same investigator performed all of the dissections of rats brain for microarray and qPCR experiments. Approximately 12h following the drug or vehicle administration, animals were euthanized by decapitation and brains were rapidly removed and washed twice in ice-cold phosphate buffered saline (PBS, pH=7.4) prior to dissection of the four regions of interested; somatosensory cortex (peri-oral region) (Bregma 0.70 mm), visual cortex (bregma -4.80 mm), ventral and lateral thalamus (bregma -3.30 mm) (Fig. 5.1) Following dissection, brain tissue was placed into 300 μl of ice-cold Trizol reagent (Invitrogen) for isolation of total RNA.

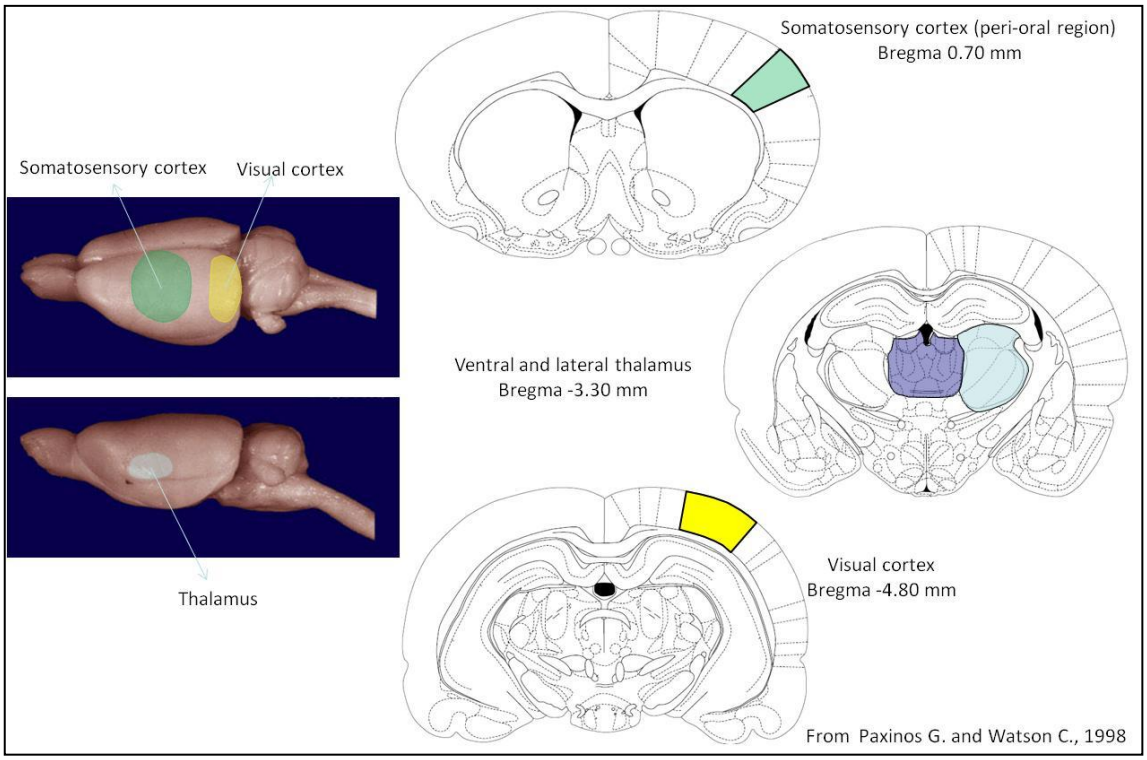


**Fig.5.1** The four rat brain regions dissected for microarray experiments.

*RNA isolation, t*otal RNA was extracted using Trizol reagent (Invitrogen) according to the manufacturer's directions. RNA from the tissues was isolated from each region per each rat individually and not pooled within treatment groups or regions (48 samples). RNA was then further purified by elution through an RNeasy minicolumn (Qiagen). Total RNA integrity and concentration were determined by an Eppendorf BioPhotometer, and RNA samples were stored at −80 °C until further analysis.

*Microarray procedures,* 0.1-3 μg of total RNA from each tissue sample was used for complementary RNA (cRNA) synthesis, labeling and amplification according to TrueLabeling-AMP 2.0 reagent Kit (Superarray) instructions. Biotin-16-UTP was purchased from EnzoLife. cRNA was purified using ArrayGrade cRNA clean-up kit (Superarray). For each sample, 2-4 μg of labeled cRNA was then hybridized to the Oligo GEArray® Rat Signal Transduction PathwayFinder™ Microarray (which consist of 115 gene-specific 60-mer oligos probe sets, fixed in 8 columns and 16 rows) in according to Chemiluminescent detection Kit (Superarray) directions. Microarrays were then scanned and probe intensities were quantified using GEArray Expression Analysis Suite software (Fig. 5.2).

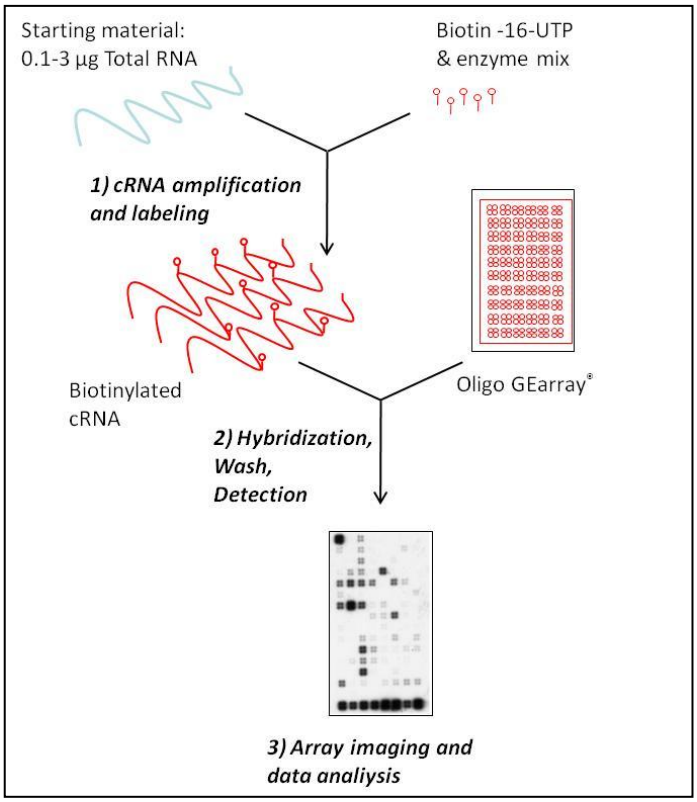


**Fig.5.2** Schematic representation of the 3 steps required for microarray analysis. In the first step RNA from each tissue sample was used for cRNA synthesis, labeling and amplification, during this phase new RNA was producted containing Biotin-16-UTP. In the second step, labeled cRNA was hybridized to the Oligo GEArray® overnight and then detection of the chemioluminescent signal was made using photosensible paper. In the last step, Microarrays were scanned and probe intensities were quantified using GEArray Expression Analysis Suite software.

*Microarray data analysis*, data from arrays were analyzed using GEArray Expression Analysis Suite (Superarray Bioscience Corporation). Quantitative expression values were corrected to the background, normalized with respect to the positive control genes included in the arrays, and reported as ratios to the mean values of normalization genes.

In order to reveal changes in expression of different genes subsets, we prompted a comparative analysis of the profiles expression; in details, we compared Vigabatrin vs PBS treated animals, and epileptic 9 months old vs non epileptic 4 months old rats, calculating the ratio between the corrected and normalized value of expression of every gene.

Moreover microarray data were subject to hierarchical clustering . Clustergram shows the correlation of the genes across the sperimental groups, genes that are more similar are joined. Dendogram showing clusters of genes based on average signal intensity for each experimental group were obtained.

## 5.3 RESULTS

Comparative analysis of the gene expression profiles of epileptic Wag/rij 9 months old vs non epileptic Wg/rij 4 months old rats (ignoring treatment and region) was made. In table 5.1 are reported the ratios of all the 113 genes.

| *Position* | *Gene Symbol* | *Gene Description* | *Fold change* |
|---|---|---|---|
| 1 | Ppia | Peptidylprolyl isomerase A | 1.00 |
| 2 | Atf2 | Activating transcription factor 2 | 1.09 |
| 3 | Bax | Bcl2-associated X protein | 0.82 |
| 4 | Bcl2 | B-cell leukemia/lymphoma 2 | 1.25 |
| 5 | Bcl2a1 | B-cell leukemia/lymphoma 2 related protein A1 | 1.27 |
| 6 | Bcl2l1 | Bcl2-like 1 | 0.92 |
| 7 | Birc1b | Baculoviral IAP repeat-containing 1b | 0.96 |
| 8 | Birc3 | Baculoviral IAP repeat-containing 3 | 1.15 |
| 9 | RGD1562883 | Similar to livin inhibitor of apoptosis isoform beta (predicted) | 0.97 |
| 10 | Bmp2 | Bone morphogenetic protein 2 | 0.91 |
| 11 | Bmp4 | Bone morphogenetic protein 4 | 1.02 |
| 12 | Brca1 | Breast cancer 1 | 0.75 |
| 13 | Ccl2 | Chemokine (C-C motif) ligand 2 | 1.14 |
| 14 | Ccl20 | Chemokine (C-C motif) ligand 20 | 1.75 |
| 15 | Ccnd1 | Cyclin D1 | 0.89 |
| 16 | Cd5 | CD5 antigen | 0.82 |
| 17 | Cdh1 | Cadherin 1 | 1.10 |
| 18 | Cdk2 | Cyclin dependent kinase 2 | 0.72 |
| 19 | Cdkn1a | Cyclin-dependent kinase inhibitor 1A | 0.99 |
| 20 | Cdkn1b | Cyclin-dependent kinase inhibitor 1B | 0.50 |
| 21 | Cdkn1c | Cyclin-dependent kinase inhibitor 1C (P57) | 0.92 |
| 22 | Cdkn2a | Cyclin-dependent kinase inhibitor 2A | 0.74 |
| 23 | Cdkn2b | Cyclin-dependent kinase inhibitor 2B (p15, inhibits CDK4) | 1.14 |
| 24 | Cdkn2c | Cyclin-dependent kinase inhibitor 2C (p18, inhibits CDK4) | 1.50 |
| 25 | Cdkn2d | Similar to cyclin-dependent kinase inhibitor 2D | 0.89 |
| 26 | Cebpb | CCAAT/enhancer binding protein (C/EBP), beta | 1.05 |
| 27 | Csf2 | Colony stimulating factor 2 (granulocyte-macrophage) | 0.92 |
| 28 | Csn2 | Casein beta | 0.77 |
| 29 | Ctsd | Cathepsin D | 0.97 |
| 30 | Cxcl1 | Chemokine (C-X-C motif) ligand 1 | 1.20 |
| 31 | Cxcl9 | Chemokine (C-X-C motif) ligand 9 | 2.58 |
| 32 | Cyp19a1 | Cytochrome P450, family 19, subfamily a, polypeptide 1 | 2.31 |
| 33 | Egfr | Epidermal growth factor receptor | 0.97 |
| 34 | Egr1 | Early growth response 1 | 0.85 |
| 35 | Ei24 | Etoposide induced 2.4 mRNA | 1.06 |
| 36 | Fasn | Fatty acid synthase | 1.08 |
| 37 | Fgf4 | Fibroblast growth factor 4 | 0.88 |

| | | | |
|---|---|---|---|
| 38 | Fn1 | Fibronectin 1 | 1.03 |
| 39 | Fos | FBJ murine osteosarcoma viral oncogene homolog | 0.68 |
| 40 | Foxa2 | Forkhead box A2 | 3.10 |
| 41 | Gadd45a | Growth arrest and DNA-damage-inducible 45 alpha | 0.88 |
| 42 | LOC690987 | Similar to glycogen synthase 1, muscle | 0.66 |
| 43 | Gys2 | Glycogen synthase 2 | 1.02 |
| 44 | RGD1564108 | Similar to hedgehog-interacting protein (predicted) | 1.59 |
| 45 | Hk2 | Hexokinase 2 | 1.03 |
| 46 | Hoxa1 | Homeo box A1 | 0.68 |
| 47 | Hoxb1 | Homeo box B1 (predicted) | 1.95 |
| 48 | Hsf1 | Heat shock transcription factor 1 | 1.41 |
| 49 | Hspb1 | Heat shock 27kDa protein 1 | 0.97 |
| 50 | Hspca | Heat shock protein 1, alpha | 1.00 |
| 51 | Hspcal3 | Heat shock 90kDa protein 1, alpha-like 3 (predicted) | 0.99 |
| 52 | Icam1 | Intercellular adhesion molecule 1 | 1.55 |
| 53 | Igfbp3 | Insulin-like growth factor binding protein 3 | 0.79 |
| 54 | Igfbp4 | Insulin-like growth factor binding protein 4 | 1.13 |
| 55 | Ikbkb | Inhibitor of kappaB kinase beta | 1.46 |
| 56 | Il1a | Interleukin 1 alpha | 3.44 |
| 57 | Il2 | Interleukin 2 | 1.10 |
| 58 | Il2ra | Interleukin 2 receptor, alpha chain | 0.81 |
| 59 | Il4 | Interleukin 4 | 0.69 |
| 60 | Il4ra | Interleukin 4 receptor, alpha | 1.04 |
| 61 | Irf1 | Interferon regulatory factor 1 | 1.02 |
| 62 | Jun | Jun oncogene | 1.08 |
| 63 | Junb | Jun-B oncogene | 1.00 |
| 64 | Klkb1 | Kallikrein B, plasma 1 | 3.72 |
| 65 | Lef1 | Lymphoid enhancer binding factor 1 | 0.76 |
| 66 | Lep | Leptin | 0.66 |
| 67 | LOC685360 | Similar to Homeobox protein engrailed-1 (Mo-En-1) | 1.62 |
| 68 | Lta | Lymphotoxin A | 1.25 |
| 69 | Mdm2 | Transformed mouse 3T3 cell double minute 2 | 0.84 |
| 70 | Mmp10 | Matrix metallopeptidase 10 | 0.68 |
| 71 | Mmp7 | Matrix metallopeptidase 7 | 0.82 |
| 72 | Myc | Myelocytomatosis viral oncogene homolog (avian) | 1.41 |
| 73 | Nab2 | Ngfi-A binding protein 2 | 0.72 |
| 74 | Nfkb1 | Nuclear factor of kappa light chain gene enhancer in B-cells 1, p105 | 0.71 |
| 75 | Nfkbia | Nuclear factor of k light chain gene enhancer in B-cells inhibitor, α | 1.12 |
| 76 | Ngfg | Nerve growth factor, gamma | 0.84 |
| 77 | Nos2 | Nitric oxide synthase 2, inducible | 0.56 |
| 78 | Odc1 | Ornithine decarboxylase 1 | 0.91 |
| 79 | Pecam | Platelet/endothelial cell adhesion molecule | 1.08 |
| 80 | Pgr | Progesterone receptor | 0.74 |
| 81 | Pparg | Peroxisome proliferator activated receptor gamma | 1.70 |
| 82 | Prkca | Protein kinase C, alpha | 0.74 |
| 83 | Prkcb1 | Protein kinase C, beta 1 | 1.03 |
| 84 | Prkce | Protein kinase C, epsilon | 0.63 |
| 85 | Ptch | Patched homolog 1 (Drosophila) | 0.55 |
| 86 | Ptch1 | Patched homolog 1 (Drosophila) | 1.12 |
| 87 | Pten | Phosphatase and tensin homolog | 0.60 |
| 88 | Ptgs2 | Prostaglandin-endoperoxide synthase 2 | 0.87 |

| | | | |
|---|---|---|---|
| 89 | Pzp | Pregnancy-zone protein | 1.24 |
| 90 | Rbp1 | Retinol binding protein 1, cellular | 1.32 |
| 91 | Rbp2 | Retinol binding protein 2, cellular | 0.91 |
| 92 | Sele | Selectin, endothelial cell | 0.81 |
| 93 | Selp | Selectin, platelet | 0.45 |
| 94 | Stra6 | Stimulated by retinoic acid gene 6 homolog (mouse) | 0.41 |
| 95 | Tank | TRAF family member-associated Nf-kappa B activator | 0.68 |
| 96 | Tcf7 | Transcription factor 7, T-cell specific (predicted) | 0.90 |
| 97 | Tert | Telomerase reverse transcriptase | 1.07 |
| 98 | Tfrc | Transferrin receptor | 0.69 |
| 99 | Tmepai | Transmembrane, prostate androgen induced RNA (predicted) | 1.02 |
| 100 | Tmprss9 | Transmembrane serine protease 9 (predicted) | 0.70 |
| 101 | Tnf | Tumor necrosis factor (TNF superfamily, member 2) | 0.26 |
| 102 | Tnfrsf10b | Tumor necrosis factor receptor superfamily, member 10b (predicted) | 0.49 |
| 103 | Tnfrsf6 | Tumor necrosis factor receptor superfamily, member 6 | 0.79 |
| 104 | Faslg | Fas ligand (TNF superfamily, member 6) | 1.08 |
| 105 | Tp53 | Tumor protein p53 | 1.00 |
| 106 | Trim25 | Tripartite motif protein 25 (mapped) | 0.60 |
| 107 | Vcam1 | Vascular cell adhesion molecule 1 | 0.68 |
| 108 | Vegfa | Vascular endothelial growth factor A | 0.47 |
| 109 | Vegfc | Vascular endothelial growth factor C | 0.46 |
| 110 | Wisp1 | WNT1 inducible signaling pathway protein 1 | 0.68 |
| 111 | Wisp2 | WNT1 inducible signaling pathway protein 2 | 0.85 |
| 112 | Wnt1 | Wingless-type MMTV integration site family, member 1 (mapped) | 0.87 |
| 113 | Wnt2 | Wingless-related MMTV integration site 2 | 0.62 |
| 114 | Wsb1 | WD repeat and SOCS box-containing 1 | 0.61 |

**Tab. 5.1** Comparative analysis of the gene expression profiles of epileptic Wag/rij 9 months old vs non epileptic Wg/rij 4 months old rats (ignoring treatment and region). Data are reported as ratio (Fold Change) between the corrected and normalized value of expression of every gene in the two groups.

Genes were considered significantly over-expressed in one group when their expression values proved $\geq$ 1.25-fold higher than the expression of the same gene in the other group. On the other hand, genes were considered significantly under-expressed in one lineage when their expression values were $\leq$ 0.75-fold that of the expression of the same gene in the other group. In table 5.2 are reported all the over-expressed genes for every characteristic biological pathway. Since 5 out of 16 up-regulated genes belong to the NFkB pathway, it seems to be the biological pathway more implicated in the develop of the absence seizures in epileptic older animals.

| *NFkB Pathway* | | | |
|---|---|---|---|
| ***Position*** | ***Gene Symbol*** | ***Gene Description*** | ***Fold change*** |
| 5 | Bcl2a1 | B-cell leukemia/lymphoma 2 related protein A1 | 1.27 |
| 14 | Ccl20 | Chemokine (C-C motif) ligand 20 | 1.75 |
| 52 | Icam1 | Intercellular adhesion molecule 1 | 1.55 |
| 55 | Ikbkb | Inhibitor of kappaB kinase beta | 1.46 |
| 56 | Il1a | Interleukin 1 alpha | 3.44 |
| ***Retinoic Acid Pathway*** | | | |
| ***Position*** | ***Gene Symbol*** | ***Gene Description*** | ***Fold change*** |
| 47 | Hoxb1 | Homeo box B1 (predicted) | 1.95 |
| 67 | LOC685360 | Similar to Homeobox protein engrailed-1 (Mo-En-1) | 1.62 |
| 90 | Rbp1 | Retinol binding protein 1, cellular | 1.32 |
| ***Stress Pathway*** | | | |
| ***Position*** | ***Gene Symbol*** | ***Gene Description*** | ***Fold change*** |
| 48 | Hsf1 | Heat shock transcription factor 1 | 1.41 |
| 72 | Myc | Myelocytomatosis viral oncogene homolog (avian) | 1.41 |
| ***CREB Pathway*** | | | |
| ***Position*** | ***Gene Symbol*** | ***Gene Description*** | ***Fold change*** |
| 32 | Cyp19a1 | Cytochrome P450, family 19, subfamily a, polypeptide 1 | 2.31 |
| ***Androgen Pathway*** | | | |
| ***Position*** | ***Gene Symbol*** | ***Gene Description*** | ***Fold change*** |
| 64 | Klkb1 | Kallikrein B, plasma 1 | 3.72 |
| ***Hedgehog Pathway*** | | | |
| ***Position*** | ***Gene Symbol*** | ***Gene Description*** | ***Fold change*** |
| 40 | Foxa2 | Forkhead box A2 | 3.10 |
| ***Jak-Stat Pathway*** | | | |
| ***Position*** | ***Gene Symbol*** | ***Gene Description*** | ***Fold change*** |
| 31 | Cxcl9 | Chemokine (C-X-C motif) ligand 9 | 2.58 |
| ***Wnt Pathway*** | | | |
| ***Position*** | ***Gene Symbol*** | ***Gene Description*** | ***Fold change*** |
| 81 | Pparg | Peroxisome proliferator activated receptor gamma | 1.70 |
| ***TGF β Pathway*** | | | |
| ***Position*** | ***Gene Symbol*** | ***Gene Description*** | ***Fold change*** |
| 24 | Cdkn2c | Cyclin-dependent kinase inhibitor 2C (p18, inhibits CDK4) | 1.50 |

**Tab 5.2** List of all the over-expressed genes (Fold change ≥ 1.25) for the specifical biological pathway comparing epileptic Wag/rij 9 months old vs non epileptic Wg/rij 4 months old rats.

In table 5.3 are reported all the under-expressed genes for every characteristic biological pathway. Also in this case, the most implicated pathway seems to be the NFkB pathway (5 of the 31 total down-regulated genes).

| ***NFkB Pathway*** | | | |
|---|---|---|---|
| ***Position*** | ***Gene Symbol*** | ***Gene Description*** | ***Fold change*** |
| 74 | Nfkb1 | Nuclear factor of kappa light chain gene enhancer in B-cells 1, p105 | 0.71 |
| 77 | Nos2 | Nitric oxide synthase 2, inducible | 0.56 |
| 95 | Tank | TRAF family member-associated Nf-kappa B activator | 0.68 |
| 101 | Tnf | Tumor necrosis factor (TNF superfamily, member 2) | 0.26 |
| 107 | Vcam1 | Vascular cell adhesion molecule 1 | 0.68 |
| ***Calcium and Protein Kinase C Pathway*** | | | |
| ***Position*** | ***Gene Symbol*** | ***Gene Description*** | ***Fold change*** |
| 82 | Prkca | Protein kinase C, alpha | 0.74 |
| 84 | Prkce | Protein kinase C, epsilon | 0.63 |
| 98 | Tfrc | Transferrin receptor | 0.69 |
| ***Estrogen Pathway*** | | | |
| ***Position*** | ***Gene Symbol*** | ***Gene Description*** | ***Fold change*** |
| 12 | Brca1 | Breast cancer 1 | 0.75 |
| 80 | Pgr | Progesterone receptor | 0.74 |
| 106 | Trim25 | Tripartite motif protein 25 (mapped) | 0.60 |
| ***Wnt Pathway*** | | | |
| ***Position*** | ***Gene Symbol*** | ***Gene Description*** | ***Fold change*** |
| 108 | Vegfa | Vascular endothelial growth factor A | 0.47 |
| 109 | Vegfc | Vascular endothelial growth factor C | 0.46 |
| 110 | Wisp1 | WNT1 inducible signaling pathway protein 1 | 0.68 |
| ***Hedgehog Pathway*** | | | |
| ***Position*** | ***Gene Symbol*** | ***Gene Description*** | ***Fold change*** |
| 85 | Ptch | Patched homolog 1 (Drosophila) | 0.55 |
| 113 | Wnt2 | Wingless-related MMTV integration site 2 | 0.62 |
| 114 | Wsb1 | WD repeat and SOCS box-containing 1 | 0.61 |
| ***TGF β Pathway*** | | | |
| ***Position*** | ***Gene Symbol*** | ***Gene Description*** | ***Fold change*** |
| 20 | Cdkn1b | Cyclin-dependent kinase inhibitor 1B | 0.50 |
| 22 | Cdkn2a | Cyclin-dependent kinase inhibitor 2A | 0.74 |

| *Retinoic Acid Pathway* | | | |
|---|---|---|---|
| ***Position*** | ***Gene Symbol*** | ***Gene Description*** | ***Fold change*** |
| 46 | Hoxa1 | Homeo box A1 | 0.68 |
| 94 | Stra6 | Stimulated by retinoic acid gene 6 homolog (mouse) | 0.41 |
| ***Jak-Stat Pathway*** | | | |
| ***Position*** | ***Gene Symbol*** | ***Gene Description*** | ***Fold change*** |
| 59 | Il4 | Interleukin 4 | 0.69 |
| 70 | Mmp10 | Matrix metallopeptidase 10 | 0.68 |
| ***Androgen Pathway*** | | | |
| ***Position*** | ***Gene Symbol*** | ***Gene Description*** | ***Fold change*** |
| 18 | Cdk2 | Cyclin dependent kinase 2 | 0.72 |
| 100 | Tmprss9 | Transmembrane serine protease 9 (predicted) | 0.70 |
| ***P13 Kinase/AKT Pathway*** | | | |
| ***Position*** | ***Gene Symbol*** | ***Gene Description*** | ***Fold change*** |
| 87 | Pten | Phosphatase and tensin homolog | 0.60 |
| ***Insuline Pathway*** | | | |
| ***Position*** | ***Gene Symbol*** | ***Gene Description*** | ***Fold change*** |
| 66 | Lep | Leptin | 0.66 |
| ***P53 Pathway*** | | | |
| ***Position*** | ***Gene Symbol*** | ***Gene Description*** | ***Fold change*** |
| 102 | Tnfrsf10b | Tumor necrosis factor receptor superfamily, member 10b (predicted) | 0.49 |
| ***LDL Pathway*** | | | |
| ***Position*** | ***Gene Symbol*** | ***Gene Description*** | ***Fold change*** |
| 93 | Selp | Selectin, platelet | 0.45 |
| ***Mitogenic Pathway*** | | | |
| ***Position*** | ***Gene Symbol*** | ***Gene Description*** | ***Fold change*** |
| 73 | Nab2 | Ngfi-A binding protein 2 | 0.72 |
| ***Stress Pathway*** | | | |
| ***Position*** | ***Gene Symbol*** | ***Gene Description*** | ***Fold change*** |
| 39 | Fos | FBJ murine osteosarcoma viral oncogene homolog | 0.68 |

**Tab 5.3** List of the under-expressed genes (Fold change $\leq 0.75$) for the specifical biological pathway comparing epileptic Wag/rij 9 months old vs non epileptic Wg/rij 4 months old rats.

Comparative analysis of the gene expression profiles in Wag/Rij rats after Vigabatrin treatment vs PBS treatment (ignoring age and region) was made. In table 5.4 are reported the ratios of all the 113 genes.

| ***Position*** | ***Gene Symbol*** | ***Gene Description*** | ***Fold change*** |
|---|---|---|---|
| 1 | Ppia | Peptidylprolyl isomerase A | 0.98 |
| 2 | Atf2 | Activating transcription factor 2 | 1.52 |
| 3 | Bax | Bcl2-associated X protein | 1.62 |
| 4 | Bcl2 | B-cell leukemia/lymphoma 2 | 3.09 |
| 5 | Bcl2a1 | B-cell leukemia/lymphoma 2 related protein A1 | 2.20 |
| 6 | Bcl2l1 | Bcl2-like 1 | 2.78 |
| 7 | Birc1b | Baculoviral IAP repeat-containing 1b | 2.39 |
| 8 | Birc3 | Baculoviral IAP repeat-containing 3 | 2.54 |
| 9 | RGD1562883 | Similar to livin inhibitor of apoptosis isoform beta (predicted) | 1.62 |
| 10 | Bmp2 | Bone morphogenetic protein 2 | 2.22 |
| 11 | Bmp4 | Bone morphogenetic protein 4 | 1.86 |
| 12 | Brca1 | Breast cancer 1 | 2.78 |
| 13 | Ccl2 | Chemokine (C-C motif) ligand 2 | 2.63 |
| 14 | Ccl20 | Chemokine (C-C motif) ligand 20 | 2.28 |
| 15 | Ccnd1 | Cyclin D1 | 1.37 |
| 16 | Cd5 | CD5 antigen | 2.66 |
| 17 | Cdh1 | Cadherin 1 | 2.00 |
| 18 | Cdk2 | Cyclin dependent kinase 2 | 2.34 |
| 19 | Cdkn1a | Cyclin-dependent kinase inhibitor 1A | 1.80 |
| 20 | Cdkn1b | Cyclin-dependent kinase inhibitor 1B | 1.60 |
| 21 | Cdkn1c | Cyclin-dependent kinase inhibitor 1C (P57) | 2.30 |
| 22 | Cdkn2a | Cyclin-dependent kinase inhibitor 2A | 2.54 |
| 23 | Cdkn2b | Cyclin-dependent kinase inhibitor 2B (p15, inhibits CDK4) | 2.73 |
| 24 | Cdkn2c | Cyclin-dependent kinase inhibitor 2C (p18, inhibits CDK4) | 2.65 |
| 25 | Cdkn2d | Similar to cyclin-dependent kinase inhibitor 2D | 2.87 |
| 26 | Cebpb | CCAAT/enhancer binding protein (C/EBP), beta | 2.30 |
| 27 | Csf2 | Colony stimulating factor 2 (granulocyte-macrophage) | 1.89 |
| 28 | Csn2 | Casein beta | 2.67 |
| 29 | Ctsd | Cathepsin D | 1.11 |
| 30 | Cxcl1 | Chemokine (C-X-C motif) ligand 1 | 1.82 |
| 31 | Cxcl9 | Chemokine (C-X-C motif) ligand 9 | 3.11 |
| 32 | Cyp19a1 | Cytochrome P450, family 19, subfamily a, polypeptide 1 | 2.41 |
| 33 | Egfr | Epidermal growth factor receptor | 1.41 |
| 34 | Egr1 | Early growth response 1 | 1.16 |
| 35 | Ei24 | Etoposide induced 2.4 mRNA | 1.21 |
| 36 | Fasn | Fatty acid synthase | 1.29 |
| 37 | Fgf4 | Fibroblast growth factor 4 | 2.17 |
| 38 | Fn1 | Fibronectin 1 | 1.60 |
| 39 | Fos | FBJ murine osteosarcoma viral oncogene homolog | 1.30 |
| 40 | Foxa2 | Forkhead box A2 | 2.41 |
| 41 | Gadd45a | Growth arrest and DNA-damage-inducible 45 alpha | 2.64 |
| 42 | LOC690987 | Similar to glycogen synthase 1, muscle | 1.96 |
| 43 | Gys2 | Glycogen synthase 2 | 2.65 |

| | | | |
|---|---|---|---|
| 44 | RGD1564108 | Similar to hedgehog-interacting protein (predicted) | 3.67 |
| 45 | Hk2 | Hexokinase 2 | 4.15 |
| 46 | Hoxa1 | Homeo box A1 | 3.46 |
| 47 | Hoxb1 | Homeo box B1 (predicted) | 5.26 |
| 48 | Hsf1 | Heat shock transcription factor 1 | 2.23 |
| 49 | Hspb1 | Heat shock 27kDa protein 1 | 1.24 |
| 50 | Hspca | Heat shock protein 1, alpha | 1.00 |
| 51 | Hspcal3 | Heat shock 90kDa protein 1, alpha-like 3 (predicted) | 1.20 |
| 52 | Icam1 | Intercellular adhesion molecule 1 | 3.01 |
| 53 | Igfbp3 | Insulin-like growth factor binding protein 3 | 2.10 |
| 54 | Igfbp4 | Insulin-like growth factor binding protein 4 | 3.40 |
| 55 | Ikbkb | Inhibitor of kappaB kinase beta | 4.20 |
| 56 | Il1a | Interleukin 1 alpha | 4.92 |
| 57 | Il2 | Interleukin 2 | 2.07 |
| 58 | Il2ra | Interleukin 2 receptor, alpha chain | 1.56 |
| 59 | Il4 | Interleukin 4 | 2.79 |
| 60 | Il4ra | Interleukin 4 receptor, alpha | 1.93 |
| 61 | Irf1 | Interferon regulatory factor 1 | 2.25 |
| 62 | Jun | Jun oncogene | 1.19 |
| 63 | Junb | Jun-B oncogene | 4.24 |
| 64 | Klkb1 | Kallikrein B, plasma 1 | 7.55 |
| 65 | Lef1 | Lymphoid enhancer binding factor 1 | 2.26 |
| 66 | Lep | Leptin | 3.50 |
| 67 | LOC685360 | Similar to Homeobox protein engrailed-1 (Mo-En-1) | 4.75 |
| 68 | Lta | Lymphotoxin A | 4.81 |
| 69 | Mdm2 | Transformed mouse 3T3 cell double minute 2 | 2.94 |
| 70 | Mmp10 | Matrix metallopeptidase 10 | 4.54 |
| 71 | Mmp7 | Matrix metallopeptidase 7 | 2.96 |
| 72 | Myc | Myelocytomatosis viral oncogene homolog (avian) | 3.55 |
| 73 | Nab2 | Ngfi-A binding protein 2 | 2.82 |
| 74 | Nfkb1 | Nuclear factor of kappa light chain gene enhancer in B-cells 1, p105 | 2.54 |
| 75 | Nfkbia | Nuclear factor of k light chain gene enhancer in B-cells inhibitor, α | 1.80 |
| 76 | Ngfg | Nerve growth factor, gamma | 2.58 |
| 77 | Nos2 | Nitric oxide synthase 2, inducible | 3.15 |
| 78 | Odc1 | Ornithine decarboxylase 1 | 1.95 |
| 79 | Pecam | Platelet/endothelial cell adhesion molecule | 4.97 |
| 80 | Pgr | Progesterone receptor | 1.98 |
| 81 | Pparg | Peroxisome proliferator activated receptor gamma | 2.26 |
| 82 | Prkca | Protein kinase C, alpha | 2.24 |
| 83 | Prkcb1 | Protein kinase C, beta 1 | 1.17 |
| 84 | Prkce | Protein kinase C, epsilon | 1.82 |
| 85 | Ptch | Patched homolog 1 (Drosophila) | 2.34 |
| 86 | Ptch1 | Patched homolog 1 (Drosophila) | 3.54 |
| 87 | Pten | Phosphatase and tensin homolog | 1.92 |
| 88 | Ptgs2 | Prostaglandin-endoperoxide synthase 2 | 1.70 |
| 89 | Pzp | Pregnancy-zone protein | 2.74 |
| 90 | Rbp1 | Retinol binding protein 1, cellular | 1.66 |
| 91 | Rbp2 | Retinol binding protein 2, cellular | 1.34 |
| 92 | Sele | Selectin, endothelial cell | 1.95 |
| 93 | Selp | Selectin, platelet | 2.06 |

| | | | |
|---|---|---|---|
| 94 | Stra6 | Stimulated by retinoic acid gene 6 homolog (mouse) | 2.97 |
| 95 | Tank | TRAF family member-associated Nf-kappa B activator | 2.36 |
| 96 | Tcf7 | Transcription factor 7, T-cell specific (predicted) | 3.38 |
| 97 | Tert | Telomerase reverse transcriptase | 2.45 |
| 98 | Tfrc | Transferrin receptor | 1.71 |
| 99 | Tmepai | Transmembrane, prostate androgen induced RNA (predicted) | 1.11 |
| 100 | Tmprss9 | Transmembrane serine protease 9 (predicted) | 2.64 |
| 101 | Tnf | Tumor necrosis factor (TNF superfamily, member 2) | 1.71 |
| 102 | Tnfrsf10b | Tumor necrosis factor receptor superfamily, member 10b (predicted) | 1.86 |
| 103 | Tnfrsf6 | Tumor necrosis factor receptor superfamily, member 6 | 2.75 |
| 104 | Faslg | Fas ligand (TNF superfamily, member 6) | 2.51 |
| 105 | Tp53 | Tumor protein p53 | 1.30 |
| 106 | Trim25 | Tripartite motif protein 25 (mapped) | 2.20 |
| 107 | Vcam1 | Vascular cell adhesion molecule 1 | 1.34 |
| 108 | Vegfa | Vascular endothelial growth factor A | 1.78 |
| 109 | Vegfc | Vascular endothelial growth factor C | 1.81 |
| 110 | Wisp1 | WNT1 inducible signaling pathway protein 1 | 1.73 |
| 111 | Wisp2 | WNT1 inducible signaling pathway protein 2 | 1.76 |
| 112 | Wnt1 | Wingless-type MMTV integration site family, member 1 (mapped) | 1.63 |
| 113 | Wnt2 | Wingless-related MMTV integration site 2 | 1.35 |
| 114 | Wsb1 | WD repeat and SOCS box-containing 1 | 1.32 |

**Tab. 5.4** Comparative analysis of the gene expression profiles of all Vigabatrin treated Wag/Rij vs PBS treated (ignoring age and region). Data are reported as ratio (Fold Change) between the corrected ana normalized value of expression of every gene in the two groups.

Genes were considered significantly over-expressed in one group when their expression values proved $\geq 1.50$-fold higher than the expression of the same gene in the other group. No under-expressed genes (Fold change $\leq 0.50$) were finded out comparing Vigabatrin treaed animals with control PBS treated animals. In table 5.5 are reported all the over-expressed genes for every characteristic biological pathway.

| *NFkB Pathway* | | | |
|---|---|---|---|
| ***Position*** | ***Gene Symbol*** | ***Gene Description*** | ***Fold change*** |
| 5 | Bcl2a1 | B-cell leukemia/lymphoma 2 related protein A1 | 2,20 |
| 7 | Birc1b | Baculoviral IAP repeat-containing 1b | 2,39 |
| 8 | Birc3 | Baculoviral IAP repeat-containing 3 | 2,54 |
| 14 | Ccl20 | Chemokine (C-C motif) ligand 20 | 2,28 |
| 30 | Cxcl1 | Chemokine (C-X-C motif) ligand 1 | 1,82 |
| 52 | Icam1 | Intercellular adhesion molecule 1 | 3,01 |
| 55 | Ikbkb | Inhibitor of kappaB kinase beta | 4,20 |
| 56 | Il1a | Interleukin 1 alpha | 4,92 |
| 57 | Il2 | Interleukin 2 | 2,07 |
| 68 | Lta(TNFβ) | Lymphotoxin A | 4,81 |
| 74 | Nfkb1 | Nuclear factor of kappa light chain gene enhancer in B-cells 1, p105 | 2,54 |
| 75 | Nfkbia | Nuclear factor of k light chain gene enhancer in B-cells inhibitor, α | 1,80 |
| 77 | Nos2 | Nitric oxide synthase 2, inducible | 3,15 |
| 79 | Pecam | Platelet/endothelial cell adhesion molecule | 4,97 |
| 95 | Tank | TRAF family member-associated Nf-kappa B activator | 2,36 |
| 97 | Tert | Telomerase reverse transcriptase | 2,45 |
| 101 | Tnfα | Tumor necrosis factor (TNF superfamily, member 2) | 1,71 |
| *Wnt Pathway* | | | |
| ***Position*** | ***Gene Symbol*** | ***Gene Description*** | ***Fold change*** |
| 17 | Cdh1 | Cadherin 1 | 2,00 |
| 37 | Fgf4 | Fibroblast growth factor 4 | 2,17 |
| 65 | Lef1 | Lymphoid enhancer binding factor 1 | 2,26 |
| 81 | Pparg | Peroxisome proliferator activated receptor gamma | 2,26 |
| 96 | Tcf7 | Transcription factor 7, T-cell specific (predicted) | 3,38 |
| 108 | Vegfa | Vascular endothelial growth factor A | 1,78 |
| 109 | Vegfc | Vascular endothelial growth factor C | 1,81 |
| 110 | Wisp1 | WNT1 inducible signaling pathway protein 1 | 1,73 |
| 111 | Wisp2 | WNT1 inducible signaling pathway protein 2 | 1,76 |
| *Calcium and Protein Kinase C Pathway* | | | |
| ***Position*** | ***Gene Symbol*** | ***Gene Description*** | ***Fold change*** |
| 27 | Csf2 | Colony stimulating factor 2 (granulocyte-macrophage) | 1,89 |
| 58 | Il2ra | Interleukin 2 receptor, alpha chain | 1,56 |
| 72 | Myc | Myelocytomatosis viral oncogene homolog (avian) | 3,55 |
| 78 | Odc1 | Ornithine decarboxylase 1 | 1,95 |
| 82 | Prkca | Protein kinase C, alpha | 2,24 |
| 84 | Prkce | Protein kinase C, epsilon | 1,82 |
| 98 | Tfrc | Transferrin receptor | 1,71 |
| *Hedgehog Pathway* | | | |
| ***Position*** | ***Gene Symbol*** | ***Gene Description*** | ***Fold change*** |
| 10 | Bmp2 | Bone morphogenetic protein 2 | 2,22 |
| 11 | Bmp4 | Bone morphogenetic protein 4 | 1,86 |
| 40 | Foxa2 | Forkhead box A2 | 2,41 |
| 67 | LOC685360 | Similar to Homeobox protein engrailed-1 (Mo-En-1) | 4,75 |
| 85 | Ptch | Patched homolog 1 (Drosophila) | 2,34 |
| 86 | Ptch1 | Patched homolog 1 (Drosophila) | 3,54 |
| 112 | Wnt1 | Wingless-type MMTV integration site family, member 1 (mapped) | 1,63 |

| *TGF β Pathway* | | | |
|---|---|---|---|
| ***Position*** | ***Gene Symbol*** | ***Gene Description*** | ***Fold change*** |
| 19 | Cdkn1a | Cyclin-dependent kinase inhibitor 1A | 1,80 |
| 20 | Cdkn1b | Cyclin-dependent kinase inhibitor 1B | 1,60 |
| 21 | Cdkn1c | Cyclin-dependent kinase inhibitor 1C (P57) | 2,30 |
| 22 | Cdkn2a | Cyclin-dependent kinase inhibitor 2A | 2,54 |
| 23 | Cdkn2b | Cyclin-dependent kinase inhibitor 2B (p15, inhibits CDK4) | 2,73 |
| 24 | Cdkn2c | Cyclin-dependent kinase inhibitor 2C (p18, inhibits CDK4) | 2,65 |
| 25 | Cdkn2d | Similar to cyclin-dependent kinase inhibitor 2D | 2,87 |
| ***Jak-Stat Pathway*** | | | |
| ***Position*** | ***Gene Symbol*** | ***Gene Description*** | ***Fold change*** |
| 28 | Csn2 | Casein beta | 2,67 |
| 31 | Cxcl9 | Chemokine (C-X-C motif) ligand 9 | 3,11 |
| 59 | Il4 | Interleukin 4 | 2,79 |
| 60 | Il4ra | Interleukin 4 receptor, alpha | 1,93 |
| 61 | Irf1 | Interferon regulatory factor 1 | 2,25 |
| 70 | Mmp10 | Matrix metallopeptidase 10 | 4,54 |
| 89 | Pzp | Pregnancy-zone protein | 2,74 |
| ***P53 Pathway*** | | | |
| ***Position*** | ***Gene Symbol*** | ***Gene Description*** | ***Fold change*** |
| 3 | Bax | Bcl2-associated X protein | 1,62 |
| 41 | Gadd45a | Growth arrest and DNA-damage-inducible 45 alpha | 2,64 |
| 53 | Igfbp3 | Insulin-like growth factor binding protein 3 | 2,10 |
| 69 | Mdm2 | Transformed mouse 3T3 cell double minute 2 | 2,94 |
| 102 | Tnfrsf10b | Tumor necrosis factor receptor superfamily, member 10b (predicted) | 1,86 |
| 103 | Tnfrsf6 | Tumor necrosis factor receptor superfamily, member 6 | 2,75 |
| ***Estrogen Pathway*** | | | |
| ***Position*** | ***Gene Symbol*** | ***Gene Description*** | ***Fold change*** |
| 4 | Bcl2 | B-cell leukemia/lymphoma 2 | 3,09 |
| 12 | Brca1 | Breast cancer 1 | 2,78 |
| 54 | Igfbp4 | Insulin-like growth factor binding protein 4 | 3,40 |
| 80 | Pgr | Progesterone receptor | 1,98 |
| 106 | Trim25 | Tripartite motif protein 25 (mapped) | 2,20 |
| ***Retinoic Acid Pathway*** | | | |
| ***Position*** | ***Gene Symbol*** | ***Gene Description*** | ***Fold change*** |
| 46 | Hoxa1 | Homeo box A1 | 3,46 |
| 47 | Hoxb1 | Homeo box B1 (predicted) | 5,26 |
| 90 | Rbp1 | Retinol binding protein 1, cellular | 1,66 |
| 94 | Stra6 | Stimulated by retinoic acid gene 6 homolog (mouse) | 2,97 |

| *Androgen Pathway* | | | |
|---|---|---|---|
| ***Position*** | ***Gene Symbol*** | ***Gene Description*** | ***Fold change*** |
| 18 | Cdk2 | Cyclin dependent kinase 2 | 2,34 |
| 64 | Klkb1 | Kallikrein B, plasma 1 | 7,55 |
| 76 | Ngfg | Nerve growth factor, gamma | 2,58 |
| 100 | Tmprss9 | Transmembrane serine protease 9 (predicted) | 2,64 |
| ***Insuline Pathway*** | | | |
| ***Position*** | ***Gene Symbol*** | ***Gene Description*** | ***Fold change*** |
| 26 | Cebpb | CCAAT/enhancer binding protein (C/EBP), beta | 2,30 |
| 43 | Gys2 | Glycogen synthase 2 | 2,65 |
| 45 | Hk2 | Hexokinase 2 | 4,15 |
| 66 | Lep | Leptin | 3,50 |
| ***P13 Kinase/AKT Pathway*** | | | |
| ***Position*** | ***Gene Symbol*** | ***Gene Description*** | ***Fold change*** |
| 38 | Fn1 | Fibronectin 1 | 1,60 |
| 71 | Mmp7 | Matrix metallopeptidase 7 | 2,96 |
| 87 | Pten | Phosphatase and tensin homolog | 1,92 |
| ***LDL Pathway*** | | | |
| ***Position*** | ***Gene Symbol*** | ***Gene Description*** | ***Fold change*** |
| 13 | Ccl2 | Chemokine (C-C motif) ligand 2 | 2,63 |
| 92 | Sele | Selectin, endothelial cell | 1,95 |
| 93 | Selp | Selectin, platelet | 2,06 |
| ***Stress Pathway*** | | | |
| ***Position*** | ***Gene Symbol*** | ***Gene Description*** | ***Fold change*** |
| 2 | Atf2 | Activating transcription factor 2 | 1,52 |
| 48 | Hsf1 | Heat shock transcription factor 1 | 2,23 |
| ***Phospholipase C Pathway*** | | | |
| ***Position*** | ***Gene Symbol*** | ***Gene Description*** | ***Fold change*** |
| 63 | Junb | Jun-B oncogene | 4,24 |
| 88 | Ptgs2 | Prostaglandin-endoperoxide synthase 2 (Cox-2) | 1,70 |
| ***Mitogenic Pathway*** | | | |
| ***Position*** | ***Gene Symbol*** | ***Gene Description*** | ***Fold change*** |
| 73 | Nab2 | Ngfi-A binding protein 2 | 2,82 |
| ***Jak/Src Pathway*** | | | |
| ***Position*** | ***Gene Symbol*** | ***Gene Description*** | ***Fold change*** |
| 6 | Bcl2l1 | Bcl2-like 1 | 2,78 |

| *NFAT Pathway* | | | |
|---|---|---|---|
| ***Position*** | ***Gene Symbol*** | ***Gene Description*** | ***Fold change*** |
| 16 | Cd5 | CD5 antigen | 2,66 |
| ***CREB Pathway*** | | | |
| ***Position*** | ***Gene Symbol*** | ***Gene Description*** | ***Fold change*** |
| 32 | Cyp19a1 | Cytochrome P450, family 19, subfamily a, polypeptide 1 | 2,41 |

**Tab 5.5** List of all the over-expressed genes (Fold change ≥ 1.50) for the specifical biological pathway comparing Vigabatrin treaed Wag/rij 9 vs PBS treated Wg/Rij.

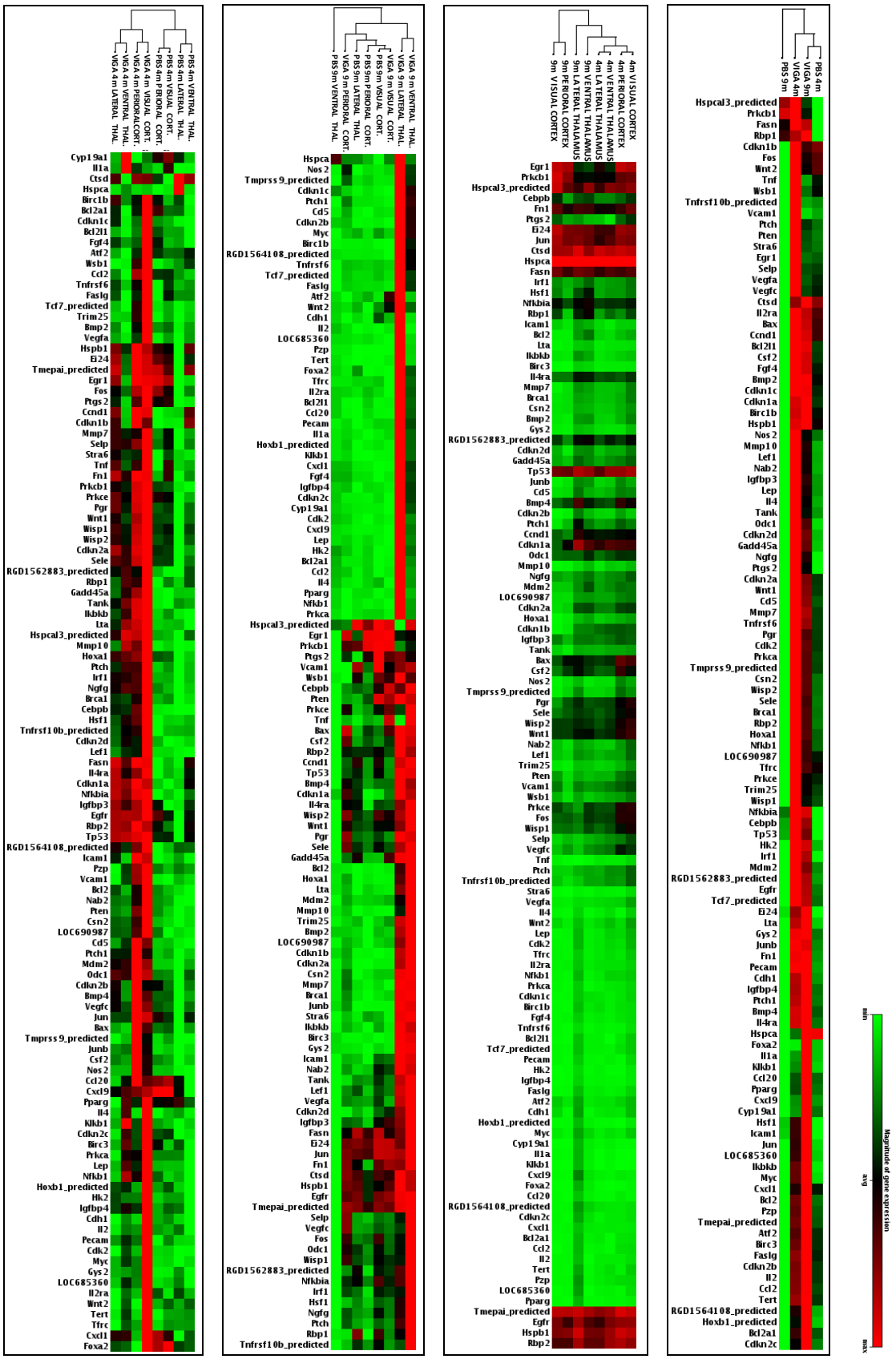


**Fig. 5.3** Clustergram shows the correlation of the genes across the sperimental groups in order to reveal changes in expressions associated to age of animals, treatment or different brain regions. Groups that have similar profile of expression are joined and showed on the top side of the dendogram, symbols of genes are along the left side.

# -6-

## EXPERIMENT 4; REAL TIME QUANTITATIVE PCR ANALYSIS (RT-qPCR)

### 6.1 INTRODUCTION TO EXPERIMENT 4

In order to validate the direction and magnitude of changes in gene expression indicated by microarray analyses, was performed real-time qPCR for analyze the expression of transcripts encoding B-cell CLL/lymphoma 2 (Bcl2), early growth response 1 (Egr1), fatty acid synthase (Fasn), tumor necrosis factor alpha (Tnf α) and tumor necrosis factor receptor superfamily, member 10b (Tnfrsf10b) .

### 6.2 MATERIAL AND METHODS

Wag/Rij treatmented with Vigabatrin (n=4; two 9 months and two 4 months) or saline (n=4; two 9 months and two 4 months) and tissues preparation and total RNA isolation were prompted in accordance with microarray experimental protocol (see experiment 3). Reverse transcription of the RNA was performed in 20 µL reaction volumes from 1.5 µg RNA using 200 ng of random primers, 4 µL 5x First strand buffer, 0.5 µL RNasi Hinibitor, 0.5mM of dNTP and 200U of MoMLV reverse-transcriptase (Superscript II). The cDNA synthesis was performed at 42˚C for 2 hour before inactivation at 70˚C for 10 minutes.

Primers pairs were designed with Primer3 software (Table 6.1). Amplification, data acquisition, and data analysis were carried out in the Biorad iQ5. Dissociation curves of PCR products were run to verify amplification of the correct product. For 25-µL reaction , 3 ng of cDNA template was mixed with 400 nM of each primer and iQ 2X SYBR Green Supermix (Biorad, Hercules CA) . The reaction was allowed to proceed for 90 seconds at 95 ˚C for for denaturation, followed by 55 cycles of 95 ˚C for 10 seconds and 62 ˚C for 30 seconds for annealing/extension. The comparative cycle threshold (Ct) method was used for relative quantification. Data were normalized to the levels of RNA encoding 18S as housekeeping gene. Relative differences were subsequently calculated using the $2^{-\Delta\Delta Ct}$ method (Livak and Schmittgen, 2001). The Threshold cycle (Ct) mean of any sample was compared with the Ct mean obtained for the control gene, so ΔCt = Ct (sample) – Ct (control). Then was calculated ΔΔCt per

groups ΔΔCT=ΔCT (target) –ΔCT (reference). (for example I want to see AGE EFFECT; ΔΔCt = ΔCt 9months-ΔCt 4months!). Fold change = $2^{-\Delta\Delta Ct}$.

| Gene | Forwad Primer 5' to 3' | Reverse Primer 5' to 3' |
|---|---|---|
| Egr1 | AGC AGC GCT TTC AAT CCT C | AGC GCC TTC TCG TTA TTC AG |
| Bcl2 | GAG CAG CGT CTT CAG AGA CA | GTG GAC AAC ATC GCT CTG TG |
| Fasn | AGC TGT TCC TCC AGC TCC TT | TTC TGA CCA GGT CCA GGA AG |
| Tnf α | GAC CCT CAC ACT CAG ATC ATC TTCT | TGC TAC GAC GTG GGC TACG |
| Tnfrsf10b | GCT GGT ACT GGC AAA TGG | CAT ATG CCG CAT GAG ACG |
| 18s | CGGCTACCACATCCAAGGAA | CCT GTA TTG TTA TTT TTC GTC ACT ACC T |
| **Egr1**, early growth response 1; **Bcl2**, B-cell CLL/lymphoma 2; **Fasn**, fatty acid synthase; **Tnf alpha**, tumor necrosis factor alpha, **Tnfrsf10b**, tumor necrosis factor receptor superfamily member 10b; **18s**, ribosomal subunit. | | |

**Tab 6.1** Sequence of primers used for real-time RT-PCR analyses

## 6.3 RESULTS

The RT-PCR analysis of the total RNA extracted from above-mentioned regions of the brain of Wag/Rij rats show that, there is a general tendency to validate the direction and magnitude of changes in gene expression indicated by microarray analyses. In table 6.2 are reported data obtained comparing all epileptic 9 months old rats with all non epileptic 4 months old rats (ignoring treatment and region). Moreover, in table 6.3 are reported data obtained comparing all Vigabatrin treated rats with all PBS treated rats.

| *Gene Symbol* | *Gene Description* | *Array Data* | *Real time qPCR* |
|---|---|---|---|
| | | *Fold Change ± st err* | *FOLD ($2^{-\Delta\Delta Ct}$) maen ± st err* |
| Bcl2 | B-cell leukemia/lymphoma 2 | 1,25 ± 0,74 (+25%) | 0,70 ± 0,24 (-30%) |
| Egr1 | Early growth response 1 | 0,85 ± 0,16 (-15%) | 0,56 ± 0,23 (-44%) |
| Fasn | Fatty acid synthase | 1,08 ± 0,12 (+8%) | 1,01 ± 0,21 (+1%) |
| Tnf | Tumor necrosis factor, α | 0,26 ± 0,12 (-74%) | 0,67 ± 0,17 (-33%) |
| Tnfrsf10b | Tnf receptor superfamily, member 10b | 0,49 ± 0,15 (-51%) | 0,99 ± 0,28 (-1%) |

**Tab 6.2** Data from Arraya and qPCR about the expression of five selected genes comparing all epileptic 9 months old rats with all non epileptic 4 months old rats. Data are reported as Fold Change mean ± st err.

| Gene Symbol | Gene Description | Array Data | Real time qPCR |
|---|---|---|---|
| | | Fold Change ± st err | FOLD ($2^{-\Delta\Delta Ct}$) maen ± st err |
| Bcl2 | B-cell leukemia/lymphoma 2 | 3,09 ± 2,99 (+309%) | 1,37 ± 0,43 (+37%) |
| Egr1 | Early growth response 1 | 1,16 ± 0,23 (+16%) | 1,10 ± 0,56 (+10%) |
| Fasn | Fatty acid synthase | 1,29 ± 0,18 (+29%) | 1.41 ± 0,42 (+41%) |
| Tnf | Tumor necrosis factor, α | 1,71 ± 0,71 (+71%) | 1,26 ± 0,47 (+26%) |
| Tnfrsf10b | Tnf receptor superfamily, member 10b | 1,86 ± 0,56 (+86%) | 1,94 ± 1,01 (+94%) |

**Tab 6.3** Data from Arraya and qPCR about the expression of five selected genes comparing all Vigabatrin treated rats with all PBS treated rats. Data are reported as Fold Change mean ± st err.

In order to point out the effect of Age of the animals on the expression of TNFα in any one of the specif considered brain region, in Table 6.4 are reported Array and qPCR results of expression of this pro-inflamamtoy mediator comparing all epileptic 9 months old rats with all non epileptic 4 months old rats.

| Brain region | Array Data | Real time qPCR |
|---|---|---|
| | Fold Change ± st err | FOLD ($2^{-\Delta\Delta Ct}$) maen ± st err |
| Somatosensory cortex (peri-oral area) | 0,21 ± 0,11 (-79%) | 0,73 ± 0,11 (-27%) |
| Visual cortex | 0,26 ± 0,25 (-74%) | 0,51 ± 0,09 (-49%) |
| Lateral thalamus | 0,10 ± 0,06 (-90%) | 0,61 ± 0,23(-39%) |
| Medial thalamus | 0,69 ± 0,49 (-31%) | 0,83 ± 0,11 (-17%) |

**Tab 6.4** Tnf-α expression from Arrays and qPCR four selected regions of interest comparing all epileptic 9 months old rats with all non epileptic 4 months old rats. Data are reported as Fold Change mean ± st err.

Moreover, in order to point out the effect of the Vigabatrin treatment on the expression of TNFα in in the four selected regions of interest, in Table 6.5 are reported Array and qPCR results of expression of this pro-inflamamtoy mediator comparing all Vigabatrin treated Wag/Rij rats vs all the PBS treated rats (ignoring age).

| Brain region | Array Data | Real time qPCR |
|---|---|---|
| | Fold Change ± st err | FOLD ($2^{-\Delta\Delta Ct}$) maen ± st err |
| Somatosensory cortex (peri-oral area) | 1,38 ± 0,66 (+38%) | 1,22 ± 0,54 (+22%) |
| Visual cortex | 1,71 ± 2,30 (+71%) | 1,15 ± 0,50 (+15%) |
| Lateral thalamus | 1,14 ± 0,89 (+14%) | 1,46 ± 0,32 (+46%) |
| Medial thalamus | 1,77 ± 0,97 (+77%) | 1,19 ± 0,10 (+19%) |

**Tab 6.5** Tnf-α expression from Arrays and qPCR four selected regions of interest comparing all Vigabatrin treated rats with all PBS treated rats. Data are reported as Fold Change mean ± st err.

# -7-

## EXPERIMENT 5: EEG RECORDING AFTER CITOKINES INJECTION

### 7.1 INTRODUCTION TO EXPERIMENT 5

The role of proinflammatory cytokines on SWDs was recently investigated in WAG/Rij rats by the administration of various doses of lipopolysaccarides (LPS) and an increase in SWDs was found (Kovacs et al., 2006). However, LPS induces and releases numerous proinflammatory mediators, e.g. IL-1β, TNF-α and IL-6. Here we want to establish separately the role of IL-1β, TNF-α on seizure activity; we have chosen these cytokines since they represent two classes of cytokines that are expressed in the central nervous system and are most widely studied in relation with epilepsy (Shandra et al., 2002; Banks et al., 2001).

In this experiment was investigated whether these cytokines when added exogenously had an effect on SWD's. Little is known about the duration, if any, of these effects after peripheral administration. Known is that there exists a diurnal rhythm in the expression of the effects of IL-1β and TNF-α and that various cytokines may trigger a cascade of events also effecting neuronal, endocrinological, behavioural parameters including the production of themselves (Rothwell and Hopkins, 1995; Szelényi, 2001). Therefore, the expression of SWD following systemic application was investigated for 72 hrs after its administration.

**This experiment, as part of a general collaborative agreement, has been performed independently by the group coordinated by Prof. G. van Luijtelaar (Radboud Nijmegen University, the Netherlands) and has been recently submitted for publication (van Luijtelaar et al., submitted).**

### 7.2 MATERIALS AND METHODS

The EEG studies in this experiment were carried out on 32 adult (9 –16 months) male WAG/Rij rats, weighing between 266-406 g. Rats lived under standard laboratory

conditions, housed in pairs before surgery, food and water ad lib available, room temperature was kept at 22-24 °C and a 24 h LD schedule with lights out from 7.00 to 19.00. After surgery, rats were individually housed in a Plexiglas cage (36*25*15 cm) suited for EEG recordings. Procedures involving animals and their care were conducted according to University guidelines that comply with international laws and policies concerning the use of the laboratory animals in the experimental trials (European Community Council Directive 86/609, OJ L 358, I, December 12, 1987). A local ethical committee (RU-DEC) approved the protocol.

*Surgical preparation*, three standard EEG electrodes (Plastic One, MS303/2) were stereotactically implanted under anesthesia with isoflurane (4.5% for induction and 2-2.5% for maintenance) in oxygen. The EEG-electrode set is fixated with acryl cement and two screws, which were placed bilaterally over the cortex. The experiments were performed at least 10 days after surgery.

*Experimental protocol*, rats were familiarized for 24 hours with the EEG recording leads that were connected to a swivel. Signals were amplified and filtered (low pass was set at 100 Hz, high pass at 1 Hz).

The recordings started immediately after the administration of the cytokines or solvent at 13.00 and persisted for 72 hrs. The behaviour of the rats was observed every day through a window from an adjacent room between 13.30 h till 15.30 h for half an hour per rat. Rats were injected i.p. with Interleukine-1β (2μg/kg in 2 ml), TNF-α (2μg/kg in 2 ml) or a bovine salt solution (0,5 % BSA in PBS)(2μg/kg in 2 ml) as control, group size n=9 to 11.

*Analysis of the EEG*, The EEG recordings were analysed with a custom made program that was previously validated. SWD were initially identified by this program and subsequently checked by a trained EEG analyst. Criteria for the detection of SWD can be found elsewhere (van Luijtelaar and Coenen, 1986). The cumulative amount of SWDs per hour is reported.

*Statistical analysis of the data*, the effects of the exogenous administration of cytokines on SWD were analysed with a repeated measures ANOVA with cytokine (3 levels) as between factor and time as a within subject factor. If necessary, univariate analysis was performed followed by Duncan's post hoc test ($\alpha<0.05$). Considering the large number

of variables (time points, hours) in relation to the number of animals, it was not possible to analyze all the EEG data in one large ANOVA. The effects of the cytokines might most likely occur in the first few hours after administration, therefore the first period (1-6) hours after injection (the dark period) and the remainder of the day, were analyzed per hour. The remainder of the recording period was subdivided into days with blocks of 2 hours.

## 7.3 RESULTS

The number of SWD as recorded over the 72 hr period in the control group is dominated by a circadian pattern with a peak in the number of SWDs in the dark period, and a smaller number in the light phase of the 24 hour light-dark cycle. A significant time-effect ($p<0.001$ and $p<0.05$ respectively) was found on day 2 and day 3. On both days the data could be described with a linear and cubic trend, suggesting that the changes over time were not due to chance and showed a maximum and minimum, reflecting the circadian distribution of SWDs.

The repeated measures ANOVA for the first 6 hours shows a time effect ($p<0.05$), a treatment effect ($p<0.01$) and a time x treatment-effect ($p<0.05$). The interaction prompted us to analyze the treatment effects per hour with an univariate analysis followed by post-hoc tests. These results are presented in Tab 7.1

The ANOVA for the first light period (7-18 hr post injection) showed a treatment effect ($p<0.01$). The subsequent post-hoc test showed that the duration of SWD was higher for the TNF-α than for the Il-1β and control group. There were no differences between the 2 groups at day 2 and 3.

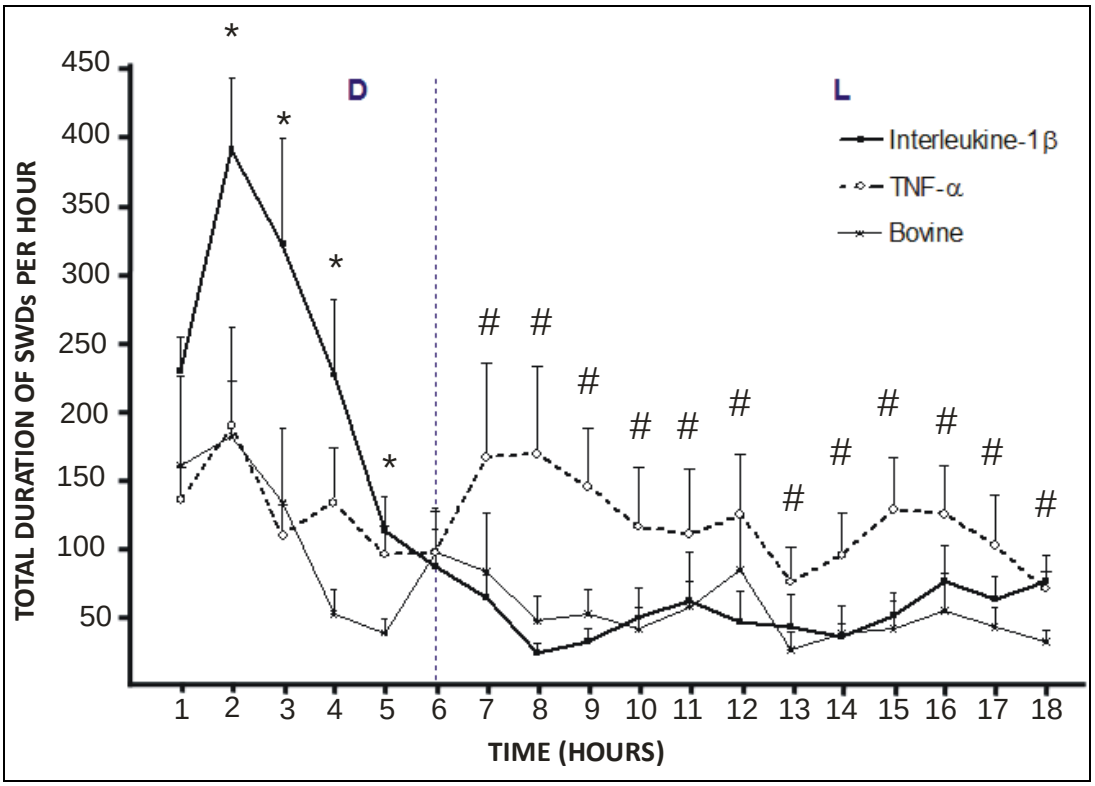


**Fig.7.1** Mean and St. errM of the total duration of SWD per hour as a function of time after injection of bovine, TNF-α and IL-1β. Note the immediate increase after IL-1β injection and the delayed increase of TNF-α in the subsequent light period (7-18 hrs after injection). D=dark period, L=light period. *; significative differently of IL-1β Vs Bovine ($p<0,05$), #; significative differently of TNF-α Vs Bovine ($p<0,05$)

| Hours | F-value | P value | Post-hoc |
|---|---|---|---|
| 0-1 | 4.26 | 0.021 | IL > Bov |
| 1-2 | 5.14 | 0.011 | IL > Bov, TNF |
| 2-3 | 3.64 | 0.044 | IL > Bov, TNF |
| 3-4 | 4.12 | 0.024 | IL > Bov, TNF |
| 4-5 | 8.63 | 0.001 | IL > Bov, TNF |
| 5-6 | 2.26 | n.s. | |

**Tab 7.1** Inferential statistics concerning the first 6 hours of the total duration of spike-wave discharges after injection of bovine, Il-1ß (Il) and TNF-α (TNF). The post-hoc tests revealed that IL-1β enhanced SWDs expression 1-5 hrs after its administration.

# -8-

## EXPERIMENT 6: CITOKINES CONCENTRATION IN BRAIN AND PLASMA

### 8.1 INTRODUCTION TO EXPERIMENT 6

In this experiment we established the role of these two cytokines in the pathogenesis of absence epilepsy by measuring their levels in brain and plasma at an age of 2, 4 and 6 months of age. Since cytokines are active during neural development as well as in the adult nervous system, both during normal function and in pathological conditions their role in causing SWD cannot be excluded at forehand.

**This experiment, as part of a general collaborative agreement, has been performed independently by the group coordinated by Prof. G. van Luijtelaar (Radboud Nijmegen University, the Netherlands) and has been recently submitted for publication (van Luijtelaar et al., submitted).**

### 8.2 MATERIALS AND METHODS

*ELISA methods*, 51 rats (25 ACI and 26 WAG/Rij) experimentally naïve were used in the ELISA study. Rats were 2, 4 and 6 months old. All rats were killed by decapitation and their brains were rapidly removed at $4^{o}$ C and frozen on dry ice. Brain tissue was weighted and homogenized in ice-cold PBS (5 gm/ml) using a Potter homogenizer (1000 rpm, 10 strokes). The homogenates were centrifuged for 10 min (5000 rpm, $4^{o}$ C). One hundred microliters of the supernatant were taken in duplicate to measure TNF-α and IL-1β content. TNF-α and IL-1β were determined using selective antibodies ("Biotrak" system from Amersham Pharmacia Biotech, USA). Absorbance was read at 405 nm. The detection limit was 4.0 pg/ml. The data are expressed in pg/mg of wet brain tissue. For each determination 0,416 mg of tissue was used in 50 mcl of investigated solution for IL-1β and ten times less- for TNF-α.

*Statistical analysis of the data,* the outcomes of the ELISA method were determined with MANOVA with strain (2 levels), age (3 levels) and operation (yes/no) as between subject variables. Since there were no main effects of operation nor interactions with

operations, the data were pooled in a final two way MANOVA, followed by univariate ANOVA's and post-hoc tests.

The number of SWDs as measured in the comparative study between 2 and 6 month WAG/Rij and ACI rats were analysed with ANOVA with strain and age as between group factors. Statistical analysis was done with SPSS version 10.0 for Windows. Graphics were made with Prism 3.0.

## 8.3 RESULTS

The data of the immunological investigations are presented in Tab 8.1. The overall ANOVA showed a strain x age effect ($p<0.05$). Univariate tests showed significant strain effect for TNFα serum levels ($p<0.05$; WAG/Rij > ACI) and an interaction between strain and age ($p<0.01$) and a similar interaction for TNFα in the brain ($p<0.01$). Subsequent post-hoc tests showed that plasma levels were higher in 2 months WAG/Rij vs age matched ACI's rats, and brain concentrations tented to be higher in 4 months old WAG/Rij rats ($p<0.01$). There were no differences in 6 months old rats.

| Strain | Indices under Investigation | Age of animals in months, (number of rats) | | |
|---|---|---|---|---|
| | | 2 | 4 | 6 |
| WAG/Rij | TNF-α, serum | 6,31 ± 2,0** (n=12) | 2,47 ± 0,89 (n=13) | 1,84 ± 0,94 (n=12) |
| | TNF-α, brain | 63,8 ± 2,6 (n=11) | 78,7 ± 8,4* (n=11) | 67,3 ± 3,2 (n=12) |
| | IL-1β, serum | 1,59 ± 0,78 (n=12) | 2,58 ± 0,74 (n=12) | 1,04 ± 0,53 (n=12) |
| | IL-1β, brain | 27,0 ± 2,8 (n=11) | 32,5 ± 3,8 (n=11) | 25,8 ± 1,7 (n=11) |
| ACI | TNF-α, serum | 0,61 ± 0,34 (n=12) | 3,53 ± 1,50 (n=12) | 1,27 ± 0,53 (n=13) |
| | TNF-α, brain | 70,3 ± 3,3 (n=11) | 62,2 ± 4,2 (n=11) | 62,3 ± 2,6 (n=11) |
| | IL-1β, serum | 1,79 ± 0,78 (n=12) | 1,96 ± 1,07 (n=12) | 1,54 ± 0,73 (n=12) |
| | IL-1β, brain | 30,9 ± 2,8 (n=11) | 31,7 ± 2,7 (n=10) | 29,2 ± 1,8 (n=12) |

**Tab. 8.1** Mean and SEM of TNF-α and IL-1β (pg/mg of wet brain tissue) content in serum and brain tissue of WAG/Rij and ACI rats at 2, 4 and 6 months of age; ** = $p<0.05$; * = $p<0.01$ - Significantly different from age matched ACI group. Two factor (Age and strain) ANOVA followed by post-hoc tests were used.

# -9-

## GENERAL DISCUSSION

Four leading theories endeavor to explain the origin of the generalized spike-wave discharges associated with absence seizures. 1) Penfield and Jasper (1954) put forward the "centrencephalic" theory, proposing that spike-wave discharges originate from a deeply located, subcortical pacemaker in upper brainstem and midline thalamus, this pacemaker having wide-spread projections to both sides of the cortex. 2) Buzsáki et al. (1988) proposed the "thalamic clock" theory, in which the reticular thalamic nucleus contains the pacemaker cells for the spike-wave discharges. It must be stressed that in these theories the cortex has only a passive function. 3) On the other hand, the "cortical" theory of Bancaud (1972) and Niedermeyer (1972) implies that the generalized spike-wave discharges originate from a focus, or foci, in the cortex. In this theory, subcortical structures are not essential for the generation of spike-wave discharges but only participate passively. 4) The 'corticoreticular' theory postulated by Gloor (1968, 1969) forms a bridge between the thalamic and cortical theories, implying that a hyperexcitable cortex responds abnormally to initially normal, thalamocortical volleys, thereby initiating, in such a way, abnormal thalamocortical oscillations. Thus, in all four views, a prerequisite for the occurrence of spike-wave discharges is a highly synchronized activity of thalamocortical or corticothalamic connections. The widespread, bilaterally synchronous spike-wave discharges are reflections of highly synchronized oscillations in thalamo–cortical–thalamic networks. Moreover, it now seems quite clear that the reticular thalamic nucleus is the driving force behind the generation of sleep spindles. Recently, Meeren et al. (2002) extensively studied the initiation and generalization of spike-wave discharges by describing the interrelationships between multisite cortical and thalamic field potentials recorded in freely moving WAG/Rij rats. Nonlinear association analysis revealed a consistent cortical "focus" within the perioral region of the somatosensory cortex. The spike-wave discharges recorded at other cortical sites consistently lagged behind this focal site, with time delays that increased with electrode distance. Intrathalamic relationships were more complex and could not account for the observed cortical propagation pattern. Cortical and thalamic sites interacted bidirectionally, whereas the direction of this coupling could vary throughout one seizure. However, during the first 500 ms, the

cortical focus was consistently found to precede the thalamus. These findings argue against the existence of one common subcortical pacemaker for the generation of generalized spike-wave discharges characteristic for absence seizures in the rat. Instead, the results suggest that a cortical focus is the dominant factor in initiating the paroxysmal oscillation within the corticothalamic loops, and that the large-scale synchronization is mediated by way of an extremely fast intracortical spread of seizure activity (Meeren et al., 2002). During the first cycles of a seizure the cortex drives the thalamus, which subsequently becomes entrained into the oscillation, thus maintaining the discharges. Once the oscillation has been set into motion, cortex and thalamus act as a unified oscillatory network. In brief, the cortex triggers the thalamus and the intact thalamus maintains the sustaining character of the discharge. The outcomes of the Meeren et al. (2002) studies provide evidence to formulate the hypothesis of a cortical focus that comprehensively drives corticothalamic networks during the occurrence of spontaneous spike-wave discharges in rats. Rather than being an aberrant form of spindle oscillations originating from the thalamus, spike-wave discharges appear to be a phenomenon that shares the general "focus-propagation-generalization" principle of cortical seizures. Moreover, independent component analyses of multisite cortical EEG recordings in absence epileptic patients have shown an early independent component in the frontal EEG (McKeown et al., 1999). Hence, the findings of Meeren et al. (2002), as well as those of McKeown et al. (1999), strongly challenge the concept of the "centrencephalic" theory of generalized absence epilepsy, but form, instead, a synthesis between the "cortical" and the "corticoreticular" theories. This "cortical-driven and thalamic-sustained" theory of the origin of spike-wave discharges, as proposed by Meeren et al. (2002), provides a new and interesting concept.

In order to raise the evidence of a focal cortical theory for absence epilepsy, we studied whether *structural* and *functional* damage or differences occurs in cerebral areas which are known more involved in absence epilepsy.

DWI alterations reflect pathological conditions in brain tissue that are only partially understood, and involve changes in the diffusion characteristics of intra- and extracellular water compartments, and water exchange across permeable boundaries (Gass et al., 2001). In general, alterations associated with acute vasogenic edema or tissue destruction usually show elevations of the DWI, while a reduction of the DWI has

been associated with acute cytotoxic edema (Gass et al., 2001). This may explain the present findings of decreased DWI value in the cortex of older rats if compare to younger ones, and the general lower DWI value after Vigabatrin treatment. Data observed in sub-cortical regions shows that DWI signal for lateral Thalamus is the lowest if compare to Hippocampus and medial Thalamus results.
Result of structural MRI analysis reveal an age dependent decrease of T2 values in somatosensory cortex (both supra- and sub-granula layer) and lateral thalamus, 3 regions involved in absence seizures. The decrease in T2 might indicate a decline in extracellular water. As alternative explanation, some authors suggest that an increased concentration of paramagnetic deoxyhemoglobin causes a decrease in T2 (Lei et al., 2003). This so-called negative BOLD effect has been shown to occur in MR studies of hypoxic hypoxia in the rat. Deoxyhemoglobin increases in situations in which the metabolic requirement for oxygen is not met by the delivery of oxygen.

Result of functional MRI reveal a general cortical decrease of rCBV after Vigabatrin treatment. Moreover, referred to subcortical data, lateral thalamus have the lowest value of rCBV. A reduction in rCBV might be a consequence of edema, resulting from imbalance of water distribution, vascular alteration or perivascular inflammation, which causes vessel compression (Nawashiro et al., 1994).
Our data indicates an increase of rCBF in all the cortical and subcortical regions in oldest epileptic animals. The increase in rCBF was hypothesized to be primarily because of increased glucose metabolism, resulting from increased inflammatory cell activation (Juhler and Paulson, 1986).

Gene array and real time RT-PCR data and Elisa analysis demonstrate a general age-related down-regulation of Tnf-α in all the four cerebral areas considered in our studies, so a general tone decrease of this mediator in the brain of epileptic animals could be present.
Regarding real time RT-PCR, data related to the expression of Tnf-α are very interesting. Results seem to attest that somatosensory cortex and visual cortex are involved in different way. Results point out a minor age-related down-regulation of Tnf-α in the peri-oral area than in the visual cortex. The same gene is also more up-regulated

in the somatosensory cortex and in lateral thalamus than in the other two brain regions after Vigabatrin treatment (which results in a increase of seizures).

It is important to note the up regulation of IL1α in the oldest epileptic Wag/Rij rats and also after vigabatrin treatment. IL-1α, IL-1β, together with IL-1 Receptor antagonist (IL-1RA) are mebers of IL1 superfamily. For the most part, IL-1α, IL-1β bind to the same cellular receptor. This receptor is composed of two related, but non-identical, subunits that transmit intracellular signals via a pathway that is mostly shared with certain other receptors. IL1α and IL-1β and also Tnf- α signals are amediated by NF-κB (nuclear factor kappa-light-chain-enhancer of activated B cells) patway. In particular, Tnf-α and IL-1β dose-dependently inhibited astrocyte glutamate uptake (Hu et al., 2000; Danbolt, 2001). NF-κB is a protein complex that controls the transcription of DNA and is found in almost all animal cell types and is involved in cellular responses to stimuli such as stress, cytokines, free radicals, ultraviolet irradiation, oxidized LDL, and bacterial or viral antigens. NF-κB plays a key role in regulating the immune response to infection. Conversely, incorrect regulation of NF-κB has been linked to cancer, inflammatory and autoimmune diseases, septic shock, viral infection, and improper immune development. NF-κB has also been implicated in processes of synaptic plasticity and memory and data presented in this study seems to demonstrate that it's the most involved signal-transduction patway in Wag/Rij animal model of absence epilepsy.

One of the main goals of this study was to establish a relationship between the cytokine IL-1β and TNF-α and absence epilepsy. We choose the WAG/Rij model for that purpose. The outcomes of the experiment 5, in which TNF-α and IL-1β were administered i.p. and the effects on SWD were determined in a 72 hour period, show an immediate and short lasting increase on SWD of IL-1β and a delayed increase in SWD after TNF-α. The intraperitoneal route of IL-1β and TNF-α administration was chosen since it has been established that cytokines reach the CNS directly by crossing at leaky areas the BBB through the circumventricular organs even in healthy, basal conditions (Shandra et al., 2002; Banks et al., 2001). In agreement with data as obtained in models of focal onset, fever or infection related (Vezzani and Granata, 2005) and in the same genetic model after the administration of LPS (Kovacs et al., 2006), IL-1β aggravated absence seizures. The present outcomes demonstrate also that the acute effects, as found

after bacterial LPS were not due to TNF-α, but to either IL-1β or to other non-tested cytokines.

The effects of IL-1β on the cumulative duration of SWD occurred rather quickly, in the first few hours after its peripheral administration. Its fast onset suggests a direct effect, while the effects after LPS occurred after 90 till 270 min. It is known that IL-1β induces its own synthesis and the synthesis of IL-6 and TNF-α in the central nervous system, mainly in astrocytes and microglia (Vezzani et al., 1999). It is not known whether IL-6 modulates SWD, however, TNF-α had only a delayed effect, the increase of SWD occurred only after 7-18 hours after the administration. Interestingly, LPS has time dependent effects on the production of TNF-α: its reaches a peak concentration 6h post treatment in a rat glial cell culture (Shemi et al., 2000). Since a direct effect on SWDs is not taking place after TNF-α, another physiological or hormonal mechanism might be at work here. Interestingly, the bioavailability and gene expression of TNF-α has a circadian rhythm with peak levels at the beginning of the light period (Krueger et al., 1998). At specifically these hours of the 24 h light dark cycle, the number of SWD is usually quite low (van Luijtelaar and Coenen, 1988; van Luijtelaar et al., 2001). These two facts suggest an inverse relationship between SWD and TNF-α levels. We consider this as another argument for our suggestion that it is not TNF-α itself that is responsible for the increase but another factor, perhaps IL-1β itself since this interleukin has SWD enhancing effects. We propose that the effects of TNF-α on SWDs are not mediated by TNF-α, but by another unknown factor.

The mechanisms through which the cytokines affect SWD activity by interfering with neurotransmitters of hormones in rats are multiple. The action of IL-1β may involve an increase in or facilitation of glutamatergic function through NMDA receptors. Activation of glutamate receptors of the NMDA subtype leads to an increase in depolarisation and burst firing of neurons. It is known that various types of NMDA agonists enhance SWD (Peeters et al., 1990). IL-1β may also directly enhance NMDA receptor function, because IL-1β receptors are associated with signal transduction pathways known to affect the response of NMDA receptors to endogenous ligands (Vezzani et al., 1999). The NMDA receptor requires both binding of glutamate and depolarization to allow entry of $Ca^{2+}$ into the cell. The pattern of excitation/inhibition provokes a massive calcium entry that specifically activates $Ca^{2+}$ dependent molecular

gates in thalamo-cortical cells involved in burst firing characterizing SWD (Sejnowski and Destexhe, 2000). Depolarizing pulses of $Ca^{2+}$ that enter the thalamic and cortical neurons may influence membrane excitability and enzyme cascades. So, IL-1β may have an effect on $Ca^{2+}$ increase in bursting cells by mediating their NMDA receptors. $Ca^{2+}$ would then be available in the cell for the generation of bursting patterns and perhaps for protein synthesis.

The delayed effects of TNF-α might be also be explained by the inhibitory effect of TNF-α on glutamate uptake (Pickering et al., 2005). A decrease in glutamate uptake increased extracellular glutamate level, which in turn resulted in glutamate-induced cell swelling; brain edema occurs commonly in epilepsy (Chang et al., 2001). Glutamate cannot enter the cell as long as TNF-α has its inhibiting effect. Brain tissue is known to have a remarkable ability to store glutamate (Danbolt, 2001). The only way this glutamate will be removed is through the working of transporter proteins, which provide glutamate to the cell for synthesis of e.g. GABA and energy production. The concentration transporter proteins will be at a relatively low level in contrast with the sudden enormous increase of extracellular glutamate after TNF-α injection. The TNF-α effect has worn out, after approximately 5-6 hours, just like IL-1β, while the concentration transporter proteins has increased because of the high abundance of glutamate. Now the accumulated glutamate massively enters the cell and has a positively effect on the occurrence of SWD on a cortical level. This hypothesis is feasible considering than NMDA aggravates SWD in WAG/Rij rats (Peeters et al., 1990; Filakovszky et al., 1999). This effect may last about 12 hours until the concentration glutamate transporters will return to basal levels.

It is also quite well possible that the presently found increase in SWDs is due to non-specific effects induced by the cytokines. Beside their well-known actions including effects on the HPA axis, fever responses, and somnogenic effects. Some of these factors have well described effects on the occurrence of SWDs. Corticosteroids and stress facilitate the occurrence of SWD (Schridde and van Luijtelaar, 2004; Tolmacheva and van Luijtelaar, 2006), while corticosteroids also induce β-endorphin release. β-endorphin is known to enhance the mu- and delta-opioid receptors, the mu-opioid receptor agonist DAMGO increased SWD in WAG/Rij rats (Przewlocka et al., 1998). Larger concentrations of TNF-α were found in plasma of WAG/Rij vs ACI rats

(irrespective of age), next to an age-dependent strain differences. The serum level of TNF-α was enhanced in young WAG/Rij rats preceding the onset of SWDs, the brain concentration tended to be increased in WAG/Rij rats when rats were 4 months of age. When SWD were fully developed at 6 months of age, there were no longer differences between the two strains. Therefore, in all, there is some evidence that TNF-α might be involved in the pathogenesis of absence seizures in WAG/Rij rats, IL-1β not. This cytokine plays a crucial role in more dramatic forms of epilepsy such as status epilepsy, or kindling. The strain difference, the large concentration of TNF-α in pre-epileptic rats and the somewhat increased brain concentrations in 4 months old rats might be considered as a form of neuroprotection towards the changes from a pro-epileptic to an epileptoformic brain. Neuroprotective effects for cytokines have been proposed e.g. by Peltola et al. (1998). Plata Salaman (2000) proposed that cytokines play a role in adaptive mechanisms associated with generalized seizure activity with implications for neuroprotection.

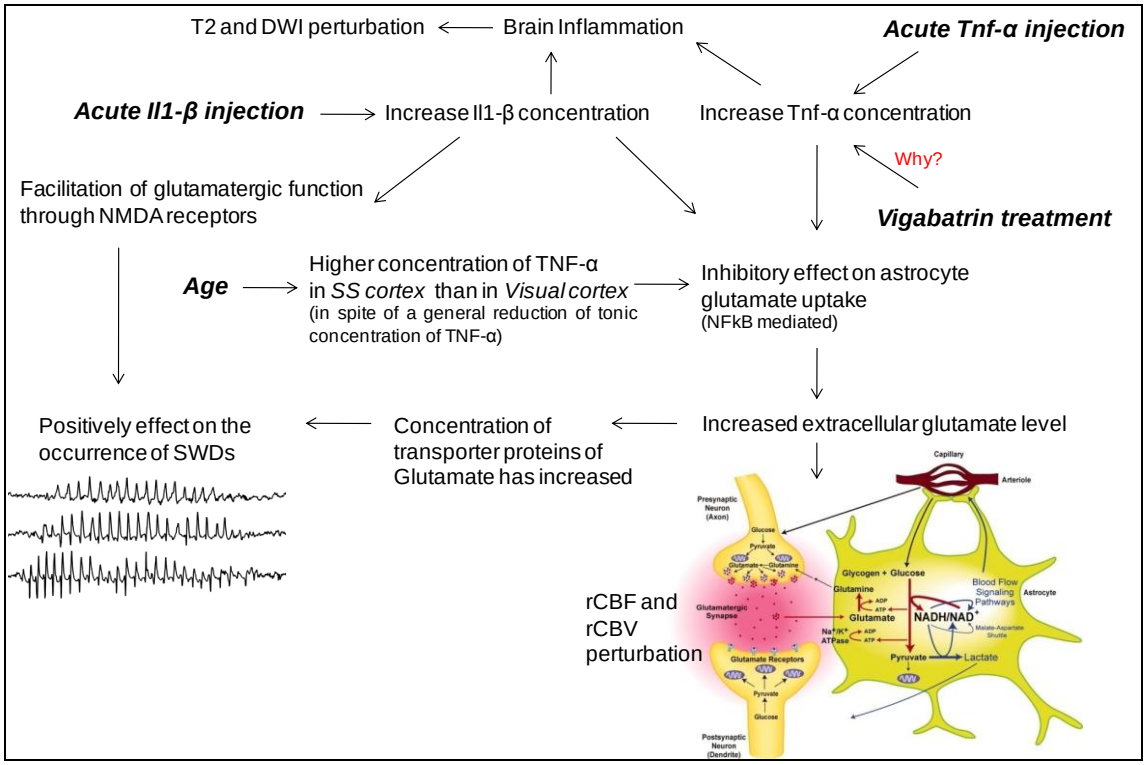


**Fig. 9.1** Schematic representation of possible pathways involved in the aetiopathogenesis of absence epilepsy, as deduced by the data reported in the present thesis. In particular, the possible neuromodulator role of inflammatory players like IL-1B and TNF-a are discussed. Many questions need still to be answered; for example, how Vigabatrin treatment induces a TNF-a increase. Further experiments have been planned and are currently ongoing in our laboratory.

**ACKNOWLEDGEMENTS**

I have worked with a great number of people whose contribution in assorted ways to the research and the making of the thesis deserved special mention. It is a pleasure to convey my gratitude to them all in my humble acknowledgment.

In the first place I would like to record my gratitude to Paolo Fabene for his supervision, advice, and professional guidance from the very early stage of this research as well as giving me extraordinary support through out the work. His truly scientific intuition has made him as a constant oasis of ideas and passions in science, which exceptionally inspire and enrich my growth as a student, a researcher and a scientist (..who I'd like to be). I am indebted to him more than he knows.

I gratefully acknowledge Prof. Gilles van Luijtelaar for his advice and crucial contribution, which made him a cornerstone of this research and so of this thesis.

It is a pleasure to express my gratitude to the staff of the laboratory coordinated by Prof. Fabene, composed by close friends more than colleagues, this thesis would certainly not have existed without them: Federica Schio, Rita Lodico, Lara Zanetti, Graciela Navarro Mora, Asmaa Chakir, Serena Becchi and Manuela Teti.

A special thanks goes to Daniele Peroni, Ilaria Scambi and Marta Bonaconsa for creating such a great friendship at the office and for the beautiful time we spend together every day.

Thanks are also due to the other scientific, technical and administrative personnel of the section of Anatomy and Histology of the Department of Morphological and Biomedical Sciences of the University of Verona, for their support during the studies presented in this thesis.

I am heartily thankful to all my friends and all the people whose presence in my life is a constant source of support, emotions and happiness.

Words fail me to express my appreciation to my family, whose dedication, love and persistent confidence in me, has taken the load off my shoulder…this thesis is dedicated to you!!!

Finally, I would like to thank everybody who was important to the successful realization of thesis, as well as expressing my apology that I could not mention personally one by one.

## REFERENCES


Adie, W.J., 1924. Pycnolepsy: a form of epilepsy occuring in children with good prognosis. Brain 47, 96–102.

Aghakhani, Y., Bagshaw, A.P., Benar, C.G., Hawco, C., Andermann, F., Dubeau, F., Gotman, J., 2004. fMRI activation during spike and wave discharges in idiopathic generalized epilepsy. Brain 127, 1127–1144.

Ahissar, E., Haidarliu, S., Zacksenhouse, M., 1997. Decoding temporally encoded sensory input by cortical oscillations and thalamic phase comparators. Proceedings of the National Academy of Sciences of USA 94, 11633–11638.

Ajmone-Marsan, C., 1965. The thalamus. Data on its functional anatomy and on some aspects of thalamo-cortical integration. Archives of Italiennes de Biologie 103, 847–882.

Aker, R.G., O¨ zkara, C., Dervent, A., Onat, F.Y., 2002. Enhancement of spike and wave discharges by microinjection of bicuculline into the reticular nucleus of rats with absence epilepsy. Neuroscience Letters 322, 71–74.

Amor, F., Navarro, V., N'Diaye, K., Garnero, L., Martinerie, J., Le van Quyen, M., 2005. Cortical synchronisation before generalised absence seizure: a magneto-encephalographic study. Epilepsia 46, 379.

Avanzini, G., de Curtis, M., Marescaux, C., Panzica, F., Spreafico, R., Vergnes, M., 1992. Role of the thalamic reticular nucleus in the generation of rhythmic thalamo-cortical activities subserving spike and waves. Journal of Neural Transmission 35 (Suppl.), 85–95.

Avanzini, G., Vergnes, M., Spreafico, R., Marescaux, C., 1993. Calcium dependent regulation of genetically determined spike and waves by the RTN of rats. Epilepsia 34, 1–7.

Avanzini, G., de Curtis, M., Franceschetti, S., Sancini, G., Spreafico, R., 1996. Cortical versus thalamic mechanisms underlying spike and wave discharges in GAERS. Epilepsy Research 26, 37–44.

Avanzini, G., Panzica, F., de Curtis, M., 2000. The role of the thalamus in vigilance and epileptogenic mechanisms. Clinical Neurophysiology 111 (S2), S19–S26.

Avoli, M., Gloor, P., 1981. The effects of transient functional depression of the thalamus on spindles and on bilateral synchronous epileptic discharges of feline generalized penicillin epilepsy. Epilepsia 22, 443–452.

Avoli, M., Gloor, P., 1982. Role of the thalamus in generalized penicillin epilepsy: observations on decorticated cats. Experimental Neurology 77, 386–402.

Bancaud, J., 1969. Physiopathogenesis of generalized epilepsies of organic nature (Stereoencephalographic study). In: Gastaut, H., Jasper, H.H.,

Bancaud, J., Waltregny, A. (Eds.), The Physiopathogenesis of the Epilepsies. Charles C. Thomas, Springfield, IL, pp. 158–185.

Bancaud, J., 1971. Role of the cerebral cortex in (generalized) epilepsy of organic origin. Contribution of stereoelectroencephalographic investigations (S.E.E.G.) to discussion of the centrencephalic concept. Presse Medicale 79, 669–673.

Bancaud, J. Mechanisms of cortical discharges in 'generalized'epilepsies in man. In H. Petsche and M. A. B. Brazier (eds.),1972. Synchronization of EEG activity in epilepsies, (pp. 368–381) New York: Springer

Bancaud, J., Talairach, J., Morel, P., Bresson, M., Bonis, A., Geier, S., Hemon, E., Buser, P., 1974. ''Generalized'' epileptic seizures elicited by electrical stimulation of the frontal lobe in man. Electroencephalography and Clinical Neurophysiology 37, 275–282.

Bauer, J., 1996. Seizure-inducing effects of antiepileptic drugs: a review. Acta Neurologica Scandinavica 94, 367–377.

Berkovic, S.F., Andermann, F., Andermann, E., Gloor, P., 1987. Concepts of absence epilepsies: discrete syndromes or biological continuum? Neurology 37, 993–1000.

Blumenfeld, H., 2005. Cellular and network mechanisms of spike-wave seizures. Epilepsia 46 (S9), S21–S33.

Bosnyakova, D., Gabova, A., Kuznetsova, G., Obukhov, Y., Midzyanovskaya, I., Salonin, D., van Rijn, C., Coenen, A., Tuomisto, L., van Luijtelaar, G., 2006. Time-frequency analysis of spike-wave discharges using a modified wavelet transform. Journal of Neuroscience Methods

Bouwman, B.M., Heesen, E., van Rijn, C.M., 2004. The interaction between vigabatrin and diazepam on the electroencephalogram during active behaviour in rats: an isobolic analysis. European Journal of Pharmacology 495, 119–128.

Brailowsky, S., Montiel, T., Boehrer, A., Marescaux, C., Vergnes, M., 1999. Susceptibility to focal and generalized seizures in Wistar rats with genetic absence-like epilepsy. Neuroscience 93, 1173–1177.

Buzsaki, G., Smith, A., Berger, S., Fisher, L.J., Gage, F.H., 1990. Petit mal epilepsy and parkinsonian tremor: hypothesis of a common pacemaker. Neuroscience 36, 1–14.

Berg, A.T., et al., 1999. Newly diagnosed epilepsy in children: presentation at diagnosis. Epilepsia 40, 445–452.

Blom, S., et al., 1978. Incidence of epilepsy in children: a follow-up study three years after the first seizure. Epilepsia 19, 343–350.

Broicher T, Kanyshkova T, Meuth P, Pape HC, Budde T, 2008. Correlation of T-channel coding gene expression, IT, and the low threshold Ca2+ spike in the thalamus of a rat model of absence epilepsy. Mol Cell Neurosci. Nov;39(3):384-99.

Buzsáki, G., Bickford, R. G., Ponomareff, G., Thal, L. J., Mandel,R., and Gage, F. H., 1988. Nucleus basalis and thalamic control of neocortical activity in the freely moving rat. J Neurosci. 8:4007–4026.

Caddick, S.J., Hosford, D.A., 1996. The role of GABAB mechanisms in animal models of absence seizures. Molecular Neurobiology 13, 23–32.

Callenbach, P.M., et al., 1998. Familial occurrence of epilepsy in children with newly diagnosed multiple seizures: Dutch Study of Epilepsy in Childhood. Epilepsia 39, 331–336.

Calmeil, L.F., 1824. De l'epilepsie etudiee sous le rapport de son siege et de son influence sur la production de l'alienation mental. Thesis, Paris.

Caplan, R., Arbelle, S., Magharious, W., Guthrie, D., Komo, S., Shields, W.D., Chayasirisobhon, S., Hansen, R., 1998. Psychopathology in pediatric complex partial and primary generalized epilepsy. Dev. Med. Child Neurol. 40, 805–811.

Caplan, R., Siddarth, P., Gurbani, S., Hanson, R., Sankar, R., Shields, W.D., 2005. Depression and anxiety disorders in pediatric epilepsy. Epilepsia 46, 720–730.

Capovilla, G., et al., 2001. A clinical spectrum of the myoclonic manifestations associated with typical absences in childhood absence epilepsy. A video-polygraphic study. Epileptic Disord. 3, 57–62.

Celio, M.R., 1986. Parvalbumin in most gamma-aminobutyric acidcontaining neurons of the rat cerebral cortex. Science 231, 995–997.

Challis, R.E., Kitney, R.I., 1991. Biomedical signal processing (in four parts). Part 3. The power spectrum and coherence function. Medical & Biological Engineering & Computing 29, 225–241.

Chen, Y., Lu, J., Pan, H., Zhang, Y., Wu, H., Xu, K., Liu, X., Jiang, Y., Bao, X., Yao, Z., Ding, K., Lo, W.H., Qiang, B., Chan, P., Shen, Y., Wu, X., 2003. Association between genetic variation of CACNA1H and childhood absence epilepsy. Annals of Neurology 54, 239–243.

Cocito, L., Primavera, A., 1998. Vigabatrin aggravates absences and absence status. Neurology 51, 1519–1520.

Coenen, A.M., van Luijtelaar, E.L., 1987. The WAG/Rij rat model for absence epilepsy: age and sex factors. Epilepsy Research 1, 297–301

Coenen, A.M., Drinkenburg, W.H., Peeters, B.W., Vossen, J.M., van Luijtelaar, E.L., 1991. Absence epilepsy and the level of vigilance in rats of the WAG/Rij strain. Neuroscience and Biobehavioral Reviews 15, 259–263.

Coenen, A.M.L., 1995. Neuronal activities underlying the electroencephalogram and evoked potentials of sleeping and waking: implications for information processing. Neuroscience and Biobehavioral Reviews 19, 447–463.

Coenen, A.M.L., Blezer, E.H.M., van Luijtelaar, E.L.J.M., 1995. Effects of the GABA-uptake inhibitor tiagabine on electroencephalogram. Epilepsy Research 21, 89–94.

Coenen AML, van Luijtelaar ELJM., 1997. The WAG/Rij rat model for absence epilepsy: age and sex factors. Epilepsy Res. ;1:297–301.

Coenen AML, Drinkenburg WHIM, Inoue M, et al., 1992. Genetic models of absence epilepsy, with emphasis on the WAG/Rij strain of rats. Epilepsy Res;12:75–86.

Coenen AML and E. L. J. M. van Luijtelaar., 2003. Genetic Animal Models for Absence Epilepsy:A Review of the WAG/Rij Strain of Rats. Behavior Genetics, Vol. 33, No. 6,

Connors, B.W., Gutnick, M.J., 1990. Intrinsic firing patterns of diverse neocortical neurons. Trends in Neurosciences 13, 99–104.

Crunelli, V., Leresche, N., 2002. Childhood absence epilepsy: genes, channels, neurons and networks. Nature Reviews Neuroscience 3, 371–382.

Danober, L., Deransart, C., Depaulis, A., Vergnes, M., Marescaux, C., 1998. Pathophysiological mechanisms of genetic absence epilepsy in the rat. Prog. Neurobiol. 55,27–57.

D'Antuono, M., Inaba, Y., Biagini, G., D'Argancelo, V., Avoli, M., 2006. Synaptic hyperexcitability of deep layer neocortical cells in a genetic model of absence epilepsy. Genes, Brain and Behavior 5, 73–84.

Davies, S., Heyman, I., Goodman, R., 2003. A population survey of mental health problems in children with epilepsy. Dev. Med. Child Neurol. 45, 292–295.

de Bruin, N.M., van Luijtelaar, E.L., Cools, A.R., Ellenbroek, B.A., 2001. Auditory information processing in rat genotypes with different dopaminergic properties. Psychopharmacology (Berlin) 156, 352–359.

de Bruin, N. M., van Luijtelaar, E. L., Cools, A. R., and Ellenbroek, B. A., 2001. Dopamine characteristics in rat genotypes with distinct susceptibility to epileptic activity: pomorphineinduced stereotyped gnawing and novelty/amphetamine-induced locomotor stimulation. Behav. Pharmacol. 12:517–525.

Depaulis, A., van Luijtelaar, G., 2006. Genetic models of absence epilepsy in the rat. In: Pitkanen, A., Schwartzkroin, P., Moshe, S. (Eds.), Models of Seizures and Epilepsy. Elsevier Inc, San Diego, CA, pp. 233–248.

Deschenes, M., Veinante, P., Zhang, Z.W., 1998. The organization of corticothalamic projections: reciprocity versus parity. Brain Research and Brain Research Review 28, 286–308.

Destexhe, A., Sejnowski, T.J., 2002. The initiation of burst in thalamic neurons and the cortical control of thalamic sensitivity. Philosophical Transactions of the Royal Society of London B 357, 1649–1657.

Drinkenburg, W.H., Coenen, A.M., Vossen, J.M., van Luijtelaar, E.L., 1991. Spike-wave discharges and sleep–wake states in rats with absence epilepsy. Epilepsy Research 9, 218–224.

Drinkenburg, W.H., van Luijtelaar, E.L., van Schaijk, W.J., Coenen, A.M., 1993. Aberrant transients in the EEG of epileptic rats: a spectral analytical approach. Physiology & Behavior 54, 779–783.

Drinkenburg, W.H., Schuurmans, M.L., Coenen, A.M., Vossen, J.M., van Luijtelaar, E.L., 2003. Ictal stimulus processing during spike-wave discharges in genetic epileptic rats. Behavioral and Brain Research 143, 141–146.

Esquirol,, J., 1838. De l' epilepsie. Traite des Maladies Mentale. Bailliere Publishers, Paris, p. 355. Fellous, J.M., Houweling, A.R., Modi, R.H., Rao, R.P., Tiesinga, P.H., Sejnowski, T.J., 2001. Frequency dependence of spike timing reliability in cortical pyramidal cells and interneurons. Journal of Neurophysiology 85, 1782–1787.

Ferrie, C.D., et al., 1995. Lamotrigine as an add-on drug in typical absence seizures. Acta Neurol. Scand. 91, 200–202.

Festing, M. F., and Bender, K., 1984. Genetic relationships between inbred strains of rats: An analysis based on genetic markers at 28 biochemical loci. Genet Res. 44:271–281.

Flint, A.C., Connors, B.W., 1996. Two types of network oscillations in neocortex mediated by distinct glutamate receptor subtypes and neuronal populations. Journal of Neurophysiology 75, 951–957.

Forsgren, I., et al., 2005a. Cost of epilepsy in Europe. Eur. J. Neurol. 12, 54–58.

Forsgren, L., et al., 2005b. The epidemiology of epilepsy in Europe a systematic review. Eur. J. Neurol. 12, 245–253.

Friedmann, M, 1906. Über die nichtepileptischen Absencen oder kurzen narkoleptischen Anfälle. Dtsch. Z. Nervenheilkd. 30, 462–492.

Gandolfo, G., Romettino, S., Gottesmann, C., van Luijtelaar, G.,Coenen, A., Bidard, J. N., and Lazdunski, M., 1989. $K^+$ channel openers decrease seizures in genetically epileptic rats. Eur. J. Pharmacol. 167:181–183

Gardiner M., 2005. Genetics of idiopathic generalized epilepsies. Epilepsia.;46 Suppl 9:15-20.

Gastaut, H., 1970. Clinical and electroencephalographical classification of epileptic seizures. Epilepsia 17,102–113.

Gauguier, D., van Luijtelaar, G., Bihoreau, M.T., Wilder, S.P., Godfrey, R.F., Vossen, J., Coenen, A., Cox, R.D., 2004. Chromosomal mapping of genetic loci controlling absence epilepsy phenotypes in the WAG/Rij rat. Epilepsia 45, 908–915.

Genton, P., Guerrini, R., Perucca, E., 2001. Tiagabine in clinical practice. Epilepsia 42 (S3), 42–45.

Gibbs, F.A., Gibbs, E.L., 1935. Atlas of Electroencephalography. Addison-Wesley, Cambridge, MA.

Gibbs FA, Davis H, Lennox WG., 1935. The electroencephalogram in epilepsy and in conditions of impaired consciousness. Arch Neurol Psychiatr 34:1133–1148

Gloor, P.,1968. Generalized cortico-reticular epilepsies: Some considerations on the pathophysiology of generalized bilaterally synchronous spike and wave discharge. Epilepsia 9:249–263

Gloor, P., 1969. Epileptogenic action of penicillin. Ann. NY Acad. Sci. 166:350–360.

Gloor, P., 1979. Generalized epilepsy with spike-and-wave discharge: a reinterpretation of its electrographic and clinical manifestations. The 1977 William G. Lennox Lecture, American Epilepsy Society. Epilepsia 20, 571–588.

Gloor, P., 1986. Consciousness as a neurological concept in epileptology: a critical review. Epilepsia 27 (S2), S14–S26.

Gloor, P., Fariello, R.G., 1988. Generalized epilepsy: some of its cellular mechanisms differ from those of focal epilepsy. Trends in Neuroscience 11, 63–68.

Gloor, P., Pellegrini, A., Kostopoulos, G.K., 1979. Effects of changes in cortical excitability upon the epileptic bursts in generalized penicillin epilepsy of the cat. Electroencephalography and Clinical Neurophysiology 46, 274–289.

Gloor, P., Avoli, M., Kostopoulos, G., 1990. Thalamo-cortical relationships in generalized epilepsy with bilaterally synchronous spike-andwave discharge. In: Avoli, M., Gloor, P., Naquet, R., Kostopoulos, G. (Eds.), Generalized Epilepsy: Neurobiological Approaches. Birkha¨ user Boston Inc., Boston, pp. 190–212.

Golshani, P., Liu, X.B., Jones, E.G., 2001. Differences in quantal amplitude reflect GluR4- subunit number at corticothalamic synapses on two populations of thalamic neurons. Proceedings of the National Academy of Sciences of USA 98, 4172–4177.

Gowers, W.R., 1881. Epilepsies and Other Chronic Convulsive Diseases: Their Causes, Symptoms and Treatment. JA Churchill, London.

Gray, C.M., McCormick, D.A., 1996. Chattering cells: superficial pyramidal neurons contributing to the generation of synchronous oscillations in the visual cortex. Science 274, 109–113.

Guerrini, R., 2005. Myoclonic astatic epilepsy. In: Roger, J., Bureau, M., Dravet, C., Genton, P, Tassinari, C.A., Wolf, P. (Eds.), Epileptic Syndromes in Infancy, Childhood and Adolescence. John Libbey, London, pp. 115–124.

Guerrini, R., et al., 1998. Antiepileptic drug-induced worsening of seizures in children. Epilepsia 39 (Suppl. 3), S2–10.

Gurbanova, A.A., Aker, R., Berkman, K., Onat, K.Y., van Rijn, C.M., van Luijtelaar, G. Effects of systemic and intracortical administration of phenytoin in two genetic models of absence epilepsy. British Journal of Pharmacology, in press.

Harrington, G. M., 1972. Strain differences in open-field behavior of the rat. Psychon. Sci. 27:51–53.

Hahn, A., et al., 2001. Atypical "benign" partial epilepsy or pseudo-Lennox syndrome. Part I: symptomatology and long-term prognosis. Neuropediatrics 32, 1–8.

Hammond and Wilder, 1985 E.J. Hammond and B.J. Wilder, Gamma-Vinyl GABA: a new antiepileptic drug, Clin. Neuropharmacol. 8 (1), pp. 1–12

Hirose, S., Mitsudome, A., Okada, M., Kaneko, S., 2005. Epilepsy genetic study group Japan. Epilepsia 46 (S1), 38–43.

Holmes, M.D., Brown, M., Tucker, D.M., 2004. Are generalized seizures truly generalized? Evidence of localized mesial frontal and frontopolar discharges in absence epilepsy. Epilepsia 45, 1568–1579.

Hosford, D.A., Clark, S., Cao, Z., Wilson, W.A., Lin, F., Morrisett, R.A., Huin, A., 1992. The role of GABAB receptor activation in absence seizures of lethargic (lh/lh) mice. Science 257, 398–401.

Houser, C.R., Vaughn, J.E., Barber, R.P., Roberts, E., 1980. GABA neurons are the major cell type of the nucleus reticularis thalami. Brain Research 200, 341–354.

Inoue, M., Peeters, B.W., van Luijtelaar, E.L., Vossen, J.M., Coenen, A.M., 1990. Spontaneous occurrence of spike-wave discharges in five inbred strains of rats. Physiology & Behavior 48, 199–201.

Inoue, M., van Luijtelaar, E.L., Vossen, J.M., Coenen, A.M., 1992. Visual evoked potentials during spontaneously occurring spike-wave discharges in rats. Electroencephalography and Clinical Neurophysiology 84, 172–179.

Inoue, M., Duysens, J., Vossen, J.M.H., Coenen, A.M.L., 1993. Thalamic multiple unit activity underlying spike-wave discharges in anesthetized rats. Brain Research 612, 35–40.

Jallon, P., Latour, P., 2005. Epidemiology of idiopathic generalized epilepsies. Epilepsia 46 (Suppl. 9), 10–14.

Jasper, H.H., Kershman, J., 1941. Electroencephalographic classification of the epilepsies. Archives of Neurology and Psychiatry 45, 903–943. Jones, E.G., 1985. The Thalamus. Plenium Press, New York, 955pp.

Jones, J.E., Watson, R., Sheth, R., Caplan, R., Koehn, M., Seidenberg, M., Hermann, B., 2007. Psychiatric comorbidity in children with new onset epilepsy. Dev. Med. Child Neurol. 49, 493–497.

Jones, N.C., Salzberg, M.R., Kumar, G., Couper, A., Morris, M.J., O'Brien, T.J., 2008. Elevated anxiety and depressive-like behavior in a rat model of genetic generalized epilepsy suggesting common causation. Exp. Neurol. 209, 254–260.

Kandel, A., Buzsaki, G., 1997. Cellular-synaptic generation of sleep spindles, spike-and-wave discharges, and evoked thalamocortical responses in the neocortex of the rat. Journal of Neuroscince 17, 6783–6797.

Karpova, A.V., Bikbaev, A.F., Coenen, A.M., van Luijtelaar, G., 2005. Morphometric Golgi study of cortical locations in WAG/Rij rats: the cortical focus theory. Neuroscience Research 51, 119–128.

Kapucu, L.O., Serdaroglu, A., Okuyaz, C., Kose, G., Gucuyener, K., 2003. Brain single photon emission computed tomographic evaluation of patients with childhood absence epilepsy. Journal of Child Neurology 18, 542–548.

Kawaguchi, Y., Kubota, Y., 1997. GABAergic cell subtypes and their synaptic connections in rat frontal cortex. Cerebral Cortex 7, 476–486. Kellaway, P., 1985. Sleep and epilepsy. Epilepsia 26 (S1), 15–30.

Khosravani, H., Zamponi, G.W., 2006. Voltage-gated calcium channels and idiopathic generalized epilepsies. Physiol. Rev. 86, 941–966.

Klein, J.P., Khera, D.S., Nersesyan, H., Kimchi, E.Y., Waxman, S.G., Blumenfeld, H., 2004. Dysregulation of sodium channel expression in cortical neurons in a rodent model of absence epilepsy. Brain Research 1000, 102–109.

Kleinfeld, D., Berg, R.W., O'Connor, S.M., 1999. Anatomical loops and their electrical dynamics in relation to whisking by rat. Somatosensory and Motor Research 16, 69–88.

Knake, S., Hamer, H.M., Schomburg, U., Oertel, W.H., Rosenow, F., 1999. Tiagabine-induced absence status in idiopathic generalized epilepsy. Seizure 8, 314–317.

Knight, A.R., Bowery, N.G., 1992. GABA receptors in rats with spontaneous generalized nonconvulsive epilepsy. Journal of Neural Transmission 35 (Suppl.), 189–196.

Konishi, T., Matsuzawa, J., Hongou, K., Murakami, M., Yamatani, M., Yagi, S., 1999. Partial seizures during the course in patients with absence epilepsy. No To Hattatsu 31, 395–401.

Kostopoulos, G.K., 2000. Spike-and-wave discharges of absence seizures as a transformation of sleep spindles: the continuing development of a hypothesis. Clinical Neurophysiology 111 (S2), S27–S38.

Kostopoulos, G., Avoli, M., Pellegrini, A., Gloor, P., 1982. Laminar analysis of spindles and of spikes of the spike and wave discharge of feline generalized penicillin epilepsy. Electroencephalography and Clinical Neurophysiology 53, 1–13.

Lagae, L., Pauwels, J., Monte, C.P., Verhelle, B., Vervisch, I., 2001. Frontal absences in children. European Journal of Paediatric Neurology 5, 243–251.

Lei H, Zhang Y, Zhu XH, Chen W., 2003. Changes in the proton T2 relaxation times of cerebral water and metabolites during forebrain ischemia in rat at 9.4 T. Magn Reson Med. Jun;49(6):979-84.

Lennox, W.G., et al., 1945. The petit mal epilepsies: their treatment with Tridione. JAMA 129, 1069–1074.

Lerman, P., 1986. Seizures induced or aggravated by anticonvulsants. Epilepsia 27, 706–710.

Leutmezer, F., Lurger, S., Baumgartner, C., 2002. Focal features in patients with idiopathic generalized epilepsy. Epilepsy Research 50, 293–300.

Liu, Z., Vergnes, M., Depaulis, A., Marescaux, C., 1991. Evidence for acritical role of GABAergic transmission within the thalamus in the genesis and control of absence seizures in the rat. Brain Research 545, 1–7.

Liu, Z., Vergnes, M., Depaulis, A., Marescaux, C., 1992. Involvement of intrathalamic GABAB neurotransmission in the control of absence seizures in the rat. Neuroscience 48, 87–93.

Llinas, R.R., Steriade, M., 2006. Bursting of thalamic neurons and states of vigilance. J. Neurophysiol. 95, 3297–3308.

Loiseau, P., 2002. Childhood absence epilepsy and related syndromes. In: Roger, J., Bureau, M., Dravet, C., Genton, P,Loiseau, J., et al., 1990. Survey of seizure disorders in the French southwest. I. Incidence of epileptic syndromes. Epilepsia 31, 391–396.

Lüders H., Daube, J., Johnson, J., Klass, D.W., 1980. Computer analysis generalized spike and wave complexes. Epilepsia 21, 183 [abstract].

Lüders H, Lesser RP, Dinner DS, Morris HH III., 1984. Generalized epilepsies: a review. Cleve Clin Q.51:205-226.

Luhmann, H.J., Mittmann, T., van Luijtelaar, G., Heinemann, U., 1995. Impairment of intracortical GABAergic inhibition in a rat model of absence epilepsy. Epilepsy Research 22, 43–51.

Lu, Y., et al., 2008. Photosensitivity in epileptic syndromes of childhood and adolescence. Epileptic Disord. 10, 136–143.

Lu J, Chen Y, Zhang Y, Pan H, Wu H, Xu K, Liu X, Jiang Y, Bao X, Ding K, hen Y, Wu X. 2002. Mutation screen of the GABA(A) receptor gamma 2 subunit gene in Chinese patients with childhood absence epilepsy. Neurosci Lett.Oct 31;332(2):75-8.

Manning, J.P., et al., 2003. Pharmacology of absence epilepsy. Trends Pharmacol. Sci. 24, 542–549.

Manning, J.P., Richards, D.A., Leresche, N., Crunelli, V., Bowery, N.G.,2004. Cortical-area specific block of genetically determined absence seizures by ethosuximide. Neuroscience 123, 5–9.

Malpeli, J.G., Schiller, P.H., 1979. A method of reversible inactivation of small regions of brain tissue. Journal of Neuroscience Methods 1, 143–151.

Marescaux, C., Micheletti, G., Vergnes, M., Depaulis, A., Rumbach, L., Warter, J.M., 1984. A model of chronic spontaneous petit mal-like seizures in the rat: comparison with pentylenetetrazol-induced seizures. Epilepsia 25, 326–331.

Marescaux, C., Vergnes, M., Depaulis, A., 1992. Genetic absence epilepsy in rats from Strasbourg—a review. Journal of Neural Transmission 35(Suppl.), 37–69.

Marini, C., Scheffer, I., Crossland, K., et al., 2004. Genetic architecture of idiopathic generalized epilepsy: clinical genetic analysis of 55 multiplex families. Epilepsia 45, 467–478.

Markram, H., Toledo-Rodriguez, M., Wang, Y., Gupta, A., Silberberg, G., Wu, C., 2004. Interneurons of the neocortical inhibitory system. Nature Reviews Neuroscience 5, 793–807.

Matthes, A, Schneble, H., 1999. Epilepsien: Diagnostik und Therapie für Klinik und Praxis. Thieme.

Mathivet, P., Bernasconi, R., Bittiger, H., Marescaux, C., 1996. Regional differences of the inhibition of GABAB ligand binding by the GTP analogue Gpp(NH)p. Brain Reseach and Molecular Brain Research 42, 18–24.

McKeown, M. J., Humphries, C., Iragui, V., and Sejnowski, T. J., 1999. Spatially fixed patterns account for the spike and wave features in absence seizures. Brain Topogr. 12:107–116.

Meencke, H.J., 1989. Pathology of childhood epilepsies. Cleveland Clinic Journal of Medicine 56 (Suppl. Pt 1), S111–S120.

Meeren, H.K.M., 2002. Cortico-thalamic mechanisms underlying generalized spike-wave discharges of absence epilepsy. A lesional and signal analytical approach in the WAG/Rij rat. Ph.D. Thesis, Nijmegen University.

Meeren, H.K., van Cappellen van Walsum, A.M., van Luijtelaar, E.L., Coenen, A.M., 2001. Auditory evoked potentials from auditory cortex, medial geniculate nucleus, and inferior colliculus during sleep–wake states and spike-wave discharges in the WAG/Rij rat. Brain Research 898, 321–331.

Meeren, H.K., Pijn, J.P., van Luijtelaar, E.L., Coenen, A.M., Lopes da Silva, F.H., 2002. Cortical focus drives widespread corticothalamic networks during spontaneous absence seizures in rats. Journal of Neuroscience 22, 1480–1495.

Meeren, H.K., van Luijtelaar, E.L.J.M., Lopes da Silva, F.H., Coenen, A.M., 2005. Evolving concepts on the pathophysiology of absence seizures: the cortical focus theory. Archives of Neurology 62, 371–376.

Midzianovskaia, I.S., Kuznetsova, G.D., Coenen, A.M., Spiridonov, A.M., van Luijtelaar, E.L., 2001. Electrophysiological and pharmacological characteristics of two types of spike-wave discharges in WAG/Rij rats. Brain Research 911, 62–70.

Midzyanovskaya, I., Strelkov, V., Rijn, C.V., Budziszewska, B., van Luijtelaar, E., Kuznetsova, G., 2006. Measuring clusters of spontaneous spike-wave discharges in absence epileptic rats. Journa of Neuroscience Methods

Miettinen, M., Koivisto, E., Riekkinen, P., Miettinen, R., 1996. Coexistence of parvalbumin and GABA in nonpyramidal neurons of the rat entorhinal cortex. Brain Research 706, 113–122.

Mirsky, A.F., Tecce, J.J., 1968. The analysis of visual evoked potentials during spike-wave EEG activity. Epilepsia 9, 211–220.
Nersesyan, H., Hyder, F., Rothman, D.L., Blumenfeld, H., 2004a. Dynamic fMRI and EEG recordings during spike-wave seizures and generalized tonic–clonic seizures in WAG/Rij rats. Journal of Cerebral Blood Flow and Metabolism 24, 589–599.

Nersesyan, H., Herman, P., Erdogan, E., Hyder, F., Blumenfeld, H., 2004b. Relative changes in cerebral blood flow and neuronal activity in local microdomains during generalized seizures. Journal of Cerebral Blood Flow and Metabolism 24, 1057–1068.

Ngomba, R.T., Biagioni, F., Casciato, S., Willems-van Bree, E., Battaglia, G., Bruno, V., Nicoletti, F., van Luijtelaar, E.L., 2005. The preferential mGlu2/3 receptor

antagonist, LY341495, reduces the frequency of spike-wave discharges in the WAG/Rij rat model of absence epilepsy. Neuropharmacology 49S1, 89–103.

Nicolelis, M.A., Baccala, L.A., Lin, R.C., Chapin, J.K., 1995. Sensorimotor encoding by synchronous neural ensemble activity at multiple levels of the somatosensory system. Science 268, 1353–1358.

Nicolelis, M.A., Fanselow, E.E., 2002. Thalamocortical optimization of tactile processing according to behavioral state. Nature Neuroscience 5, 517–523.

Niedermeyer, E., 1972. The generalized epilepsies: A clinical electroencephalographical study. Springfield, IL: Charles C. Thomas.

Niedermeyer, E., 1996. Primary (idiopathic) generalized epilepsy and underlying mechanisms. Clinical Electroencephalography 27, 1–21. Nunez, P.L., 1995. Neocortical Dynamics and Human EEG Rhythms. Oxford University Press, New York.

November Lennox, W. G., and Jolly, D., 1954. Seizures, brain waves and intelligence tests of epileptic twins. Proc. Assoc. Res. Nerv. Dis. 33:325–345.

O'Connor, S.M., Berg, R.W., Kleinfeld, D., 2002. Coherent electrical activity between vibrissa sensory areas of cerebellum and neocortex is enhanced during free whisking. Journal of Neurophysiology 87, 2137–2148.

Ohara, P.T., Sefton, A.J., Lieberman, A.R., 1980. Mode of termination of afferents from the thalamic reticular nucleus in the dorsal lateral geniculate nucleus of the rat. Brain Research 197, 503–506.

Ohara, P.T., Lieberman, A.R., Hunt, S.P., Wu, J.L., 1983. Neuronal elements containing GAD in the dorsal LGN of the rat: immunocytochemical studies by light and electron microscopy. Neuroscience 8, 189–211.

Olsson, I., 1988. Epidemiology of absence epilepsy. I. Concept and incidence. Acta Paediatr. Scand. 77, 860–866.

Ott, D., Siddarth, P., Gurbani, S., Koh, S., Tournay, A., Shields, W.D., Caplan, R., 2003. Behavioral disorders in pediatric epilepsy: unmet psychiatric need. Epilepsia 44, 591–597.

Panayiotopoulos, C.P., 1999. Typical absence seizures and their treatment. Arch. Dis. Child. 81, 351–355.

Panayiotopoulos, C.P., 2001. Treatment of typical absence seizures and related epileptic syndromes. Paediatr. Drugs 3, 379–403.

Panayiotopoulos, C.P., 2005a. Idiopathic generalized epilepsies: a review and modern approach. Epilepsia 46 (Suppl. 9), 1–6.

Panayiotopoulos, C.P., 2005b. Syndromes of idiopathic generalized epilepsies not recognized by the International League Against Epilepsy. Epilepsia 46 (Suppl. 9), 57–66.

Panayiotopoulos, C.P., et al., 1997. Idiopathic generalised epilepsy in adults manifested by phantom absences, generalized tonic–clonic seizures, and frequent absence status. J. Neurosurg. Psychiatry 63, 622–627.

Paxinos, G., Watson, C., 1998. The Rat Brain in Stereotaxic Coordinates, fourth ed. Academic Press, San Diego, CA.

Pavone, A., Niedermeyer, E., 2000. Absence seizures and the frontal lobe. Clinical Electroencephalography 31, 153–156.

Peeters, B.W., Kerbusch, J.M., Coenen, A.M., Vossen, J.M., van Luijtelaar, E.L., 1992. Genetics of spike-wave discharges in the electroencephalogram (EEG) of the WAG/Rij inbred rat strain: a classical mendelian crossbreeding study. Behavior Genetics 22, 361–368.

Peinado, M.A., Martinez, M., Pedrosa, J.A., Quesada, A., Peinado, J.M., 1993. Quantitative morphological changes in neurons and glia in the frontal lobe of the aging rat. Anatomical Record 237, 104–108.

Peinado, M.A., Quesada, A., Pedrosa, J.A., Martinez, M., Esteban, F.J., Del Moral, M.L., Peinado, J.M., 1997. Light microscopic quantification of morphological changes during aging in neurons and glia of the rat parietal cortex. Anatomical Record 247, 420–425.

Penfield, W., and Jasper, H., 1954. Epilepsy and the functional anatomy of the human brain. Boston: Little Brown.

Penry, J.K., et al., 1975. Simultaneous recording of absence seizures with video tape and electroencephalography. A study of 374 seizures in 48 patients. Brain 98, 427–440.

Peters, A., Jones, E.G. (Eds.), 1984. Cerebral Cortex, Vol. 1, Cellular Components of the Cerebral Cortex. Plenum Press, New York. Petsche, H., 1962. Pathophysiologie und Klinik des Petit-Mal. Wiener Zeitschrift fuer Nervenheilkrank 19, 345–442.

Pitra, P., Grzegorzewska, M., Hess, G., 2005. Synaptic transmission in somatosensory cortical slices of genetic epileptic WAG/Rij rats. Abstracts of the 7th International Congress of the Polish Neuroscience Society. Acta Neurobiologiae Experimentalis 65, 320.

Poe, B.H., Linville, C., Brunso-Bechtold, J., 2001. Age-related decline of presumptive inhibitory synapses in the sensorimotor cortex as revealed by the physical disector. Journal of Comparative Neurology 439, 65–72.

Polack, P.O., Charpier, S., 2006. Intracellular activity of cortical and thalamic neurons during high-voltage rhythmic spike discharge in Long-Evans rats in vivo. Journal of Physiology,12 January.

Pollen, D., Perot, P., Reid, K.H., 1963. Experimental bilateral wave and spike from thalamic stimulation in relation to level of arousal. Electroencephalography and Clinical Neurophysiology 15, 1017–1028.

Posner, E., 2006. Pharmacological treatment of childhood absence epilepsy. Expert Rev. Neurother. 6, 855–862.

Prevett, M.C., Duncan, J.S., Jones, T., Fish, D.R., Brooks, D.J., 1995. Demonstration of thalamic activation during typical absence seizures using H2(15)O and PET. Neurology 45, 1396–1402.

Princivalle, A.P., Richards, D.A., Duncan, J.S., Spreafico, R., Bowery, N.G., 2003. Modification of GABA(B1) and GABA(B2) receptor subunits in the somatosensory cerebral cortex and thalamus of rats with absence seizures (GAERS). Epilepsy Research 55, 39–51.

Pijn, J.P., Vijn, P.C.M., Lopes da Silva, F.H., van Emde Boas, W., Blanes, W., 1989. The use of signal analysis for the location of an epileptogenic focus: a new approach. Advances in Epileptology 17, 272–276.

Provencher S.W. 2001. Automatic quantitation of localized in vivo 1H spectra with LCModel. NMR Biomed. 14:260-264.

Pugliatti, M., et al., 2007. Estimating the cost of epilepsy in Europe: a review with economic modeling. Epilepsia 48, 2224–2233.

Rodin, E., Ancheta, O., 1987. Cerebral electrical fields during petit mal absences. Electroencephalography and Clinical Neurophysiology 66, 457–466.

Rogawski, M.A., Loscher, W., 2004. The neurobiology of antiepileptic drugs. Nat. Rev. Neurosci. 5, 553–564.

Rouiller, E.M., Welker, E., 2000. A comparative analysis of the morphology of corticothalamic projections in mammals. Brain Research Bulletin 53, 727–741.

Rudolf, G., Bihoreau, M.T., Godfrey, R.F., Wilder, S.P., Cox, R.D., Lathrop, M., Marescaux, C., Gauguier, D., 2004. Polygenetic control of idiopathic generalized epilepsy phenotypes in the genetic absence rats from Strasbourg (GAERS). Epilepsia 45, 301–308.

Sabers, A., Moller, A., Scheel-Kruger, J., Mouritzen Dam, A., 1996. No loss in total neuron number in the thalamic reticular nucleus and neocortex in the genetic absence epilepsy rats from Strasbourg. Epilepsy Research 26, 45–48.

Salek-Haddadi, A., Lemieux, L., Merschhemke, M., Friston, K.J., Duncan, J.S., Fish, D.R., 2003. Functional magnetic resonance imaging of human absence seizures. Annals of Neurology 53, 663–667.

Sauer, H., 1916. Über gehäufte kleine Anfälle bei Kindern (Pyknolepsie). Mschr Psychiatr. Neurol. 40, 276–300.

Schridde, U., van Luijtelaar, G., 2005. The role of the environment on the development of spike-wave discharges in two strains of rats. Physiology & Behavior 84, 379–386.

Seidenbecher, T., Pape, H.C., 2001. Contribution of intralaminar thalamic nuclei to spike-and-wave-discharges during spontaneous seizures in a genetic rat model of absence epilepsy. European Journal of Neuroscience 13, 1537–1546.

Seidenbecher, T., Staak, R., Pape, H.C., 1998. Relations between cortical and thalamic cellular activities during absence seizures in rats. European Journal of Neuroscience 10, 1103–1112.

Semba, K., Komisaruk, B.R., 1984. Neural substrates of two different rhythmical vibrissal movements in the rat. Neuroscience 12, 761–774.

Semba, K., Szechtman, H., Komisaruk, B.R., 1980. Synchrony among rhythmical facial tremor, neocortical 'alpha' waves, and thalamic nonsensory neuronal bursts in intact awake rats. Brain Research 195, 281–298.

Shaw, F.Z., 2004. Is spontaneous high-voltage rhythmic spike discharge in Long Evans rats an absence-like seizure activity? Journal of Neurophysiology 91, 63–77.

Shaw, F.Z., Liao, Y.F., 2005. Relation between activities of the cortex and vibrissae muscles during high-voltage rhythmic spike discharges in rats. Journal of Neurophysiology 93, 2435–2448.

Silva, L.R., Amitai, Y., Connors, B.W., 1991. Intrinsic oscillations of neocortex generated by layer 5 pyramidal neurons. Science 251, 432–435.

Sirven, J.I., 2002. Classifying seizures and epilepsy: a synopsis. Semin. Neurol. 22, 237–246.

Sitnikova, E., van Luijtelaar, G., 2004. Cortical control of generalized absence seizures: effect of lidocaine applied to the somatosensory cortex in WAG/Rij rats. Brain Research 1012, 127–137.

Sitnikova, E., van Luijtelaar, G., 2005. Reduction of adrenergic neurotransmission with clonidine aggravates spike-wave seizures and alters activity in the cortex and the thalamus in WAG/Rij rats. Brain Research Bulletin 64, 533–540.

Snead, O.C., 1992. Pharmacological models of generalized absence seizures in rodents. Journal of Neural Transmission 35 (Suppl.), 7–19.

Spreafico, R., Mennini, T., Danober, L., Cagnotto, A., Regondi, M.C., Miari, A., De Blas, A., Vergnes, M., Avanzini, G., 1993. GABA-a receptor impairment in the genetic absence epilepsy rats from Strasbourg (GAERS): an immunocytochemical and receptor binding autoradiographic study. Epilepsy Research 15, 229–238.

Stefan, H., 1982. Basic temporal structure of absence symptoms. In: Kazamatsuri, H., Seino, M., Ward, A.A. (Eds.), Advances in Epileptology: The 13th Epilepsy International symposium. Raven Press, New-York.

Steriade, M., 2001. Impact of network activities on neuronal properties in corticothalamic systems. Journal of Neurophysiology 86, 1–39.

Steriade, M., 2003. Neuronal Substrates of Sleep and Epilepsy. Cambridge University Press, Cambridge.

Steriade, M., 2005. Sleep, epilepsy and thalamic reticular inhibitory neurons. Trends Neurosci. 28, 317–324.

Steriade, M., 2006. Spike wave seizures in cortico-thalamic systems. In: Arzimanoglou, A., Chauvel, P., Engel, J., Hirsch, E., Luders, H. (Eds.), Progress in Epileptic Disorders. ‘‘Generalized Seizures: From Clinical Phenomenology to Underlying Systems and Networks’’. John Libey Eurotext, Montrouge, France.

Steriade, M., Amzica, F., 1994. Dynamic coupling among neocortical neurons during evoked and spontaneous spike-wave seizure activity. Journal of Neurophysiology 72, 2051–2069.

Steriade, M., Deschenes, M., Domich, L., Mulle, C., 1985. Abolition of spindle oscillations in thalamic neurons disconnected from the nucleus RT. Journal of Neurophysiology 54, 1473–1497.

Strauss, U., Kole, M.H., Brauer, A.U., Pahnke, J., Bajorat, R., Rolfs, A., Nitsch, R., Deisz, R.A., 2004. An impaired neocortical Ih is associated with enhanced excitability and absence epilepsy. European Journal of Neuroscience 19, 3048–3058.

Tancredi, V., Biagini, G., D’Antuono, M., Louvel, J., Pumain, R., Avoli, M., 2000. Spindle-like thalamocortical synchronization in a rat brain slice preparation. Journal of Neurophysiology 84, 1093–1097.

Tehovnik, E.J., Sommer, M.A., 1997. Effective spread and timecourse of neural inactivation caused by lidocaine injection in monkey cerebral cortex. Journa of Neuroscience Methods 74, 17–26.

Tellez-Zenteno, J.F., Patten, S.B., Jette, N., Williams, J., Wiebe, S., 2007. Psychiatric comorbidity in epilepsy: a population-based analysis. Epilepsia 48, 2336–2344.

Tenney, J.R., Duong, T.Q., King, J.A., Ferris, C.F., 2004. FMRI of brain activation in a genetic rat model of absence seizures. Epilepsia 45, 576–582.

Temkin, O., 1971. The Falling Sickness. A History of Epilepsy from the Greeks to the Beginnings of Modern Neurology, second ed. Johns Hopkins Press, Baltimore.

Tissot, S.A., 1770. Traite de l'epilepsie, faisant le tome troisieme du traite des nerfs et de leurs maladies. Didot Le Jeune, Paris.

Tolmacheva, E.A., van Luijtelaar, G., Chepurnov, S.A., Kaminskij, Y., Mares, P., 2004. Cortical and limbic excitability in rats with absence epilepsy. Epilepsy Research 62, 189–198.

van de Bovenkamp-Janssen, M.C., Akhmadeev, A., Kalimullina, L., Nagaeva, D.V., van Luijtelaar, E.L., Roubos, E.W., 2004a. Synaptology of the rostral reticular thalamic nucleus of absence epileptic WAG/Rij rats. Neuroscience Research 48, 21–31.

van de Bovenkamp-Janssen, M.C., Korosi, A., Veening, J.G., Scheenen, W.J.J.M., van Luijtelaar, E.L.J.M., Roubos, E.W., 2004b. Neuronal parvalbumin and absence epilepsy in WAG/Rij rats. In: van Luijtelaar, E.L.J.M., Kuznetsova, G.D., Coenen, A.M.L., Chepurnov, S.A. (Eds.), The WAG/Rij Model of Absence Epilepsy: The Nijmegen-Russian Federation Papers. NICI, Nijmegen, pp. 29–36.

van de Bovenkamp-Janssen, M.C., van der Kloet, J.C., van Luijtelaar, G., Roubos, E.W., 2006. NMDA-NR1 and AMPA-GluR4 receptor subunit immunoreactivities in the absence epileptic WAG/Rij rat. Epilepsy Research

van Luijtelaar, E.L.J.M., Coenen, A.M.L., 1986. Two types of electrocortical paroxysms in an inbred strain of rats. Neuroscience Letters 70,393–397.

van Luijtelaar, E. L. J. M., and Coenen, A. M. L., 1988. Circadian rhythmicity in absence epilepsy in rats. Epilepsy Res. 2:331–336.

van Luijtelaar, E. L. J. M., van der Staay, F. J., and Kerbusch, J. M. H., 1989. Spatial memory in rats: A cross validation study. Q. J. Exp. Psychol. 41B:287–306.

van Luijtelaar, E.L., van der Werf, S.J., Vossen, J.M., Coenen, A.M., 1991. Arousal, performance and absence seizures in rats. Electroencephalography and Clinical Neurophysiology 79, 430–434.

van Luijtelaar, E.L., Ates, N., Coenen, A.M., 1995. Role of L-type calcium channel modulation in nonconvulsive epilepsy in rats. Epilepsia 36, 86–92.

van Luijtelaar, G., Wiaderna, D., Elands, C., and Scheenen, W., 2000. Opposite effects of T- and L-type Ca(2+) channels blockers in generalized absence epilepsy. Eur. J. Pharmacol. 406:381–389

van Luijtelaar, G., Welting, J., 2001. Sleep spindles and spike-wave discharges in rats: effects of thalamic lesions. In: Alex van Bemmel, A., et al. (Eds.), Sleep–Wake in the Netherlands, pp. 81–86.

van Luijtelaar, E.L., Drinkenburg, W.H., van Rijn, C.M., Coenen, A.M., 2002. Rat models of genetic absence epilepsy: what do EEG spikewave discharges tell us about drug effects? Methods and Findings in Experimental and Clinical Pharmacology 24 (Sl D), 65–70.

Vergnes, M., Marescaux, C., 1992. Cortical and thalamic lesions in rats with genetic absence epilepsy. Journal of Neural Transmission 35 (Suppl.), 71–83.

Vergnes, M., Marescaux, C., Micheletti, G., Depaulis, A., Rumbach, L., Warter, J.M., 1984. Enhancement of spike and wave discharges by GABAmimetic drugs in rats with spontaneous petit-mal-like epilepsy. Neuroscience Letters 44, 91–94.

Vergnes, M., Boehrer, A., Reibel, S., Simler, S., Marescaux, C., 2000. Selective susceptibility to inhibitors of GABA synthesis and antagonists of GABAA receptor in rats with genetic absence epilepsy. Experimental Neurology 161, 714–723.

Victor, M., Ropper A.H., 2001. Adams and Victor's Principles of Neurology. McGraw-Hill, 7th ed.

von Krosigk, M., Bal, T., McCormick, D.A., 1993. Cellular mechanisms of a synchronized oscillation in the thalamus. Science 261, 361–364.

Vuilleumier, P., Assal, F., Blanke, O., Jallon, P., 2004. Distinct behavioural and EEG topographic correlates of loss of consciousness in absences. Epilepsia 41, 687–693.

Wallace RH, Marini C, Petrou S, Harkin LA, Bowser DN, Panchal RG, Williams DA,Sutherland GR, Mulley JC, Scheffer IE, Berkovic SF., 2001. Mutant GABA(A) receptor gamma2-subunit in childhood absence epilepsy and febrile seizures. Nat Genet. May;28(1):49-52.

Waltregny, A. (Eds.), The Physiopathogenesis of the Epilepsies. Charles C. Thomas, Springfield, IL, pp. 209–236.

Wiest, M.C., Nicolelis, M.A., 2003. Behavioral detection of tactile stimuli during 7–12Hz cortical oscillations in awake rats. Nature Neuroscience 6, 913–914.

Willoughby, J.O., Mackenzie, L., 1992. Nonconvulsive electrocorticographic paroxysms (absence epilepsy) in rat strains. Laboratory Animal Science 42, 551–554.

Williams, D., 1953. A study of thalamic and cortical rhythms in ‘‘petit mal’’. Brain 76, 50–69.